UNIVERSITY OF BELGRADE

MEDICAL FACULTY

Maja M. Životić

THE ROLE OF INTERACTION BETWEEN FIBROBLAST GROWTH FACTOR RECEPTOR AND NEURAL CELL ADHESION MOLECULE IN RENAL FIBROSIS

Doctoral dissertation

Belgrade, 2018

UNIVERZITET U BEOGRADU

MEDICINSKI FAKULTET

Maja M. Životić

ULOGA INTERAKCIJE RECEPTORA ZA FIBROBLASTNI FAKTOR RASTA SA NEURALNIM ĆELIJSKIM ADHEZIONIM MOLEKULOM U FIBROZI BUBREGA

Doktorska disertacija

Beograd, 2018

Mentor:

Prof. dr Jasmina Marković-Lipkovski, redovni profesor Medicinskog fakulteta Univerziteta u Beogradu

Članovi komisije za ocenu završne doktorke disertacije:

1. **Doc. dr Sanja Radojević Škodrić,** docent Medicinskog fakulteta Univerziteta u Beogradu
2. **Prof. dr Radomir Naumović,** vanredni profesor Medicinskog fakulteta Univerziteta u Beogradu
3. **Prof. dr Gerhard A. Müller**, redovni profesor Medicinskog fakulteta Univerziteta u Getingenu, Nemačka - Universitätsmedizin Göttingen, Georg-August-Universität Göttingen; gostujući profesor (visiting professor) Medicinskog fakulteta Univerziteta u Beogradu

ACKNOWLEDGEMENTS

I would like to express my special appreciation and thanks to my scientific advisor Professor Dr. Jasmina Marković-Lipkovski - thank you for encouraging my research and for allowing me to grow as a research scientist. Your advice on both research, as well as on my career have been priceless. Thank you for unconditional trust - you have been a tremendous mentor for me.

Financial support for research was mainly provided by Ministry of Education, Science and Technological Development of the Republic of Serbia (Project No. OI 175047), as well as by Alexander von Humboldt (Project No. 3.4-IP-DEU/1019337) and DAAD (bilateral PPP-DAAD project between Serbia and Germany, number 451-03-01858/2013-09/6) Foundations. Since a part of my Ph.D. research period was conducted through these two bilateral projects between Serbia and Germany (Alexander von Humboldt Foundation and DAAD Foundation), all these merits go to the chiefs of the projects: Professor Dr. Gerhard Müller, Professor Dr. Claudia Müller, Professor Dr. Michael Zeisberg and Professor Dr. Jasmina Marković-Lipkovski. I am grateful so much to Department of Nephrology and Rheumatology, Göttingen University Medical Center, Georg-August University, Germany, as well as laboratory of AG Zeisberg group for kindly provided equipment and regents necessary for my research ideas. Nevertheless, I would especially like to thank my colleagues included in the research group (Dr. Sanja Ćirović, Dr. Jelena Filipović, Dr. Björn Tampe), as well as others employed in Georg-August University in Germany (Dr. Xingbo Xu, Dr. Xiaoying Tan, Dr. Gunsmaa Nyamsuren, Dr. Fouzi Alnour, Dr. Shoji Saito) - all of you have been there to introduce me in new methodological procedures and to support me when I recruited patients, conducted experiments, collected, analyzed and interpreted data for my Ph.D. thesis, helping me to put it in this written Ph.D. form. Thanks to all technicians whose supports were really important in many steps through the goals realizations.

I would also like to thank my committee members, Professor Dr. Gerhard Müller, Assistant Professor Dr. Sanja Radojević Škodrić and Professor Dr. Radomir Naumović for your brilliant comments and suggestions and for letting my defense be an enjoyable moment.

Finally, a special thank to my family and friends! All of you were somewhere on the way together with me helping me to achieve this goal, but only one of you was born during this scientific journey – my daughter Jana, thank you too!

SUMMARY

Background Progression of chronic kidney disease (CKD) remains an unsolved problem in clinical nephrology since approaches to reverse or repair chronic renal injury are not yet available. Independent of the underlying disease, loss of functional kidney parenchyma and tubulo-interstitial fibrogenesis are commonly observed when kidney injury progresses towards CKD. In this regard, epithelial-to-mesenchymal transition (EMT) in tubular epithelial cells (TECs) and consecutive G2/M arrest have been shown to determine maladaptive kidney repair in response to injury, ultimately associated with renal fibrogenesis and progression into CKD. Transforming growth factor β1 (TGF-β1) is considered as a key mediator of intrarenal EMT program and renal fibrosis. Neural cell adhesion molecule (NCAM) and fibroblast growth factor receptor (FGFR) signaling during EMT program have already been described and it has been noticed that both molecules are fundamental for EMT program *in vitro.* However, their cross-talk has been widely studied mainly in neural tissues and cancer cells, but there is a lacking of evidence for the contribution of their interplay to fibrogenesis, although several studies confirmed that both molecules can be separately involved in such process. Moreover, FGFR has been widely studied in many fields of research, including fibrosis, whereas NCAM contribution to renal fibrogenesis has been only suggested by two research groups (including our team). Thus, it encouraged us to investigate aforementioned molecules in human kidneys and to evaluate their significance in fibrotic response within the renal interstitial compartment. For the first time, here we present a functional significance of NCAM and FGFR co-operation in the induction of renal fibrosis, mediated by TGFβ-1.

Material and methods In order to achieve goals of the study, we examined human kidney biopsy samples and performed cell culture experiments to clarify functional significance of NCAM/FGFR1 signaling in model of renal fibrosis. Immunostaining (immunohistochemistry and immunofluorescence) was performed to detect NCAM expressing cells in human kidneys in order to further characterize these cells and to label them for laser capture microdissection (LCM) which allows pure NCAM+ cells collecting for the subsequent qRT-PCR and gene expression analysis. Moreover, clinical relevance of both NCAM expressing renal interstitial cells and TGFβ-1 downstream effectors detection in human kidney biopsies were also examined. By using an established model of EMT program in human proximal tubular epithelial cells (HK-

2 cells) in response to TGF-β1 (10ng/mL) exposure, NCAM/FGFR1 signaling responses were analyzed by light microscopy, immunolabeling, qRT-PCR and scratch assays. Modulation of NCAM/FGFR pathway was performed using PD173074 (100nM) - a small FGFR inhibitor.

Results Significantly increased number of interstitial NCAM expressing cells has been detected in the adult kidneys with incipient interstitial renal fibrosis (incipient IRF, <25% of renal tissue affected with fibrosis), compared to advanced stages of renal fibrosis ($p<0.001$). Among 90 biopsy samples of various glomerulonephritises and glomerulopathies, an increased NCAM positivity was found in 45.6% of cases and was found to be independent of the underlying disease. After applying qRT-PCR using mRNA obtained from laser captured NCAM+ positive cells, NCAM-140 isoform was significantly over-expressed in NCAM+ cells laser captured from incipient IRF ($p=0.006$), and in the same cells significant αSMA ($p=0.014$) and SLUG ($p=0.004$) mRNAs up-regulations were detected. These cells were highly heterogeneous, whereby sub-populations shared some markers involved in fibrosis, such as HE4. However, interstitial NCAM expression did not have long term impact on disease outcome and could not be used as predictor for the impairment of kidney function. Moreover, NCAM interstitial positivity was frequently found in patients with lower proteinuria values. Since TGF-β is the main cytokine involved the fibrogenic response, here we underlined the influence of this signaling pathway (SMADs, SNAIL) on morphology of renal tubulointerstitial compartment suggesting its signaling cascade was closely related to tubular atrophy and interstitial fibrosis, resulting in higher creatinine and urea values, lower eGFR, CDK development and disease progression. Beside SMAD2 influence on morphology of renal tubulointerstitial compartment and patients' outcome, SNAIL expression in podocytes was also associated with nephrotic range proteinuria. EMT program of TECs, induced by TGF-β, was morphologically noticed 48h after treatment and was clearly apparent after 72 hours, associated with loss of CDH1 (encoding E-Cadherin) and transcriptional induction of SNAI1 (encoding SNAIL), SNAI2 (encoding SLUG), TWIST1, MMP2, MMP9, CDH2 (encoding N-Cadherin), ITGA5 (encoding integrin-α5), ITGB1 (encoding integrin-β1), ACTA2 (encoding α-SMA) and S100A4 (encoding FSP1). During early EMT program, transcriptional induction of several NCAM isoforms (mostly NCAM-140 isofrom) along with FGFR1 was observed after 24 hours of TGF-β1 exposure, implicating a mechanistic link between NCAM/FGFR1 signaling and induction of EMT program. These observations were

further supported by inhibition of EMT program by PD173074 to specifically block FGFR1 signaling responses. Beside significant suppression of mRNA and proteins of genes de-regulated during EMT, FGFR inhibitor succeeded to reduce cell migration previously enhanced by TGF-β1.

Conclusion NCAM expressing cells do not only increase during fibrogenesis but also switch the isoforms. Compared to NCAM expressing in normal human kidneys, these cells under fibrotic microenvironment highly express NCAM-140 isoform. NCAM expression in renal interstitial compartment is disease independent, representing a trait of early fibrogenesis in the human kidney. Furthermore, TGF-β signaling pathway activation, is found to be associated with chronic renal parenchymal damage (tubular atrophy and interstitial fibrosis), resulting in impaired renal excretory function and CDK development and progression. Modulation of NCAM/FGFR1 signaling by PD173074 blocks EMT program in cultured human proximal tubular epithelial cells, implicating novel insights into maladaptive repair and parenchymal damage during renal fibrosis. Unequivocally, FGFR inhibitor could be a promising anti-fibrotic strategy for kidney diseases and has to be further explored in details. Collectively, the most important finding in our study reflects a robust induction of NCAM expression in incipient renal fibrosis and an important role of NCAM/FGFR interplay in the initiation step of fibrogenic response that could be effectively suppressed by inhibition of their cross-talk applying FGFR inhibitor (PD173074).

Key words NCAM, FGFR, PD173074, fibrosis

Scientific field: Medicine

Scientific discipline: Molecular medicine/ Pathology / Nephropathology

UDK number:_____

SAŽETAK

Uvod Progresija hronične bubrežne insuficijencije predstavlja gotovo nerešiv problem kliničke nefrologije, imajući u vidu da su terapijski postupci koji bi doveli do zaustavljanja ili reverzibilnosti hroničnih oštećenja parenhima bubrega još uvek nedostupni. Sva hronična oboljenja bubrega dovode do progresivnog gubitka funkcionalnog parenhima i tubulointersticijske fibroze, indukujući pojavu hronične bubrežne insuficijencije. U tom pogledu, smatra se da je supstrat nemogućnosti regeneracije oštećenog parenhima bubrega zapravo fenomen epitelno-mezenhimne transformacije (EMT) sa sledstvenim G2/M zastojem u fazi ćelijskog ciklusa koji dovodi do nastanka fibroze i progresije hronične bubrežne insuficijencije. Smatra se da je glavni medijator EMT programa i fibroze u bubregu transformišući faktor rasta β1 (TGF-β1). Opisano je da se tokom EMT programa indukuje ekspresija neuralnog ćelijskog adhezionog molekula (NCAM) i receptora za fibroblastni faktor rasta (FGFR), koji imaju važnu ulogu u *in vitro* EMT. Međutim, značaj međusobnih interakcija NCAM i FGFR molekula do sada je prevashodno ispitivan u neuralnom tkivu i različitim malignim oboljenjima, dok nema podataka o značaju ovih interakcija tokom procesa fibroze, iako je nekoliko studija potvrdilo da individualno NCAM i FGFR molekul mogu biti uključeni u ovaj proces. Štaviše, FGFR je izučavan u mnogim patološkim procesima, uključujući i fibrozu, dok je povezanost NCAM molekula sa procesom fibroze u bubregu sugerisana od strane samo dva istraživačka tima (uključujući i naš). Stoga smo poželeli da ispitamo prethodno pomenute molekule u bubrezima čoveka i da procenimo njihov značaj u procesu fibrogeneze. Po prvi put, u ovoj studiji prikazujemo funkcionalni značaj NCAM/FGFR interakcija u indukciji fibroze bubrega, posredovanoj TGF-β1.

Materijal i metode U svrhu ispitivanja zadatih ciljeva studije, korišćeni su uzorci humanih biopsija bubrega kao i eksperimenti na ćelijskim kulturama kako bi se razjasnio funkcionalni značaj NCAM/FGFR1 signalnog puta u modelu fibroze bubrega. Primenjene su imunohistohemisjke i imunofluorescentne tehnike detektovanja NCAM eksprimirajućih ćelija sa ciljem njihove bolje krakterizacije i vizuelizacije, kao i radi sprovođenja laserske mikrodiskcije (LCM) koja omogućava sakupljenje izolovanih NCAM+ ćelija za dalja ispitivanja genske ekspresije metodom real-time RT-PCR (qRT-PCR). Takođe, ispitan je klinički značaj prisustva NCAM+ ćelija u intersticijumu bubrega kao i značaj detekcije nishodnih efektora TGF-β1

signalnog puta u biopsijskim uzorcima. Korišćenjem modela EMT programa indukovanog uz pomoć TGF-β1 (10ng/mL) na humanoj ćelijskoj liniji proksimalnih tubulskih epitelnih ćelija bubrega (HK-2 ćelijka linija), analiziran je značaj NCAM/FGFR1 signalnog puta uz pomoć metoda svetlosne mikroskopije, imunobojenja, qRT-PCR i migracionog eseja (scratch assays). Modulacija NCAM/FGFR1 interakcija sprovedena je korišćenjem PD173074 (100nM) - FGFR inhibitora.

Rezultati Značajan porast broja NCAM eksprimirajućih ćelija u intersticijumu bubrega detektovan je u početnoj fazi interstcijske fibroze (<25% tkiva zahvaćeno fibrozom), poređenjem sa uznapredovalijim stadijuma fibroze ($p<0.001$). Analizom 90 biopsijskih uzoraka različitih glomerulonefritisa i glomerulopatija, povećan broj NCAM ćelija uočen je kod 45.6% ispitanika i nalaz je bio nezavistan od patohistološke dijagnoze. Primenom qRT-PCR metode, korišćenjem mRNA dobijene iz NCAM+ ćelija prikupljenih laserskom mikrodisekcijom, uočeno je da NCAM+ ćelije u početnoj fazi fibroze imaju povećanu ekspresiju NCAM-140 izoforme ($p=0.006$), kao i da pojačano eksprimiraju αSMA ($p=0.014$) i SLUG ($p=0.004$) gene. NCAM+ ćelije pokazivale se međusobno značajnu heterogenost, pri čemu su pojedine populacije ovih ćelija eksprimirale neke od molekula značajnuh u procesu fibrogeneze, kao što je HE4. Međutim, prisustvo intersticijske ekspresije NCAM molekula nije imalo dugotrajan uticaj na tok i ishod bolesti bubrega, tako da ovaj parametar ne može biti korišćen kao prediktor pogoršanja ekskretorne funkcije bubrega. Štaviše, NCAM intersticijska imunoreaktivnost češće je detektovana kod pacijanata sa nižim vrednostima proteinurije. S obzirom na to da je TGF-β glavni citokin uključen u proces fibrogeneze, imunomorfološkom detekcijom efektora ovog signalnog puta (SMAD proteini, SNAIL) uočili smo da je njihovo prisustvo značajno povezno sa morfološkim karakteristikama hroničnog oštećenja bubrežnog parenhima (tubulska atrofija i intersticijska fibroza), kao i da klinički korelira sa značajno višim vrednostima serumskog kreatinina i uree, ali i sa sniženim vrednostima jačine glomerulske fitracije (eGFR), te sa razvojem hronične bubrežne insuficijencije i njene progresije u više CKD stadijume. SNAIL je, kao i SMAD2, bio povezan hroničnim lezijama u tubulointerstcijumu i ishodom bolesti bubrega, ali je pored ovih obrazaca ispoljavanja uočena i značana detekcija ovog molekula u podocitima pacijenata sa nefrotskim vrednostima proteinurije. TGF-β1 indukovan EMT program u ćelijskoj liniji, morfološki je bio primetan 48h nakon stimulacije TGF-β1, ali su se jasni morfološki znaci

EMT mogli uočiti tek 72h od započinjanja eksperimenta i bili su udruženi sa gubitkom ekspresije CDH1 (enkodira E-Cadherin) i sa transkripcionom indukcijom SNAI1 (enkodira SNAIL), SNAI2 (enkodira SLUG), TWIST1, MMP2, MMP9, CDH2 (enkodira N-Cadherin), ITGA5 (enkodira integrin-α5), ITGB1 (enkodira integrin-β1), ACTA2 (enkodira α-SMA) and S100A4 (enkodira FSP1). U toku rane, inicijalne faze EMT, već 24h nakon stimulacije TGF-β1 detektovana je jasna indukcija ekspresije sve tri NCAM izoforme (najviše NCAM-140 izoforme) kao i FGFR1, sugerišući mehanističku povezanost između NCAM/FGFR1 signalnog puta i indukcije EMT programa. Ove opservacije su dalje potkrepljene činjenicom da je EMT uspešno suprimiran kada se blokirao FGFR signalni put uz pomoć PD173074. Pored značajne inhibicije ekspresije mRNA i proteina značajnih u procesu EMT, FGFR inhibitor je takođe uspešno usporio migraciju ćelija koja je prethodno bila stimulisana TGF-β1 uticajem.

Zaključak U toku procesa fibrogeneze u bubregu, NCAM eksprimirajuće ćelije pored toga što postaju brojnije u ranoj fazi ovog procesa, one takođe menjaju značajno i izoformu molekula. U poređenju sa NCAM+ ćelijama u normalnom intesticijumu, ćelije u fibrozi značajno više eksprimiraju NCAM-140 izoformu. Ekspresija NCAM molekula nezavisna je od bolesti koja u osnovi zahvata bubreg, već prestavlja karaktersitiku ranih faza fibroze bubrega kod čoveka. Takođe, aktivacija TGF-β signalnog puta udružena je sa hroničnim oštećenjima parenhima bubrega (atrofija tubula i fibroza intersticijuma), dovodeći do poremećaja ekskretorne funkcije bubrega i razvoja i progresije hronične bubrežne insuficijencije. Modulacija NCAM/FGFR1 signalnog puta korišćenjem PD173074 blokira EMT u kulturi epitelnih ćelija proksimalnih tubula bubrega, ukazujući na nove mehanizme uključene u proces oštećenja parenhima bubrega i reparacije. Nedvosmisleno, FGFR inhibitor bi mogao biti obećavajući anti-fibrotski agens u bubregu i trebalo bi ga dalje detaljnije ispitivati. Sveobuhvatno, najvažniji nalaz u našoj studiji ukazuje na izraženu indukciju NCAM ekspresije u početnim fazama intersticijske fibroze i značaj NCAM/FGFR interakcija u incijaciji procesa fibroze koja bi mogla biti uspešno suprimirana inhibicjom ovog signalnog puta primenom FGFR inhibitora (PD173074).

Ključne reči NCAM, FGFR, PD173074, fibroza

Naučna oblast: Medicina

Uža naučna oblast: Molekularna medicina/ Patologija / Nefropatologija

UDK broj:_____

Table of Contents

1. INTRODUCTION

Proper kidney function is important for the regulation of many physiological processes and consequently plays an important role in homeostasis. Excretory and homeostatic kidney functions include elimination of metabolic products through the urine, regulation of the fluid volume, as well as acid-base balance and electrolyte concentration. Additionally, kidney is also recognized as endocrine organ which produce and secrete hormones such as erythropoietin (EPO), renin, calcitriol and klotho. Through these endocrine functions kidney regulates erythropoiesis, blood pressure and mineralization of the bones. All these kidney functions require preserved kidney morphology and integrity of molecular pathways. Thus, any impairment on these levels could also induce disturbance in essential functions of kidney, either transient or permanent, with ability or disability to recover it (1, 2).

The majority of kidney diseases have chronic course. Either primarily glomerular or tubulointerstital diseases, during the chronic course, result in the excessive accumulation of fibrous tissue, especially within the tubulointerstital compartment. Thus, renal interstitial fibrosis could be the common feature of all kidney diseases, leading to chronic renal failure (3).

Fibrosis is considered as an injury-induced tissue response composed of inflammation, cytokines release, fibroblast activation/proliferation and deposition of matrix scaffold. It resemble normal tissue repair in many aspects and differ from it only in terminal phase. While normal tissue repair terminates with resolution of inflammation, matrix scaffold degradation and myofibroblasts apopotosis, fibrosis represent dysregulated repair seems as permanently active biosynthetic process with excessive deposition of extracellular matrix (ECM) components, accompanied by accumulation of fibroblasts and inflammatory cells, rarefactions of peritubular microvasculature and tubular damages (tubular atrophy and loss of tubular epithelial cells) (4-7). Only severe fibrosis resulting in scaring formation could be macroscopically visible. Like many organs, kidneys with severe and widespread fibrosis are stiff due to excessive ECM deposition, pale due to rarefaction of peritubular microvasculature, and have bumpy surface due to fibroblast contraction. Usually, slight and less severe fibrosis is visible under the microscope and is characterized by widening of interstitial space filled with ECM components (qualitatively

different from normal), fibroblasts (very rare in normal kidney tissue) and other cells (such as inflammatory cells) (8).

Persistent effort to modulate this natural course of kidney diseases has led the scientists to better understanding of molecular mechanisms driving renal fibrosis. Preclinical studies found many effective strategies to mellow-down interstitial fibrosis in the animal kidneys, however, only a few of them are applicable in humans (9-13). Further investigations in the field of molecular background of renal interstitial fibrosis and signaling pathways driving initiation, maintenance and progression of such process could contribute to better understanding of the complex network involved in renal fibrosis and permit development of new potential strategies to treat renal fibrosis in humans. Moreover, a special focus should be on the activation of genes highly expressed during embryonic kidney development and its potential reactivation during wound healing events in the kidney.

1.1.Pathophysiology and morphology of renal fibrosis

Extracellular matrix

In addition to quantitative changes in the matrix, fibrosis could be also followed by the qualitative modifications of ECM (9). The main feature is the accumulation of collagens fibers, types I and III, and several fibronectin splice variants that modulate fibrogenesis. Moreover, fragments of collagen IV could be also detected within the fibrotic interstitium, although this collagen type normally constitutes basement membranes of the tubular epithelium and vascular endothelium. Fibrillar collagen assemble depends on numerous interaction partners *in vivo*, such as fibronectin, collagen type V, integrins (fibronectin and collagen binding), fibrillins (i.e. latent TGF-β binding proteins - LTBP), and secreted protein acidic and rich in cysteine (SPARC). Fibronectin co-localizes with pro-collagen secretion on fibroblasts. Collagen type V assists in the assembly of collagen type I. α5β1 integrin cooperates in cell adhesion, proliferation and differentiation and plays a role in extracellular matrix assembly (5, 14, 15). LTBP facilitate the secretion of pro-TGF-β and support its release and activation. SPARC serves as protective, antiproliferative actor, since it stimulates matrix metalloproteinases (MMPs) and plasminogen activator inhibitor-1 (PAI-1). All these mechanisms modulate collagen matrix both in normal and altered tissues (6).

At the beginning, fibrosis is a focal feature with tendency to be widespread in the persistence of profibrotic microenvironment. Expansion of ECM in renal fibrosis, which induces the widening of interstitial space, appears due to excessive production by matrix-producing cells and/or decreased degradation due to suppressed activities of tissue proteases (5, 9, 16, 17).

Matrix-producing cells

The major role in renal fibrosis belongs to activated fibroblasts, also known as myofibroblasts (4, 18). However, the origin of abundantly observed myofibroblasts within fibrotic areas is still debatable, especially considering that, in contrast to other human organs, normal renal tissue contains scarce fibroblasts (1). Thus, it is difficult to assign a collagen secretion to any particular cell type found within the fibrotic area. Instead, applying different strategies it is possible only to insinuate a collagen secretory function. Usually, in situ hybridization of mRNA encoding collagen chains, collagen poromoter activity and collagen containing cells are used as surrogate

markers of secretory activity. Otherwise, endoplasmic expression of HSP47, collagen type I chaperone could be even more related to secretion (19). Some of the supposed ECM-producing cells are shown on the Figure 1.

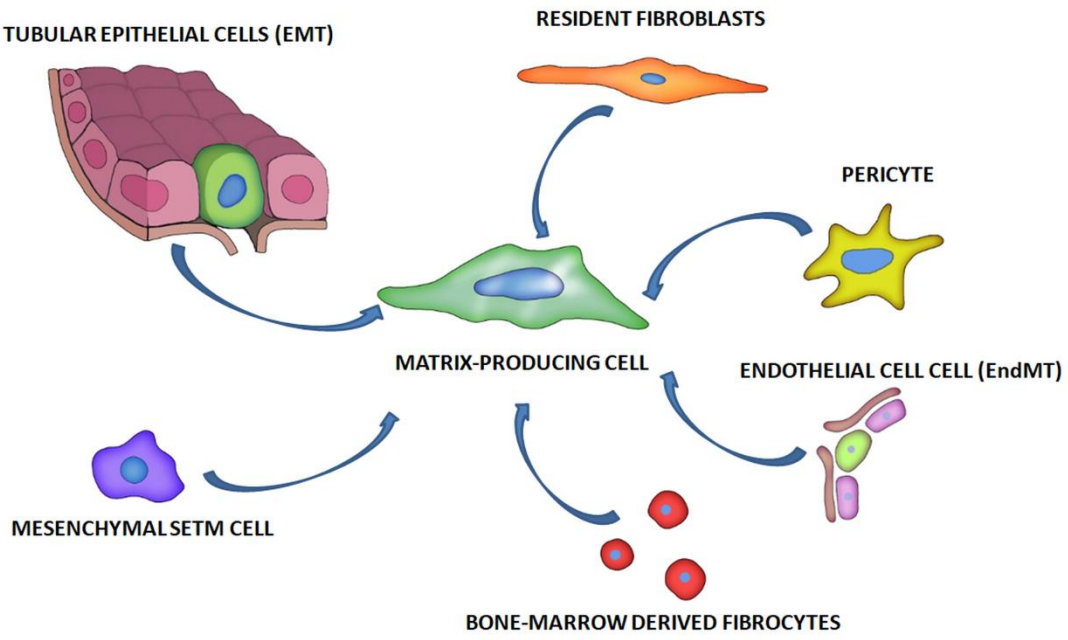

Figure 1. Origin of matrix-producing cells.

Fibroblasts

Unlike other organs, normal human kidneys are devoid of numerous fibroblasts. An increased number of fibroblasts appear during renal fibrosis, as a common event of all chronic kidney diseases. However, these fibroblasts display huge phenotypic heterogeneity, probably relay on the different origin. It has been suspected that the pool of fibrogenic fibroblasts could derive from resident fibroblasts, tubular epithelial and vascular endothelial cells (during epithelial to mesenchymal transformation (EMT) and endothelial to mesenchymal transformation (EndMT) processes initiated by tissue injury), bone marrow-derived fibrocytes, and from pericytes. Unfortunately, the conclusions of the previous studies manly derived from the cell culture experiments and from the manipulations on animal models. Thus, it is not easy to realize what really happens in the humans. Otherwise, it is not yet clear whether the aforementioned pool of fibrogenic cells should be considered as true fibroblasts or only as a separate phenotype of

collagen-producing cells. Moreover, it is less likely that all tissue fibroblasts are potentially fibrogenic (16, 20, 21).

Overall, it clear that fibroblast population is highly heterogeneous. According to the molecules expressed by these cells, their functions can be discovered. Thus, it has been accepted that fibroblasts must be activated to produce ECM components and during such activation they acquire new phenotype and convert to myofibroblasts (21). During that process, the main characteristic is acquisition of α-smooth muscle actin (α-SMA) that is normally expressed by smooth muscle cells, such as vascular. Additionally, activated fibroblasts acquire various phonotypical characteristics making them different from normal kidney fibroblast. Some of the fibroblasts traits are expression of CD90, CD73, PDGF receptors and S100A4 (FSP-1) (22).

The main differences among resident fibroblast in normal renal tissue and those in renal fibrosis are related to their proliferative capacity and ECM synthesis capacity (23). One of the molecules involved in fibroblast activation and proliferation is fibroblast growth factor receptor 1 (FGFR1) that can be activated by FGF and many different ligands including neural cell adhesion molecule (NCAM) (24, 25). Activation of FGFR1 by NCAM interaction additionally promotes FGFR1 recycling, resulting in sustained FGFR1 signaling that is important for fibroblast migration (26, 27). It has been also shown that α5β1 integrin expressed by fibroblasts promotes acquisition of a myofibroblastic phenotype (with a typical α-SMA expression pattern), which constitute the dominant interstitial cells in a pro-fibrotic microenvironment (4, 5, 16). Another up-regulated gene in myofibroblasts is human epididymis protein-4 (HE4), also found in non-α-SMA expressing cells (28). HE4 is a protein which suppresses the activity of multiple proteases, including serine proteinase and matrix metalloproteinases, and inhibits their capacity to degrade type I collagen (29).

Bone-marrow derived fibrocytes

Possible mechanism consider the influx of bone-marrow derived fibrocytes (collagen I/CD34/CD45 expressing cells) into the area of local injury, able to differentiate into the matrix producing myofibroblasts in response to local TGF-β stimuli (30, 31). However, it has been shown that influx of these fibrocytes in the fibrotic kidney is scarce and these fibrocytes did not significantly contrutibuted to interstitial fibrosis (32).

Tubular epithelium

Tubular epithelial cells are also considered as contributors of renal interstitial fibrosis, through synthesis of ECM components. This phenomenon is well studied in the *in vitro* cell culture experiments, through the induction of EMT. The well known EMT inducers are hypoxia, TGF-β and EGF which stimulate broad spectrum of epithelial cells changes until they complete transition and become fibroblasts (33). Through such transformation, many intermediate cell phenotypes appear means they start to lose their epithelial and acquire mesenchymal traits (34). Low rate turn-over of tubular epithelial cells is a limiting factor in tubular regeneration after injury (35). Tubular injury can be acute, with ability to recover damages if the cause of damage is removable. Unfortunately, if the cause of injury persists, tubular epithelial cells are chronically exposed to bad stimuli and should undergo adaptive response. Step by step, these reactions lead to terminal dysfunction of tubular epithelial cells, morphologically characterized by tubular atrophy (36).

Tubular atrophy could appear in the case of primarily tubulointerstitial injuries, as well as a secondary phenomenon of various forms of glomerular diseases with subsequent affection of tubulointerstitial compartment. Once become atrophic, regeneration would not be possible. Since the main consequence of chronically affected tubulointerstitial compartment would be deterioration in kidney function, leading to terminal insufficiency, there are an increasing efforts to prevent this chronic injury (37).

Pericytes end endothelial cells

Several studies identified pericytes and vascular endothelial cells as the major sources of interstitial myofibroblasts (32, 38-41). Thus, the scientific focus switched from tubular to vascular injury in many research groups.

Mesenchymal stem cells

Considering and ability of mesenchymal stem cells to differentiate in several cell lineage, including fibroblasts, they are also recognized as one of the putative origin of matrix producing cells in fibrogenic microenvironment (42).

Tissue proteases

Endogenous potential to remove excessively produced ECM depends on protease activity, preferably MMPs and members of plasmin dependant pathway. These families of proteases are able to fragment components of ECM further suitable for removal. Unfortunately, under certain circumstances they are also able to release profibrotic growth factors triggering undesirable events. MMP family includes 25 members of zinc-dependant endopeptidases. They are divided in several categories: collagenases (MMP1, MMP8, MMP13), gelatinases (MMP2, MMP9), stromelysins (MMP3, MMP10, MMP11), membrane-type MMPs (MMP14, MMP15, MMP16, MMP17, MMP24, MMP25), matrilysin (MMP7, MMP26), enamelysin (MMP20), metalloelastase (MMP12), other types (MMP19, MMP21, MMP23A, MMP23B, MMP27, MMP28). Tissue inhibitors of metalloproteinases (TIMPs) control their activities and they are named TIMP1-4. Among MMPs, gelatinases (MMP2 and MMP9) are the most frequently studied in the kidney. It has been found that both MMP2 and MMP9 are able to degrade collagen type IV, as a main component of basement membrane (both tubular end endothelilal), and has been suspected that they could be able to affect also collagens type I and III, however without evidence of antifibrotic potential in interstitial compartment. Moreover, the effect of these MMPs could be "stage specific", since their inhibition in advanced disease stage could accelerate fibrosis, while inhibition before the onset of fibrosis could be protective. MMP2 overexpression in tubular epithelium could be sufficient to induce fibrosis itself. Overall, it seems that MMP2 and MMP9 profibrotic potential outweigh their antifibrotic activities in the kidney. TGF-β mediated activation of MMP2 and MMP14 (a membrane-bound activator of secreted MMP2 and MMP9 in fibroblasts) is associated with basement membrane destruction, as one of the initial events during EMT. MMP14 expression is induced by SNAIL transcription factor that is one of the key down-stream mediators of TGF-β signaling pathway and EMT process. Plasmin-dependant pathway is also involved in the extracellular matrix remodeling. Whole network is really complex and the effects tissue proteases depend on the biochemical microenvironment. Shortly, tissue-type plasminogen activator (tPA) produces active plasmin by the proteolytic plasminogen cleavage. Active plasmin is able to destroy some ECM components such as laminin and fibronectin, as well as to change cell behavior through activation of MMPs. Thus, interplay between MMPs and plasmin dependant pathway could serve as a profibrotic mechanism inducing renal interstitial fibrosis and tubular cells loss (43, 44).

Inflammatory cells

Infiltration with inflammatory cells is usually seen in the area of renal interstitial fibrosis, at least in some extent. This cell population is composed of lymphocytes, macrophages, dendritic and mast cells. Some subsets of these cells could be profibrotic, while the others could even serve as antifibrotic strategies. Lymphocytes are highly heterogeneous and represent the first cell population that infiltrate the interstitium and come even before macrophages. Among them, CD3+ T lymphocytes are well established contributors to renal fibrosis, while on the other hand the involvement of B lymphocytes is not clear. Interstitial macrophages have very important regulatory role in interstitial fibrosis. Depending on the way of their activation, classically or alternatively, two main macrophages populations are defined: M1 and M2. M1 macrophages accelerate renal interstitial fibrosis, while M2 macrophages are anti-inflammatory and provide tissue repair. Dendritic cells are antigen presenting cells in tubulointerstitial injury. However, they are not widely studied in the context of renal fibrosis. Although mast cells are considered as contributors to fibrosis in many organs, in the kidney they paradoxally suppresses fibrosis. Currently, some purposed therapeutic strategies to modulate fibrogenesis are based on the modulation of inflammatory cell response. Thus, blocking of TGF-β, TNF-α and IL-1 signaling are already investigated and effects are promising (8, 45).

Microvasculature

At the beginning, transient ischemia, trough activation of pro-apoptotic stimuli, causes the damage of peritubular microvasculature that becomes completely remodeled during progression of renal interstitial fibrosis. Peritubular microvasculature in advanced stages is scarce, either due to imbalance between pro- and antiangiogenic stimuli or due to loss of endothelial cells underwent EndMT. Rarefaction of microvasculature in kidney emphasize hypoxic conditions, serving as a great medium for further matrix synthesis by fibroblasts (known as a cells “enjoy” in hypoxic conditions) and leading to progression of tubulointerstitial fibrosis (46, 47).

1.2.Mechanisms and molecular background of renal interstitial fibrosis

Fibrosis in parenchymal organs can be presented by three-step model.

1) Primary injury of epithelial cells stimulate them to release cytokines which afterwards attract inflammatory cells to the site of the primary damages
2) Infiltrating inflammatory cells also produce cytokines which in turns affect epithelial parenchymal cells and also activate fibroblasts to produce ECM components and stimulate their proliferation
3) Fibrogenesis includes maintenance and progression of fibrotic tissue response and depends on the presence of self-stimulating mechanisms persisting even after primary cause of injury and inflammation disappears

Myofibroblasts are the main highly specialized cells responsible for ECM production, both in normal tissue repair and during fibrogenesis, and represented activated fibroblasts with typical expression of α-SMA. The major initial fibroblasts activator is TGF-β, released locally from the injured epithelial cells and inflammatory cells (20, 48). Once activated, myofibroblasts produce TGF-β themselves providing self-sustaining mechanisms characteristic of fibrosis (49, 50). Nevertheless, TGF-β is a powerful stimulus for ECM synthesis especially collagen type I and fibronectin, as well as a potent inducers of EMT *in vitro*. Collagen and fibronectin together act as EMT facilitators stimulating cell migration (51). Widened interstitial space due to expansion of ECM leads to limited oxygen supply to parenchymal cells additionally causing epithelial injury and providing deeper and deeper tissue hypoxia which in turns further stimulates fibrogenesis.

Epithelial to mesenchymal transition (EMT) and fibrosis

EMT is a mechanisms involved in many events during embryogenesis such as formation of mesoderm and neural crest, aimed to create cells with ability to move and produce matrix (50).

Tubular EMT is a highly regulated process consisting of four steps: (1) loss of epithelial cell adhesion, (2) de novo expression of mesenchymal markers such as α-SMA and reorganization of actin cytoskeleton, (3) disruption of TBM, and (4) enhancement of cell migration and invasion. Thus, the main features during EMT are epithelial cell detachment from the neighboring cells

and basement membrane, as well as movement into interstitium where they may start to produce matrix (33).

Following the transformation, epithelial cells pass through many transient phenotypes progressively losing their epithelial and acquiring mesenchymal characteristics. Thus, E-cadherin down-regulation is one of the earliest molecular hallmarks of EMT, which afterwards leads to loss of cell-cell adhesion and detachment from the neighboring epithelial cells. At this step, activity of proteases (such as MMP-2, MMP-9 and MMP-14) is up-regulated aimed to digest basement membranes and allow cell migration into interstitial space. Transcription factors underlying EMT events (such as β-catenin, SMADs and SNAIL family) are also up-regulated and/or translocated into nuclei. Rho GTPase (Ras homologues guanosine triphosphatase) – mediated cytosceletal reorganization favor changes in cell shape and promote cell motility. Additionally, rearrangement in cytosceleton could be supported by activation of integrin-linked kinase (ILK) and β-catenin pathway. Upon EMT, cells start to express mesenchymal markers such as vimentin and S100A4 (FSP-1), and also markers of myofibroblasts such as α-SMA (52).

Normal epithelial cells make a contact with basement membrane which separate them from interstitial compartment and prevent contact with ECM components. When basement membrane is degraded, the contact of epithelial cells with interstitial microenvironment (such as collagens, fibronectin and perhaps TGF-β) allows them to further destabilize epithelial phenotype and enhance EMT. Three main molecular pathways are crucial in the induction of EMT process, including Wnt/β-catenin, extracellular matrix/ILK and TGF-β/SMAD signaling (Figure 2). The central common downstream target of the aforementioned pathways is SNAIL family of transcription factors. Transcription activity of SNAIL results in down-regulation of epithelial and up-regulation of mesenchymal molecules (10, 52-54).

In normal epithelial cells, glycogen synthase kinase-3β (GSK-3β) is constitutively active and phosphorylates SNAIL thereby targeting it for cytoplasmic degradation and preventing its nuclear translocation, thus acting as negative regulator of SNAIL activity. Both ILK and Akt kinase are able to phosphorylate GSK-3β and inhibit its activity which afterwards leads to increase SNAIL activity that enhances EMT. TGF-β/SMADs directly stimulate SNAIL transcription and also transcription of ILKs that in turns cooperate in additional promotion of SNAIL activity (55). TGF-β stimulates pathways involving Rho GTPase that is responsible for

reorganization of cytoskeleton in order to favor cell shape changes and improve cell motility (56).

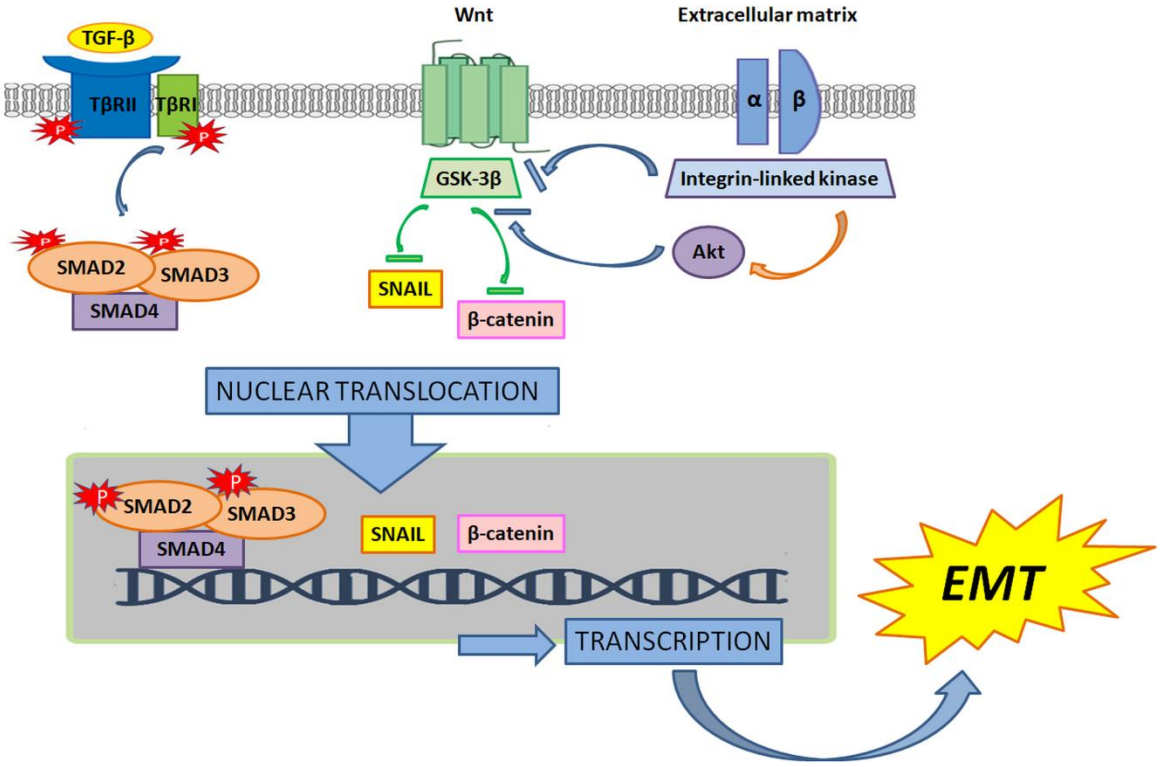

Figure 2. Signaling pathways involved in EMT and fibrosis in kidney.

Transforming growth factor-β (TGF-β) / SMAD pathway

TGF-β, secreted by inflammatory and injured epithelial cells, binds to its receptors type I and type II. Signaling pathway is initiated by TGF-β binding to type II receptor which recruits and phosphorylates type I receptor. After that, type I receptor further phosphorylates cytoplasmic SMAD2 and SMAD3 proteins which then make a complex with SMAD4 protein. SMAD complex then translocate into nucleus and bind to specific DNA sequence motifs, acting as transcription activator of many genes including SNAIL. At this point, SMADs complex also induce transcription of ILK which suppresses E-cadherin and up-regulates MMP-2 and fibronectin. SMADs are involved in the activation of Rho/Rho kinase (ROK) pathway and in the transcription of α-SMA (10, 54, 57). TGF-β ligands and receptors are summarized in Table 1.

Table 1. TGF-β ligands and receptors.

TGF-β superfamily ligand	Type II receptor	Type I receptor	R-SMADs	Co-SMAD	Ligand inhibitors
Activin A	ACVR2A	ACVR1B (ALK4)	SMAD2/3	SMAD4	Follistatin
GDF1	ACVR2A	ACVR1B (ALK4)	SMAD2/3	SMAD4	
GDF11	ACVR2B	ACVR1B (ALK4), TGFβRI (ALK5)	SMAD2/3	SMAD4	
BMPs	BMPR2	BMPR1A (ALK3), BMPR1B (ALK6)	SMAD1/5/8	SMAD4	Noggin, Chordin, DAN
Nodal	ACVR2B	ACVR1B (ALK4), ACVR1C (ALK7)	SMAD2/3	SMAD4	Lefty
TGF- βs	TGFβRII	TGFβRI (ALK5)	SMAD2/3	SMAD4	LTBP1, THBS1, Decorin

There are three distinct SMADs classes based on their roles in TGF-β family signaling transduction: R-SMADs (receptor-regulated SMADs), Co-SMAD (common SMAD) and I-SMADs (inhibitory SMADs). They are summarized in the Table 2.

Table 2. SMAD proteins divided in three classes.

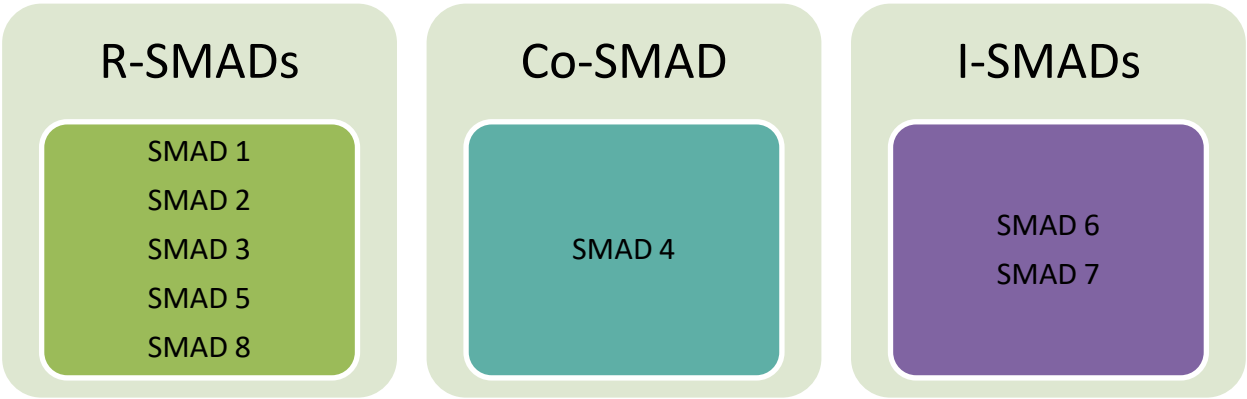

R-SMADs become phophorylated after TGF-β binding to its type I and type II receptors. Phosphorylated R-SMADS then bind to Co-SMAD making a complex that translocate into nucleus and regulate gene transcription. I-SMADs attenuate TGF-β signaling by blocking the interaction with TGF-β receptors and/or compete with Co-SMAD for the generation of R-SMAD/Co-SMAD complex. TGF-β/SMAD signaling can be modulated by Wnt/GSK-β, Rho GTPase, p53, MAPK (mitogen-activated protein kinase) and PI3K-Akt/PKB (54, 58).

In TGF-β-mediated renal fibrosis the major down-stream R-SMADs are SMAD2 and SMAD3, while SMAD7 controls inflammation (57). Regulation of the cellular SMADs concentration is mainly regulated by ubiquitin-mediated degradation through Smufr1 and Smurf2. Polyubiquitinatination of SMAD2 is reported to be mediated by SMURF2, NEDD4L, or WWP1, while SMAD3 is polyubiquitinated by CHIP. Phosphorylated SMAD2/3 can be polyubiquitinated by ARKADIA after the target gene transcription is initiated (59).

Extracellular matrix / ILK pathway

Integrin-linked kinase (ILK) is cytoplasmic serin-threonine kinase that interacts with cytoplasmic domain of β-integrin. Thus, ILK is transducer of integrin-mediated signals from extracellular matrix. Moreover, ILK can be activated by growth factors-mediated and cytokine-mediated ligands. As mentioned above, TGF-β/SMAD can also induce ILK transcription and participate in this signaling pathway. Activated ILK phosphorylate GSK-3β and inhibit its activity, whereby influence up-regulation of SNAIL and enhance β-catenin pathway (52).

Wnt / β-catenin pathway

Wnt cell surface receptors can be stimulated with extracellular Wnt glycoproteins leading to activation of this pathway which results in inhibition of GSK-3β and cytoplasmic accumulation of β-catenin. Finally, β-catenin translocates into nuclei acting as transcription activator of SNAIL, MMPs, vimentin and fibronectin. Without Wnt-mediated signals, β-catenin makes junction complex with E-cadherin. Free non-bound cytoplasmic β-catenin rapidly become phosphorylated by GSK-3β and marked for proteasomal degradation. Indirectly, Wnt pathway can be stimulated by ILK activity which inhibits GSK-3β and leads to β-catenin accumulation (53).

Rho GTPases

Rho GTPase is family that regulates balance between inactive (GDP) and active (GTP) form, influencing assembly or disassembly of actin-based structures. Rho activates ROK which in turns stimulate assembly of actin-myosin filaments by increasing the level of phosphomyosin. The result of the activation of Rho GTPase axis is enhanced cellular contractility underling movement – one of the crucial events during EMT (56).

1.3.Clinical relevance of signaling pathways and implication of anti-fibrotic therapies

TGF-β/SMADs in renal diseases

Precursor of TGF-β

Three major TGF-β isoforms (β1, β2, β3) are widely expressed and secreted in latent forms, forming a complex with the relevant LTBPs (latent TGF-β binding proteins) (54). Proteolytic cleavage enable forming active TGF-β forms, and TGF-β1 is considered as a major mediator in fibrosis. However, a latent TGF-β is not only a simple precursor of active form, but also acts as a protective agent in renal fibrosis (60-61). The precise mechanism is not completely clear, however, it might be that protective effects of the latent TGF- β relay on the elevation of endogenous SMAD7.

TGF-β receptors

TGF- β signaling depends on the phosphorylation of TGF- β receptors, types I and II (TβRI, TβRII), which further phosphorylate SMADs. In the experimental models of fibrosis, *in vivo* and *in vitro*, TβRI was highly over-expressed, thus specific inhibitor of this receptor (SD-208) was able to diminish fibrogenic response (62). Nevertheless, the involvement of TβRII in fibrosis is highly organ and cell-dependant. Thus, disruption of this receptor in tubular epithelial cells and in fibroblasts results in the inhibition of TGF-β/SMAD3 signaling and protects from fibrosis. However, such approach is not able to block ERK/p38 MAP kinase pathway. On the other hand, blocking of TβRII in collecting ducts is rather adverse, leading to enhanced renal fibrosis perhaps due to paracrine TGF-β signaling between epithelial and interstitial cells. Both TβRI and TβRII interact with Hsp90 (heat-shock protein 90kDa) resulting in prevention of TGF-β receptors' degradation. Thus, inhibition of Hsp90 reduces TGF-β signaling and related fibrogenic response, by elevation of SMAD7/Smurf2 dependant ubiqutination of TβRI and TβRII receptors (63-64).

Roles of R-SMADs

Both SMAD2 and SMAD3 are major TGF-β down-stream mediators in renal fibrosis. Several *in vivo* models of Smad3-knockout mice showed significant fibrotic response, and suggested that SMAD3 can be a critical mediator of TGF-β induced renal fibrosis. Furthermore, Hsp-72 suppressed TGF-β induced phosphorylation of SMAD3 and prevented its nuclear translocation leading to inhibition of tubulointerstitial fibrosis in rat model. Moreover, SMAD3 has been also associated with many fibrogenic genes, such as several collagen types, as well as TIMMP-1. Specific SMAD3 inhibitor could block TGF-β induced EMT and attenuate diabetic glomerulosclerosis. However, the role of SMAD2 in renal fibrosis is still controversial, since several studies demonstrated protective role of SMAD2 in fibrogenic response by regulating SMAD3 signaling. TGF-β mediated gene expressions could decrease through BMP-7 activities which block the activation of SMAD-dependant and SMAD-independent pathways (such as ERK and MAPK through SMAD1 and SMAD5 activations). It has been also reported that SMAD2 and SMAD3 can be activated independently of TGF-β signaling, such as direct and angiotensin dependant MAPK-SMAD crosstalk. Moreover, SMAD3 plays an adverse role even in acute kidney injury enhancing TGF-β mediated tubular cell apoptosis by activation of pro-apoptotic genes, such as Bcl-2-associated death promoter (BAD) (58).

Roles of Co-SMAD

SMAD4 is not only important for nuclear translocations of SMAD3, but also plays an important role in the initiation of SMAD3 targeted genes transcription. Blocking of SMAD4 up-regulation results in the reduced accumulation of ECM (58).

Roles of I-SMADs

In animal models, decreased SMAD7 expression potentiates TGF-β signaling paving the way to progressive renal fibrosis, and also increases renal inflammation by activation NF-κB response. Nevertheless, SMAD7 over-expression reduces renal inflammation by suppressing the release of cytokines (IL-1, TNF-α), adhesion molecules (ICAM-1, VCAM-1), macrophages and T cells (58).

Implications for therapies

Suppression of TGF-β1 and its receptors, blockade of SMAD signaling and suppression of its downstream effectors are three global approaches for further perspectives in the treatment of renal fibrosis. Some of the purposed agents are: neutralizing TGF-β antibodies, TβR inhibitors, Hsp90 inhibitors, SMAD3 inhibitors and SMAD7 agonist. Gene therapy is also considered, but far away from the clinical application. Ferulic acid (FA) blocks pSMAD2/3 activation and suppresses TGF-β1induced EMT program (65). It might be that specific inhibition of SMAD3, as well as stimulation of SMAD7 activities would provide improvements in targeting fibrotic and inflammatory tissue responses in the various kidney diseases. Furthermore, SMAD7 might be also suitable for treatment of acute kidney injury since it can prevent tubular cell apoptosis. However, further studies are warranted to make more conclusive information.

Moreover, several studies showed protective effects of these therapeutic strategies on the podocytes which are mainly affected in kidney diseases with proteinuria. It has been suggested that these therapies can even reduce deposition of immune complexes, reverse podocyte injuries and prevent interstitial fibrosis as the last stage of many kidney diseases.

SNAIL

SNAIL is an attractive target for the development of pharmaceutical agents, especially considering that it be induced by numerous factors and signaling involved in EMT. Recently, a Co (III)-DNA conjugate, Co(III)-E-box, has been developed for selective inhibition of Snail family of transcription factors and were considered in oncology research area (66, 67).

1.4.Fibroblast growth factor receptor (FGFR) and neural cell adhesion molecule (NCAM)

1.4.1. NCAM structure

There are two Neural Cell Adhesion Molecules (NCAMs) in mammals (NCAM1 and NCAM2), encoded by two different genes, but here we will focus on NCAM1 because NCAM2 has not been widely studied yet. NCAM1 (simply termed as NCAM), also known as CD56, is a cell surface molecule encoded by a single gene, located on chromosome 11 in humans. NCAM exists in three major isoforms and is also found in soluble secreted form. Three major NCAM isoforms result from alternative splicing and are named according to heir molecular weight: NCAM-120kDa (NCAM-C), NCAM-140kDa (NCAM-B) and 1 NCAM-80kDa (NCAM-A). All of them are cell surface molecules, whereby NCAM120 is attached to the cell membrane via a glycophosphatidyl inositol (GPI-) anchor while NCAM140 and NCAM180 are single spanning transmembrane proteins and differ in the length of their cytoplasmic domains (68-70).

NCAM belongs to the immunoglobulin (Ig) superfamily and is composed of five extracellular Ig domains and two fibronectin type III (FN3) domains and intracellular cytoplasmic part of varying length. NCAM gene contains more than 26 exons. The extracellular part of NCAM is encoded by exons 1–14 (two exons per module) and is similar for the three major isoforms. NCAM180 is defined by additional 16–19exons, while NCAM140 does not include exon 18 compared to NCAM180. The smallest one isoform (NCAM120), beside common exons 1–14 contains only additional exon 15 (68-70).

NCAM molecules can be post-translationally modified either on extracellular or intracellular parts. All three isoforms can be extracellularly modified by attachment of long chains of polysialic acid (PSA) to the fifth Ig module and the first F3 module. Attachment of the negatively charged sugar PSA to the fifth Ig domain influences NCAM adhesive properties, changing it form a pro-adhesive to a pro-migratory molecule. Transmembrane isoforms (NCAM140 and NCAM180) can be also palmitoylated on intracellular domains (C-terminal sites), thereby determining NCAMs association with lipid rafts in the membrane and defining its signaling properties (71-74).

1.4.2. NCAM functions and signaling pathways

During embryonic development, NCAM is heavily polysialilated and is widely expressed in many organs, including kidneys. However, in the adults it is mainly found in tissues of neural origin, but also appears during carcinogenesis. Thus, NCAM is thought be expressed in areas which retain a high degree of plasticity. Since during wound healing and repair many cells change their phenotype in order to recover injury, it has been considered that induction of NCAM expression in such area could appear, especially if in particular organ NCAM is expressed during organogenesis. Thus, re-induction of NCAM in epithelial structures could be considered as reversed organogenesis, through the process of epithelial to mesenchymal transition (EMT) (14, 24-27, 68-74).

NCAM signaling can be induced by homophilic and various heterophilic interactions with other molecules such as fibroblast growth factor receptor (FGFR), heparin, heparan/chondroitin sulfates, various types of collagen, glial cell line derived neurotrophic factor (GDNF), GDNF family receptor a, ATP, platelet-derived growth factor (PDGF), and various cytoskeletal components (24, 69).

NCAM homophilic interactions

Precise mechanism of NCAM homophilic binding is not completely clarified and several alternative models have been proposed. Since extracellular parts of all three NCAM isoforms have Ig-like domains, NCAM's homophilic binding mechanisms involve binding between multiple NCAM modules in various configurations (24-27, 68-74).

Rao et al. suggested that third Ig module of NCAM was important for the NCAM *trans*-homophilic binding in the model where the third Ig module binds to itself. They also found that the first three modules and can bind to each other, meaning that the third Ig domain binds to itself while the second binds to fourth and the first binds to fifth Ig domain (75, 76). However, one of the most sensitive methods currently available– NMR and surface plasmon resonance (SPR) analysis could not detected proposed interactions.

Using SPR, NMR and crystallography experiments, binding between the first and second Ig modules of NCAM was detected and the importance of the third Ig module for the homophilic

binding was also demonstrated. Soroka et al. discovered NCAM/NCAM interactions combining the first three Ig modules. Specific interactions between Ig1 and Ig2 modules mediate dimerization of NCAM molecules expressed on the same cell surface (*cis*-interactions), whereas interactions between NCAM molecules on the surfaces of opposing cells (*trans*-interactions) are mediated by Ig3 domain and its simultaneously binding to Ig1 and Ig2 (69, 77).

Signaling cascade stimulated during these homophilic interactions includes NCAM association with $p59^{Fyn}$ (Src family kinase) and its subsequent phosphorylation which in turns phosphorylates and activates its effector FAK. Activated FAK then acts by inducing CREB (c-AMP response element binding protein), through Ras/Raf/MAPK/ERK up-stream effectors (78-80). However, this specific intracellular signaling transduction is attributed only to NCAM-140 isoform and does not engage NCAM-180 (79).

This type of signaling cascade promotes adhesion properties of NCAM-expressing cells. However, de-adhesion processes can also appear during these NCAM homophilic bindings and they are primarily stimulated by post-translational modifications of NCAM molecule by polysialic acid (PSA) residues which then interferes with NCAM homophilic interactions (81-82).

NCAM and FGFR interactions

NCAM is also involved in heterophilic interactions and is able to induce FGFR signaling acting through this pathway. All NCAM isoforms (120kDa, 140 kDa, 180 kDa) are able to bind to all FGFRs (FGFR1-4). The prototypical FGFRs consist of three Ig modules, a transmembrane domain and a cytoplasmic tyrosine kinase domain. The Ig1 and Ig2 modules are separated by a very long linker containing a stretch of acidic residues, termed the acid box. FGF binding to the FGFR results in the receptor dimerization, leading to auto-phosphorylation of the receptor tyrosine kinase domains. The FGF-receptor family consing of four closely related receptor tyrosine kinases (FGFR 1–4), can be activated their main ligands - FGFs (FGF1–FGF23), and also by cell adhesion molecules such as NCAM, L1 and N-cadherin. However, a direct binding to the FGFR has only been demonstrated for NCAM. These interactions occur between FN3 NCAM domain and Ig2 and Ig3 FGFR domains, whereby both FN3 modules of NCAM are required for an efficient binding, whilst interaction involving amino acids located in the FG loop

region of the second FN3 module of NCAM and the FGFR1 results in weak binding. Beside an involvement of Ig2 and Ig3 modeule of FGFR in the interaction with NCAM, acid box region of the FGFR is proposed to be also a binding NCAM site but there is no strong evidence of this type of interplay. CHD (Cell adhesion molecule Homology Domain) region located in the second Ig module of the FGFR has been previously suggested to be involved in binding to NCAM, L1 and N-cadherin, however despite structural possibility of interaction at this site it has been indicated CHD is not necessary for the NCAM/FGFR interaction (83; 69). Molecular sites of NCAM/FGFR interactions are illustrated on Figure 3.

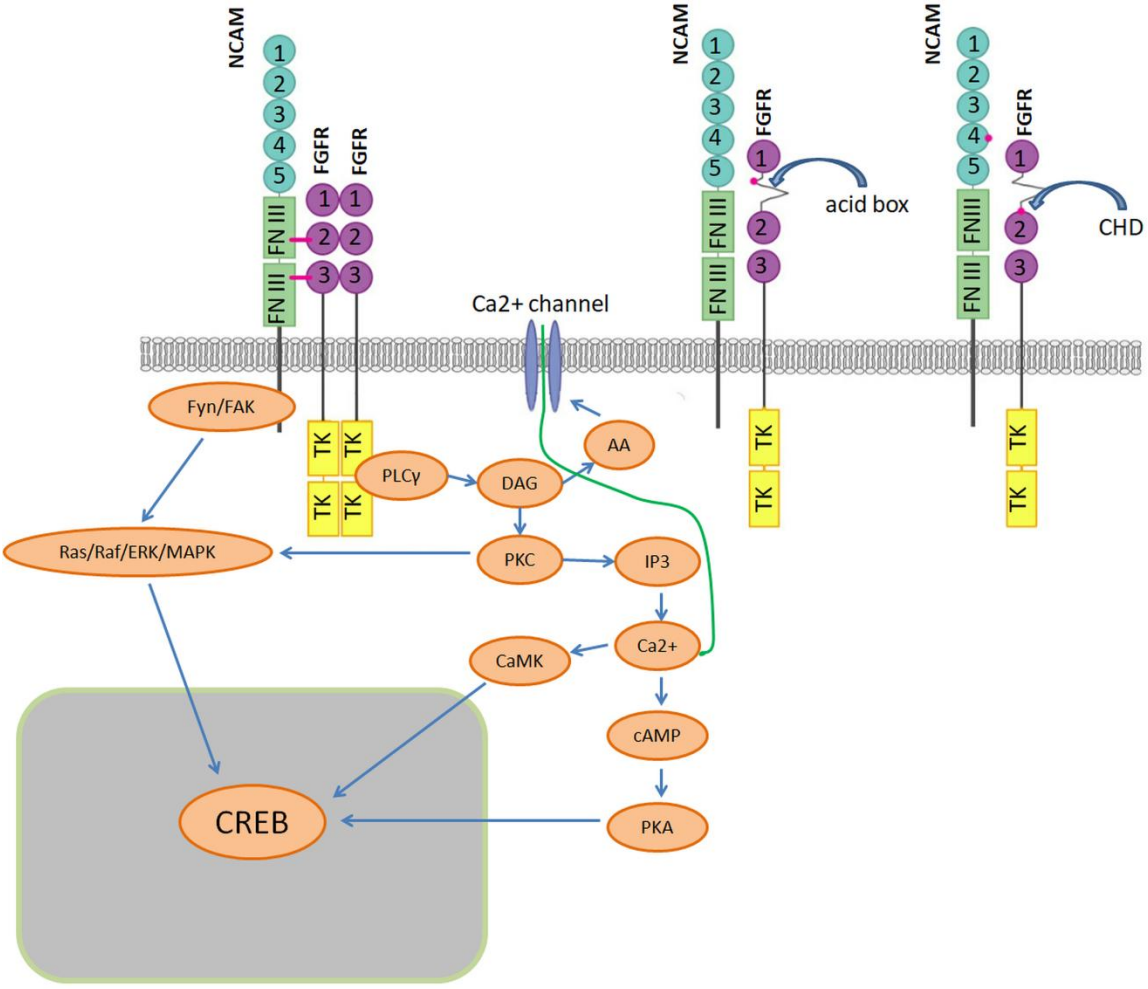

Figure 3. NCAM and FGFR interactions.

After binding to FGFR, NCAM induce its dimerisation and activation through auto-phosphorylation. Activated FGFR then recruits phospholipase Cγ (PLCγ) cleaving its substrate phosphatidylinositol 4,5-bisphosphate (PIP2) and generating the second messenger molecules inositol 1,4,5-trisphosphate (IP3) and diacylglycerol (DAG). IP3 induces the release of Ca^{2+} by binding to intracellular $Ca2^{+}$-channels. DAG remains at the membrane and can either activate protein kinase C (PKC) or can be converted into 2-arachidonylglycerol (2-AG) and arachidonic acid (AA), inducing various downstream signaling events (70, 80).

Cross-talk between NCAM/NCAM and NCAM/FGFR interactions

Moreover, cross talk between two NCAM signaling pathways is also possible. Thus, NCAM homophilic interactions (inducing $p59^{Fyn}$/FAK) and NCAM heterophilic interaction with FGFR can converge at level of ERK activation. Ras-Raf-MAPK-Erk signaling cascade could be induced both by NCAM/NCAM and NCAM/FGFR interactions, making difficult to assign ERK activation to particular pathway involved in its induction, especially under in vivo observation where many extracellular and intracellular ligands and pathways can co-operate at the same time (84).

1.5.Further directions

The growing interest in field of renal fibrosis management is reasonable, especially considering that the majority of kidney diseases could have chronic course and progressively develop impairment of kidney function that is morphologically presented with chronic tubulointerstitial damage and fibrosis. For patients and clinicians it is equally important to mellow-down, stop and reverse the putative adverse outcomes. Thus, a scientific attempts balancing between beneficial and adverse effects of proposed therapies are growing, but often hard to be archived. Further investigation should be focused on therapy options which target the underling mechanism of the earliest changes observed upon kidney injury.

Since normal renal interstitium contains scarce fibroblasts, the origin of abundantly observed fibroblasts during fibrogenesis brings many controversies and several proposed models are available. In addition to rare fibroblasts, scarce NCAM positive cells with spindle shaped or dendritic morphology can be detected within the interstitium of the normal adult human kidney (16, 85). These cells seemed to have arisen from metanephric mesenchymal cells expressing NCAM during kidney development, and selectively persist within the renal interstitium after birth (86). Previously, it has been suspected that in early phases of repairing processes of a damaged kidney interstitial NCAM+ cells could increase (85). The origin of such $NCAM^+$ cells in fibrogenesis or kidney repair and their relation to fetal $NCAM^+$ mesenchymal cells is still unknown and remains to be clarified, as well as their pathophysiological significance.

Considering an early induction of NCAM expression during fibrogenesis and taking into account that its signaling pathway could also involve FGFR activation, we thought that investigation in this field could bring new insights into renal fibrosis pathogenesis, especially considering that human renal interstitium under fibrotic conditions exhibits highly heterogeneity, mostly with regard to molecular markers expressed by interstitial cells (1). Since NCAM is one of the receptors essential during kidney organogenesis (86), we would like to clarify whether the increase of $NCAM^+$ interstitial cell lineage during kidney repair could differ from rare $NCAM^+$ cells situated within normal renal interstitium and if they could share some of the markers involved in tissue wound healing processes, either those which contribute or those which could ameliorate fibrosis.

Moreover, since FGFR1 is involved in fibroblast activation and proliferation and can be activated by different ligands including NCAM, the interplay between these molecules is required to be clarified during fibrogenesis, mostly due to the fact that activation of FGFR1 by NCAM additionally promotes FGFR1 recycling, resulting in sustained FGFR1 signaling that is important for fibroblast migration (24-27).

2. AIMS

The following aims were purposed:

- Explore quantitative relationship between NCAM expressing renal interstitial cells with the degree of renal interstitial fibrosis and underlying pathohistological diagnosis, using human kidney biopsy samples

- Investigate molecular profile (including the presence of proteins and defining the mRNA levels) of NCAM expressing renal interstitial cells with regard to three NCAM isoforms (NCAM-120, NCAM-140, NCAM-180), molecules whith regulatory role in renal fibrosis (FGFR1, HE4, α-SMA, MMP-2, MMP-9, SLUG, SNAIL, BMP 7, ALK 3), as well as molecules involved in TGF-β signaling pathway (SMAD2, SMAD3)

- Compare mRNA expression levels of NCAM, FGFR1, ITGA5, ITGB1, RUNX1 and RUNX1T1 between kidney tissue samples of different degrees of interstitial fibrosis, and also compare it among various pathohistological diagnosis

- Define the involvement of TGF-β in cell migration and explore its impact on molecular profile and dynamics of gene expression changes in TGF-β treated tubular epithelial cells (HK-2 cell line), both in the presence and the absence of FGFR inhibitor (PD173074), comparing with control (non-treated) HK-2 cells; investigate NCAM isoforms (NCAM-120, NCAM-140, NCAM-180), FGFR1 and FGFR2 (their IIIb and IIIc isoforms), SLUG, SNAIL, TWIST 1, MMP-2, MMP-9, RUNX1, RUNX1T1, N-cadherina, E-cadherina, ITGA5, ITGB1, α-SMA, BMP 7, SMAD2 and SMAD3

3. MATERIAL AND METHODS

3.1.Human kidney samples

The study was carried out in accordance with the Code of Ethics of the World Medical Association (Declaration of Helsinki) and was approved by the Ethic Committee of Medical Faculty University of Belgrade (approval no. 29/II-15).

In order to explore quantitative relationship between NCAM expressing renal interstitial cells with the degree of renal interstitial fibrosis and underlying pathohistological diagnosis, as well as to perform further characterization of NCAM expressing cells, 93 biopsy specimens of various kidney diseases were included in this study after routine diagnostic procedures.

Moreover, additional 50 kidney biopsies of patients clinically presented with nephrotic syndrome or isolated proteinuria were analyzed in order to investigate clinicopathological features comparing them with the presence and expression pattern of TGF-β signaling pathway downstream effectors (SMAD3, SMAD2, SNAIL).

For the assessments of gene expression, mRNA was isolated from the rest of frozen tissues of 24 patients. Relative mRNA levels were analyzed according the degree of renal interstitial fibrosis among heterogeneous diagnosis.

Renal tissue from the first core needle biopsy of each patient was formalin-fixed, paraffin-embedded, routinely stained with H&E, PAS, silver methenamine and Masson trichrome, and further used for immunohistochemistry. The second renal biopsy core was put into cell culture medium RPMI 1640 (PAA Laboratories GmbH, Austria) immediately after removal, snap-frozen in liquid nitrogen, used for routine immunofluorescent diagnosis, and the rest of the tissue stored at -80^{o}C for further immunostaining. In the cases where we had enough tissue, a piece of tissue sample was conserved in RNAlater (Qiagen Ltd., Hilden, Germany), a RNA stabilization reagent, for subsequent efficient reverse transcriptase PCR (RT-PCR) analysis. Normal renal tissues were obtained from 10 cadaveric kidneys that were not transplanted, as well as from 10 non-tumor renal tissues obtained after nephrectomies due to renal tumors.

3.1.1. Patients data

Clinical and laboratory patients data recorded at the time of biopsy, as well as at the time of last medical examination were collected from the medical records. Patients were clinically classified in chronic kidney disease (CKD) stages, following the widely accepted recommendations (87). Follow-up period was also noted in order to perform survival analysis aimed to define predictors of disease progression.

3.1.2. Assessment of interstitial renal fibrosis and tubular atrophy

Extension of interstitial renal fibrosis (IRF) was semi-quantitatively assessed on biopsies stained with PAS and Massone-trichrome, applying a scale from 0 to 3 with 0 meaning no IRF, 1 – less than 25% of renal tissue with IRF, 2 - 25% to 50% of renal tissue with IRF, and 3 - more than 50% of renal tissue with IRF. Using the same rule, the abundance of tubular atrophy (TA) was assessed (TA-0 – no tubular atrophy; TA-1 – less than 25% of atrophic tubuli; TA-2 – 25-50% of atrophic tubuli; TA-3 – more than 50% of atrophic tubuli).

3.1.3. Immunohistochemistry

Immunohistochemistry was performed both on paraffin and cryo sections. Tissues embedded in paraffin blocks are previously fixed in 4% formalin and dehydrated in alcohol. Thus, before proceeding to staining procedures, 5 μm kidney tissue sections from paraffin blocks were deparaffinized in xylene and rehydrated through decreasing alcohol percentage series (100%, 96% and 70%) finished with washing step into distillated water. Five μm thick frozen sections cut from each tissue were fixed in acetone for 10 min, air-dried at room temperature for 1 hour. Heat-induced antigen retrieval was performed for 20 min either in low (pH 6.0) or in high pH (pH 9.0) buffers, depending on the antibody. After antigen retrieval both frozen and paraffin samples were incubated for 1 hour at room temperature with primary antibodies listed in Table 3.1.

Table 3.1. List of primary antibodies used for immunohistochemistry in human kidneys.

No.	Primary antibody (clone)	Source	Dilution	Manufacture (Cat. No.)
1	NCAM (Eric-1)	Mouse	1:100	*Ancell Corporation* (208-020)
2	NCAM (123C3.D5)	Mouse	RTU	*LabVision* (MS-204-R7)
3	MMP2	Rabbit	1:50	*Sigma-Aldrich* (HPA001939)
4	MMP9	Rabbit	1:50	*Sigma-Aldrich* (HPA001238)
5	SMAD2 (clone 31H15L4)	Rabbit	1:100	*Thermo scientific* (700048)
6	SMAD3 (clone EP568Y)	Rabbit	1:500	*Abcam* (ab40854)
7	SNAIL	Rabbit	1:100	*Abcam* (ab180714)

NCAM (Eric-1) was used on cryostat samples, while paraffin samples were incubated with NCAM (123C3.D5). The EnVision^{TM} Detection System (Dako) was applied to label anti-mouse or anti-rabbit polymer. Visualization of antigen-antibody reaction was carried out by 3,3'-diaminobenzidine (DAB) or 3-amino-9-ethylcarbazole (AEC) and subsequently counterstaining with hemalaun (Merck, USA). Specimens were mounted with non-aqueous permanent mounting medium (Ultramount, Dako) or with aqueous-based mounting medium (Faramount, Dako). Controls were performed as previously described (85), and for mouse monoclonal antibodies as isotype control mouse IgG1 (ab91353, Abcam, UK) antibody was also used. Slides were evaluated using the light microscope BX53 with DP12 CCD camera (Olympus, Germany).

3.1.3.1. Semi-quantification of NCAM interstitial positivity

Examining the relationship of NCAM expressing interstitial cells with degree of interstitial renal fibrosis (IRF), immunostaining was performed on paraffin sections and evaluated by light microscopy, as a number of positive cells per field of view on the magnification x400 in the region with the most extensive interstitial NCAM positivity in a biopsy core. 20 cases of normal renal tissue were also assessed for the number of NCAM positive cells within the interstitium. All assessments were done independently by two pathologists.

3.1.4. Double immunofluorescence labeling

Five μm-thick cryostat sections were treated as previously described (85). In brief, frozen section were dried for 1h at room temperature, and fixed in acetone for 10 min. Since NCAM (EP2567Y) was produced in rabbit, it was used for double immunofluorescent labeling when the second antibody originated from mouse.

Thus, in order to obtain double fluorescent labeling NCAM/granzyme B, NCAM/αSMA cells and NCAM/MMP9, we applied rabbit monoclonal antibody against NCAM clone EP257Y, followed by Cy3- conjugated goat anti-rabbit antibody (1:2000, Dianova), and mouse monoclonal antibodies against granzyme B, αSMA or MMP9 were added followed by goat anti-mouse IgG-Alexa 488 (1:1000, Invitrogen). For NCAM/HE4 and NCAM/EPO cells detection, mouse monoclonal NCAM/Eric-1 antibody followed by goat anti-mouse IgG-Alexa 488, and rabbit polyclonal HE4 antibody, as well as rabbit polyclonal anti-EPO, followed by Cy3-conjugated goat anti-rabbit antibody were applied. Nuclei were identified by 4,6-diamino-2-phenylindolyl-dihydrochloride (DAPI; 1 μg/ml). List of primary antibodies with corresponding dilutions is shown in Table 3.2.

Table 3.2. List of primary antibodies used for immunofluorescence in human kidneys.

No.	Primary antibody (clone)	Source	Dilution	Manufacture (Cat. No.)
1	NCAM (Eric-1)	Mouse	1:100	*Ancell Corporation* (208-020)
2	NCAM (EP2567Y)	Rabbit	1:200	*Epitomics* (2433-1)
4	MMP9	Mouse	1:100	*Calbiochem*
6	MMP24	Rabbit	1:100	*Calbiochem*
9	α-SMA (1A4)	Mouse	1:400	*Dako*
10	Granzyme B (2C5)	Mouse	1:50	*Santa Cruz* (sc-8022)
11	EPO	Rabbit	1:100	*Abcam* (ab126876)
12	HE4	Rabbit	1:100	*Abcam* (ab85179)
13	CD73	Mouse	1:50	*Abcam* (ab81720)

For assessment of TGF-β signaling and relation to molecules involved in EMT or fibrosis, the following stainings were performed: pSMAD2/MMP2, pSMAD3/MMP9, SNAIL/α-SMA, TWIST/N-cadherin. Antibodies dilutions and detail are shown in Table 3.3.

Table 3.3. List of primary and secondary antibodies used for immunofluorescence in human kidneys.

Primary antibodies	**Source**	**Dilution**	**Manufacturer**
P-Smad3 (9520S)	rabbit	1:100	*Cell Signaling*
p-Smad2 (3108S)	rabbit	1:100	*Cell Signaling*
MMP-2 (sc-13594)	mouse	1:50	*Santa Cruz*
MMP-9 (sc-393859)	mouse	1:50	*Santa Cruz*
Twist1 (ABD29)	rabbit	1:100	*EMD Millipore*
SNAIL (ab180714)	rabbit	1:100	*Abcam*
Alpha-SMA (A5228)	mouse	1:100	*Sigma*
N-Cadherin (610920)	mouse	1:50	*BD Transduction Laboratory*
HIF-1α (hydroxy P402) (ab72775)	rabbit	1:50	*Abcam*
HIF-2α (ab109616)	rabbit	1:100	*Abcam*
Secondary antibodies			
Anti-mouse IgG (H+L), Alexa Fluor 594 (A21203)	donkey	1:200	*Life technologies*
Anti-rabbit IgG (H+L), Alexa Fluor 488 (A21206)	donkey	1:200	*Life technologies*

Controls were performed in all experiments as previously described (85). Sections were mounted with Fluoro Preserve Reagent (Calboichem, Germany). Slides were analyzed either on LSM 510 Confocal Microscope with Apotome (Carl Zeiss, Germany) using the AxioVision Release 4.8.2 (Carl Zeiss, Germany) software version for analysis and documentation, or on epifluorescence microscopy with F-View CCD camera (Olympus, Germany), whereby digital pictures of each fluorescence channel were taken and superimposed for the specific antibody staining using the software AnalySIS from Soft Imaging Systems (Olympus) as previously published (85).

3.1.5. Laser capture microdissection, RNA isolation and quantitative real-time reverse transcription PCR

Frozen renal tissues obtained from normal kidneys and from biopsies with incipient IRF were stained with NCAM/Eric-1 antibody. Only $NCAM^+$ cells localized within renal interstitum exhibiting dendritic morphology were marked for catapulting in laser capture microdissection (LCM) procedure. Between 35 and 50 $NCAM^+$ cells were captured from each sample using PALM MicroBeam (Zeiss, Germany) and afterward stored on -80°C in microtubes with 100µl RNAlater reagent until further analysis.

RNA isolation was carried out using Arcturus® PicoPure® RNA isolation kit (Applied Biosystems, Germany), suitable for high quality RNA extraction from small samples.

The quality of the isolated RNA was assessed using NanoDrop 2000 spectrophotometer (Thermo Scientific, Germany). 50 ng of total RNA was digested with DNaseI (Sigma) and used for cDNA synthesis using SuperScript II Reverse Transcriptase (Life Technologies). For quantitative real-time reverse transcription PCR (qRT-PCR) analysis, diluted cDNA (1/10) was used as a template in a Fast SYBR Green Master Mix (Life Technologies, Germany) and run in StepOnePlus™ Real-Time PCR System (Applied Biosystems) in a total reaction volume of 20 µL. Primers were designed and purchased from PrimerDesign. Primer sequences are shown in Table 3.4. Samples were run in triplicates and the mRNA expression levels were quantitatively analyzed and normalized to the level of glyceraldehyde 3-phosphate dehydrogenase (GAPDH) housekeeping gene. Before decision to use GAPDH as housekeeping gene in qRT-PCR procedure, we also tested 18s and β-actin. As signals for GAPDH were the most consistent within the analyzed samples we used it further analyses in qRT-PCR. GAPDH primers are also provided by PrimerDesign, but the sequences are undisclosed.

Table 3.4. Primer sequences used for qRT-PCR procedures.

	Forward primer 5' to3'	Reverse primer 5' to3'
NCAM-120	GAACCTGATCAAGCAGGATGACGG	CTAACAGAGCAAAAGAAGAGTC
NCAM-140	GTCCTGCTCCTGGTGGTTGTG	CCTTCTCGGGCTCCGTCAGT
NCAM-180	CGAGGCTGCCTCCGTCAGCACC	CCGGATCCATCATGCTTTGCTCTC
FGFR1	GGCTACAAGGTCCGTTATGCC	GATGCTGCCGTACTCATTCTC
FGFR1 IIIb	AATGTGACAGAGGCCCAGAG	GGAGTCAGCAGACACTGT
FGFR1 IIIc	ACTGCTGGAGTTAATACCAC	GGAGTCAGCAGACACTGT
FGFR2	GCGTTTTCCTTGCAGCGGCTGG	GTAAGTCACAGGATTCCCGTC
FGFR2 IIIb	CACTCGGGGATAAATAGTT	ACTCGGAGACCCCTGCCA
FGFR2 IIIc	CGGTGTTAACACCACGGAC	ACTCGGAGACCCCTGCCA
WFDC2 (HE4)	AGAACTGCACGCAAGAGTG	TTGAGGTTGTCGGCGCATT
α-SMA	AAGCACAGAGCAAAAGAGGAAT	ATGTCGTCCCAGTTGGTGAT
FSP-1	TCTTTCTTGGTTTGATCCTG	GCATCAAGCACGTGTCTGAA
SLUG	ACTCCGAAGCCAAATGACAA	CTCTCTCTGTGGGTGTGTGT
SNAIL	GGCAATTTAACAATGTCTGAAAAGG	GAATAGTTCTGGGAGACACATCG
TWIST	CTCAAGAGGTCGTGCCAATC	CCCAGTATTTTTATTTCTAAAGGTGTT
MMP2	TACAGGATCATTGGCTACACACC	GGTCACATCGCTCCAGACT
MMP9	TGTACCGCTATGGTTACACTCG	GGCAGGGACAGTTGCTTCT
ALK3	GGACATTGCTTTGCCATCATAG	GGGCTTTTGGAGAATCTTTGC
BMP7	CCTCCATTGCTCGCCTTG	TATGCTGCTCATGTTTCCTAATAC
ITGA5	GGCTTCAACTTAGACGCGGAG	TGGCTGGTATTAGCCTTGGGT
ITGB1	GTAACCAACCGTAGCAAAGGA	TCCCCTGATCTTAATCGCAAAAC
E-cadh	CATGAGTGTCCCCCGGTATC	CAGTATCAGCCGCTTTCAGA
N-cadh	TCAGGCGTCTGTAGAGGCTT	ATGCACATCCTTCGATAAGACTG
RUNX1	TGAGCTGAGAAATGCTACCGC	ACTTCGACCGACAAACCTGAG
RUNX1T1	ATGCCAGACTCACCTGTGGAT	GGCTGTAGGAGAATGGCTCG
PRMT1	ACAAAGACTACAAGATCCACTGGTG	CGGTATAGATGTCCACCTCCTTTATG

3.2.Cell culture (HK-2 cells)

3.2.1. Experimental procedure

Human proximal tubular epithelial cells (HK-2 cell line) were cultured in 6-well plates in 2ml of growing medium (DMEM medium supplemented with 10% FCS and 1% penicillin/streptomycin) at 37°C in 5% CO_2 air. They were seeded in the concentration of 4×10^4/ml of medium. Next day, growing medium was removed and serum-free DMEM was added. Experimental procedures started on the third day (24h after starvation) and completely were conducted under serum-free conditions. HK-2 cells were seeded in 4 wells divided in control, TGF-β1, PD173074, and TGF-β1+PD173074 treated groups. HK-2 cells were treated with 100nM PD173074 (Santa Cruise, CAS 219580-11-7) and stimulated with recombinant human TGF-β1 (R&D Systems) in the concentration of 10ng/ml. Treatment with PD173074 was done 1h prior to TGF-β1 stimulation. Cells were monitored by light microscopy at different time point, depending on the further experimental procedures.

3.2.2. Scratch assay

In order to estimate cell migration capacity in 4 experimental groups, we made scratches in the wells (in 6-well plate) using 1000µl pipette tips. Scratch was done immediately prior to TGF-β1 stimulation. Distance between cells separated with the scratch was measured under the microscope, using Olympus XM10 camera and cellSence software (under the 10x magnification), at three distinct points which were labeled in order to repeat measurements at the same points later. Measurements were repeated 24, 48 and 72 hours after TGF-β1 application.

3.2.3. RNA isolation and real-time RT-PCR analysis

Cells were detached using trypsin and after washing with PBS they were centrifuged. Cell pellet was used for RNA isolation which was carried out using TRIzol reagent (Invitrogen) and PureLink® RNA Mini Kit (Life Technologies) following manufacturer instructions. The quality of the isolated RNA was assessed using NanoDrop 2000 spectrophotometer (Thermo Scientific). 100 ng of total RNA, digested with DNaseI (Sigma), was used for cDNA synthesis using SuperScript II Reverse Transcriptase (Life Technologies). For quantitative real-time reverse transcription PCR (qRT-PCR) analysis, diluted cDNA (1/10) was used as a template in a Fast

SYBR Green Master Mix (Life Technologies) and run in StepOnePlus™ Real-Time PCR System (Applied Biosystems) in a total reaction volume of 20 μL. Primer sequences are shown in Table 3.4. Samples were run in triplicates and the mRNA expression levels were quantitatively analyzed and normalized to the level of glyceraldehyde 3-phosphate dehydrogenase (GAPDH) housekeeping gene. GAPDH primers are provided by PrimerDesign, but the sequences are undisclosed. RNA isolation and qRT-PCR were done, depending on the genes of interest, at several time points: 6, 12, 24, 48 and 72 hours after TGF-β1 stimulation.

3.2.4. Double immunofluorescence

On the first day, 10^4 HK-2 cells resuspended in 500μL of growing medium were seeded in 8 well culture slides (Falcon® 8 Well culture slide, glass slide with polystyrene vessel, Product #354118). Next day starvation was performed by removing the growing medium and changing into serum-free DMEM. On the third day experiment started, as described. After finishing the experimental procedures, immunofluorescent staining was performed as follows. Medium was removed from the chamber slides and slides were briefly washed with PBS. Then, -20°C pre-cold 100% methanol was added in each well and culture slides were put on -20°C for 20min. When removed from -20°C, methanol was discarded and slides were washed briefly with PBS, preparing the slides for permeabilization step which was performed with 0.2% Triton X-100 in PBS for 15min at RT°. After 2 times washing with PBS, blocking with 5% BSA dissolved in 0.1% Tween 20 in PBS was performed for 1h at RT°. Next, slides were washed with PBS and afterwards incubated with primary antibodies overnight on 4°C (two primary antibodies of different sources, i.e. one rabbit and one mouse or goat). Antibodies were diluted in 1% BSA dissolved in 0.1% Tween 20 in PBS and details are summarized in the Table 3.5. The second day of immunofluorescent staining started with washing step (3x5min with 0.1% Tween 20 in PBS on shaking plate) followed by application of secondary antibodies for 1h at RT°. Afterwards slides were washed 2 times for 5 min with 0.1% Tween 20 in PBS on shaking plate and prepared for incubation with DAPI (1:1000 diluted in pure PBS) on RT° for 5min. Chambers were removed and slides were finally washed with PBS for 15 min on shaking plate and covered using Immu-Mount (Thermo Scientific, #9990412) medium.

Table 3.5. List of primary and secondary antibodies used for cell culture double immunofluorescent staining.

Primary antibodies	**Manufacturer**	**Source**	**Dilution**
P-Smad3 (9520S)	Cell Signaling	rabbit	1:100
p-Smad2 (3108S)	Cell Signaling	rabbit	1:100
Ki-67 (9449S)	Cell Signaling	mouse	1:200
Twist1 (ABD29)	EMD Millipore	rabbit	1:100
SNAIL (ab180714)	Abcam	rabbit	1:100
Alpha-SMA (A5228)	Sigma	mouse	1:100
Vimentin (AB1620)	EMD Millipore	goat	1:20
N-Cadherin (610920)	BD Transduction Laboratory	mouse	1:50
Secondary antibodies			
Anti-mouse IgG (H+L), Alexa Fluor 594 (A21203)	Life technologies	donkey	1:200
Anti-rabbit IgG (H+L), Alexa Fluor 488 (A21206)	Life technologies	donkey	1:200
Anti-goat IgG (H+L), Alexa Fluor 488 (A11055)	Life technologies	donkey	1:200

3.3.Statistical analysis

Statistical analysis was performed using the IBM SPSS software, version 20.0. Each numerical variable was tested for normality of distribution, using Shapiro–Wilk and Kolmogorov–Smirnov tests, as well as considering skewness and kurtosis before the decision of implementation parametric or nonparametric statistical tests. For the assessments numerical data differences between two groups, Student t-test or Mann-Whitney U were applied depending on the normality of data distribution. ANOVA was used for the assessment of numerical data among more than two groups, only if Levene's test of homogeneity of variances allowed it ($p>0.050$), otherwise Kruskall-Wallis test, followed by Mann-Whitney U were applied. Correlations between numerical variables are analyzed by Pearson's (if data followed normal distribution) or Spearman's correlation (if data did not follow normal distribution). Nominal/ordinal data are analyzed by $\chi 2$ test or Fisher exact test or by Kruskall-Wallis test, followed by Mann-Whitney U, depending on the number of groups. Univariate analysis was performed using the Kaplan–Meier estimator in order to identify variables significantly associated with adverse outcome. Differences between two groups of patients (with and without adverse outcome) were assessed by two-sided log rank test. In univariate analysis, potential predictors of kidney dysfunction development were identified using a significance value of $p<0.05$. *P* values <0.05 were also considered to be significant in other applied statistical tests.

4. RESULTS

4.1.NCAM expressing renal interstitial cells and renal fibrosis

Renal interstitial NCAM$^+$ cells were rarely present in the tubulointerstitial compartments of normal human kidneys, used as a control group (Fig. 4.1.1). However, in 93 paraffin-embedded biopsy specimens with various degrees of interstitial fibrosis, NCAM$^+$ interstitial cells were seen in 58 cases (62.4%). NCAM$^+$ interstitial cells were detected in 100% of MesPGN, 76.0% of LN, 69.2% of MGN, 62.5% of MPGN, 61.1% of FSGS, 50% of IgA nephropathy, 33.3% of renal grafts, 25% of RPGN, while NCAM$^+$ interstitial cells were not detected in 4 cases of minimal change disease (Fig. 4.1.1).

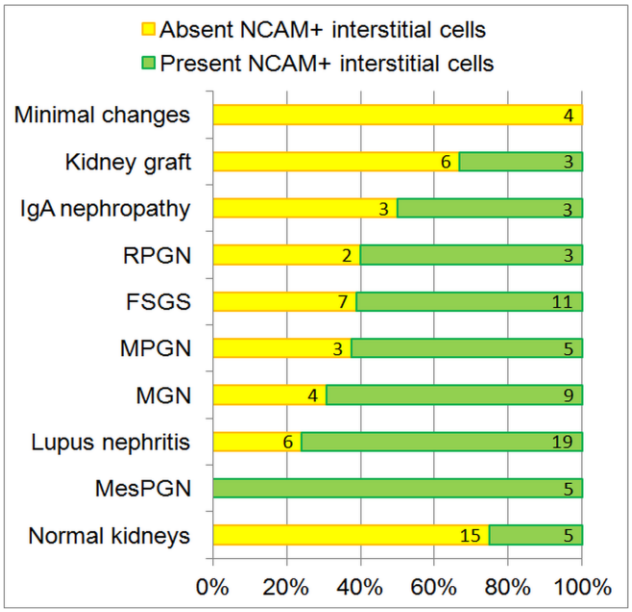

Figure 4.1.1. Frequency of interstitial NCAM positivity among various kidney diseases and in control normal kidneys.

Mean number of NCAM$^+$ cells were significantly higher in diseased kidneys (mean 2.45 NCAM$^+$ cells, 95% CI (1.83-3.07)) compared to controls (mean 0.25 NCAM$^+$ cells, 95% CI (0.4-0.46)), t=6.731; p<0.001.

A statistically significant increase of NCAM$^+$ interstitial cells was present in incipient IRF, assessed as scale 1, compared to all others scales of fibrosis independently of the pathohistological diagnosis, as it is presented on Fig. 4.1.2.

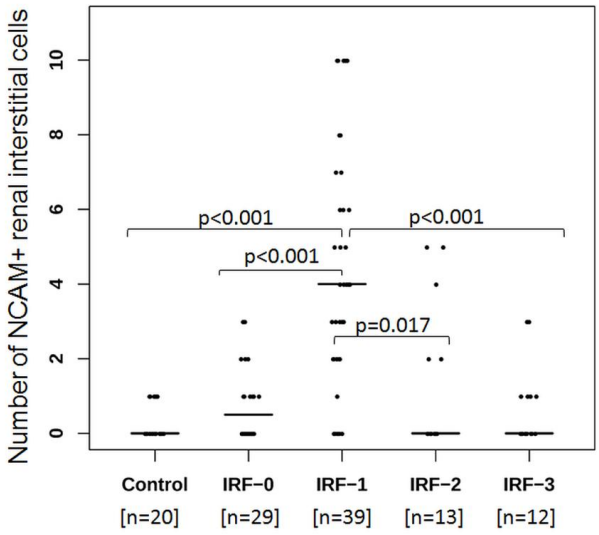

Figure 4.1.2. NCAM and severity of renal fibrosis. Number of detected NCAM$^+$ cells per field of view on ×400 magnification in controls and in diseased kidneys with regard to severity of interstitial renal fibrosis (IRF); p values after applying Mann-Whiteny U test.

Relationship between number of NCAM$^+$ cells and underlying kidney diseases classified according to IRF stages was further analyzed (Table 4.1.1.), however, there were no significant differences. These data support our previous findings that increase of interstitial NCAM$^+$ was independent of diagnosis, but depends only on extent of interstitial fibrosis, appearing almost exclusively in early stages (IRF-1), as illustrated in Fig.4.1.2.

Table 4.1.1. Distribution of diagnosis and neural cell adhesion molecule (NCAM) interstitial positivity (including the number of NCAM positive interstitial cells presented with mean ±SD) observed among stages of interstitial renal fibrosis (IRF).

Diagnosis	IRF-0		IRF-1		IRF-2		IRF-3	
	Total N (NCAM+ cases)	mean*±SD	Total N (NCAM+ cases)	mean*±SD	Total N (NCAM+ cases)	mean*±SD	Total N (NCAM+ cases)	mean*±SD
FSGS	6 (3/6)	0.8±1.2	11 (8/11)	3.6±3.6	1 (0/1)	0.0±NA	-	-
Kidney graft	-	-	3 (2/3)	3.0±3.0	1 (1/1)	2.0±NA	5 (0/5)	0.0±0.0
MGN	7 (4/7)	1.0±1.2	4 (4/4)	6.5±4.4	-	-	2 (1/2)	1.5±2.1
Lupus nephritis	5 (2/5)	0.6±0.9	13 (12/13)	5.3±3.3	6 (4/6)	3.5±3.8	1 (1/1)	1.0±NA
MesPGN	1 (1/1)	2.0±NA	4 (4/4)	3.8±1.7	-	-	-	-
MPGN	2 (1/2)	0.5±0.71	3 (3/3)	3.7±2.1	3 (1/3)	1.7±2.9	-	-
Minimal changes	4 (0/4)	0.0±0.0	-	-	-	-	-	-
IgA nephropathy	4 (2/4)	0.5±0.6	1 (1/1)	4.0±NA	1 (0/1)	0.0±NA	-	-
RPGN	-	-	-	-	1 (0/1)	0.0±NA	4 (3/4)	0.8±0.5
Statistical analysis	-	$p=0.527^{\#}$	-	$p=0.657^{\#}$	-	$p=0.831^{\#}$	-	$p=0.137^{\#\#}$

N- number of cases; *- mean number of NCAM+ cells per field of view x400; NA- not applicable; #- ANOVA test was applied; ##- Kruskall-Wallis test was applied because Levene's test of homogeneity of variances was <0.050 and consequently ANOVA could not be used.

Fig. 4.1.3., panel A illustrates routine PAS staining with diffuse incipient renal fibrosis (IRF-1) of patient with FSGS. Applying immunohistochemical staining, within the same area many peritubular $NCAM^+$ cells were detected in the interstitial compartment (panel B).

However, $NCAM^+$ interstitial cells were usually detected focally around tubuli in the area with slight IRF (IRF-1), as it is shown in Fig. 4.1.4. A-C.

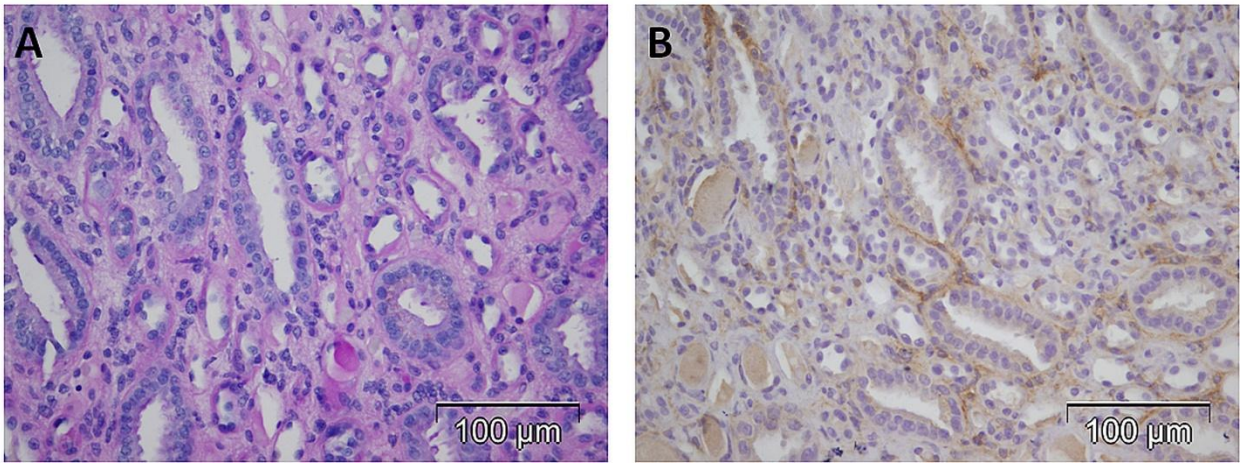

Figure 4.1.3. Morphology of interstitial fibrosis and NCAM interstitial positivity. FSGS with slight interstitial fibrosis (IRF-1) without tubular atrophy exhibiting an increased diffuse NCAM interstitial positivity detected on slides from paraffin-embedded tissue. (A) PAS, x400. (B) Immunoperoxidase staining, NCAM clone 123C3.D5, x400.

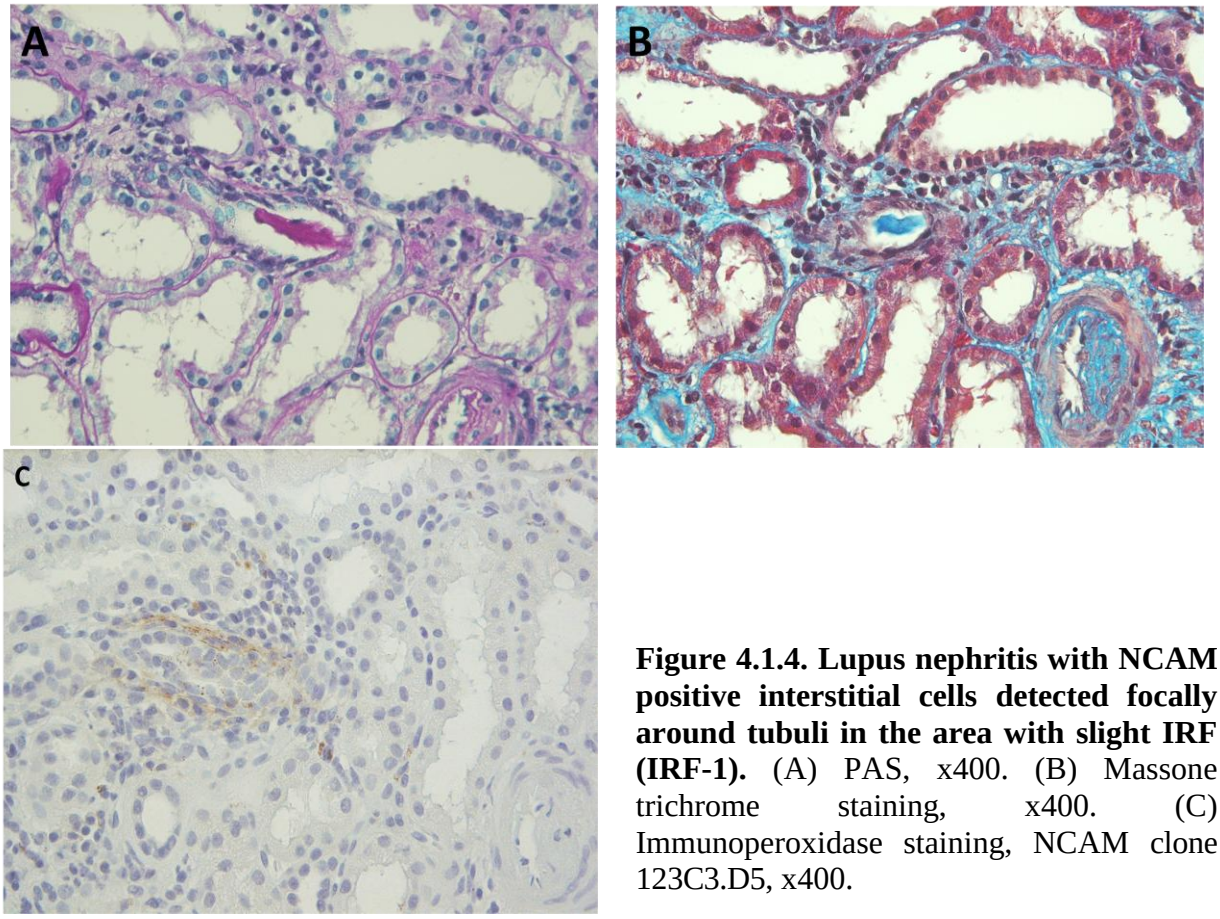

Figure 4.1.4. Lupus nephritis with NCAM positive interstitial cells detected focally around tubuli in the area with slight IRF (IRF-1). (A) PAS, x400. (B) Massone trichrome staining, x400. (C) Immunoperoxidase staining, NCAM clone 123C3.D5, x400.

4.2.Molecular profile of NCAM expressing renal interstitial cells

Since NCAM expressing renal interstitial cells were detected in early fibrosis, we performed several double immunolabelings aimed to better define molecular characteristics of these cells, especially with regard to their regulatory role in fibrosis.

Previous studies at our Institute reveled some of the markers that NCAM+ interstitial cells could share, such as FGFR1 and α5β1 integrin. These two markers are known to be expressed by fibroblasts. Thus, we further consider an opportunity to see whether these cells could represent a population of activated fibroblasts, so-called myofibroblasts. Beside α-SMA, HE4 expression is newly established characteristic of some myofibroblasts.

Despite widespread interstitial expression of both NCAM and α-SMA in many cases with early fibrosis, the overlapping of these two molecules did not appear albeit sometimes it looked possible. Although both NCAM and α-SMA were localized within the same compartments, they did not expressed by the same cells. Moreover, NCAM+ and α-SMA+ interstitial cells represented two distinct cell populations, as illustrated on Fig. 4.2.1.

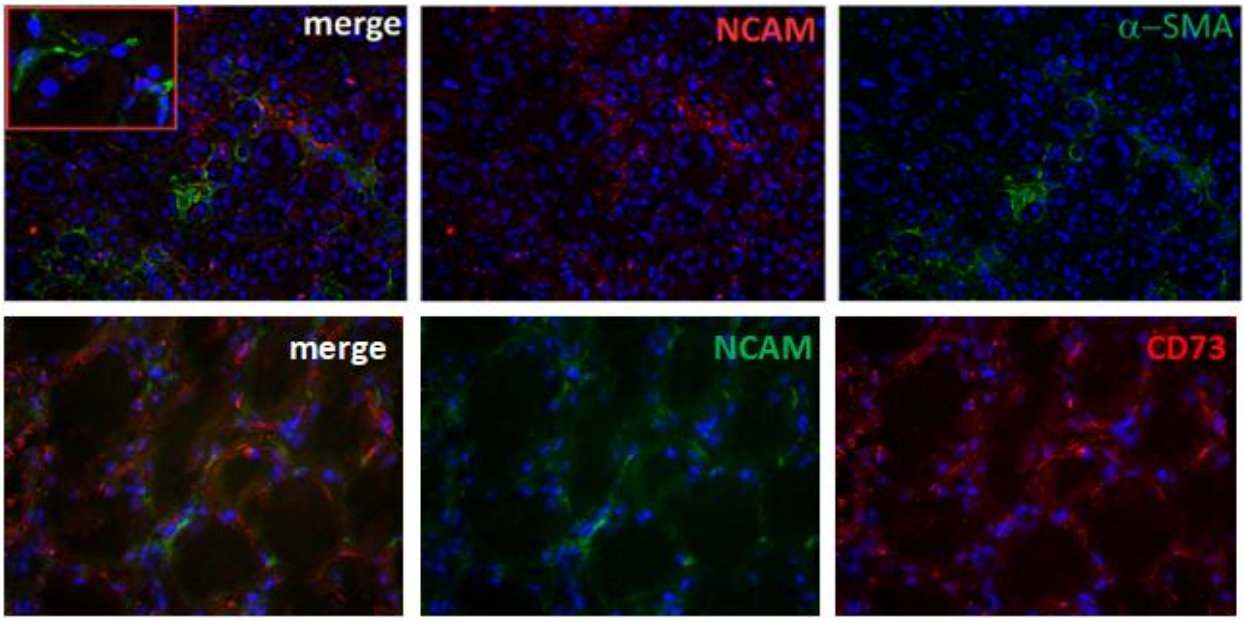

Figure 4.2.1. NCAM and α-SMA double immunolabeling.

CD73 has been previously characterized as marker of some population of renal fibroblasts, including those with EPO producing features. Here we examined if NCAM positive renal

interstitial cells could express CD73, and despite abundant expression of both NCAM and DC73 in the renal interstitial compartment in cases with incipient fibrosis, co-expression was found only in few interstitial cells (Fig. 4.2.1).

HE4 was also expressed by renal interstitial cells. In normal, control kidneys HE+ interstitial cells were rare. It was not surprising, because fibroblasts are consider to be scant in normal interstitium. However, we detected some overlapping between HE4 and NCAM that is also rarely present in normal renal interstitium. Furthermore, in the cases of incipient renal fibrosis, where NCAM+ cells could be prominent, HE4 was more frequently detected in the same cells as NCAM. HE4 and NCAM double immunolabeling is presented on the Fig. 4.2.2.

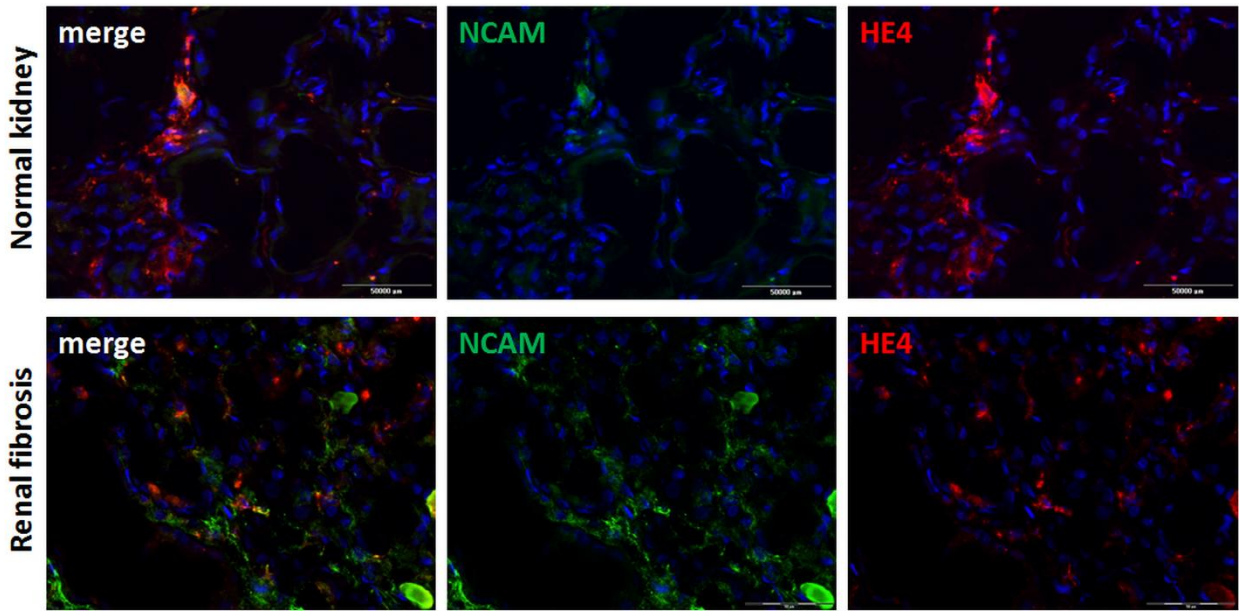

Figure 4.2.2. NCAM and HE4 double immunolabeling.

Modulation of fibrotic tissue response partly depends on the time-dependant activity of various tissue proteases, such as MMPs. Galatinases (MMP2 and MMP9) are the most popular in renal pathology. Their substrate is mainly collagen type IV, thus, their enhanced activity is noted in tubular epithelium affecting the integrity of basal membrane. Indeed, in this step their activity is considered as undesirable. However, if fibrosis is already initiated, activity of these gelatinases in the interstitial compartment would be useful to protect kidney tissue from the excessive ECM

deposition. Since NCAM+ interstitial cells are present in early fibrosis, we further investigated their relation with MMP2 and MMP9. Interestingly, MMP2 was not detected in the interstitium, but was abundantly expressed in tubuli usually surrounded with fibrosis. Nevertheless, MMP9 was sometimes expressed by glomerular basement membrane components and was rarely found in the interstitium. Sometimes MMP9 was found in interstitium in the NCAM expressing cells, implicating some capacity of NCAM+ cells to degrade ECM in fibrosis. MMP24 was observed diffusely in tubular basement membrane in the cases with increased interstitial NCAM expression, and consequently overlapping of these two molecules was not observed (Fig. 4.2.3).

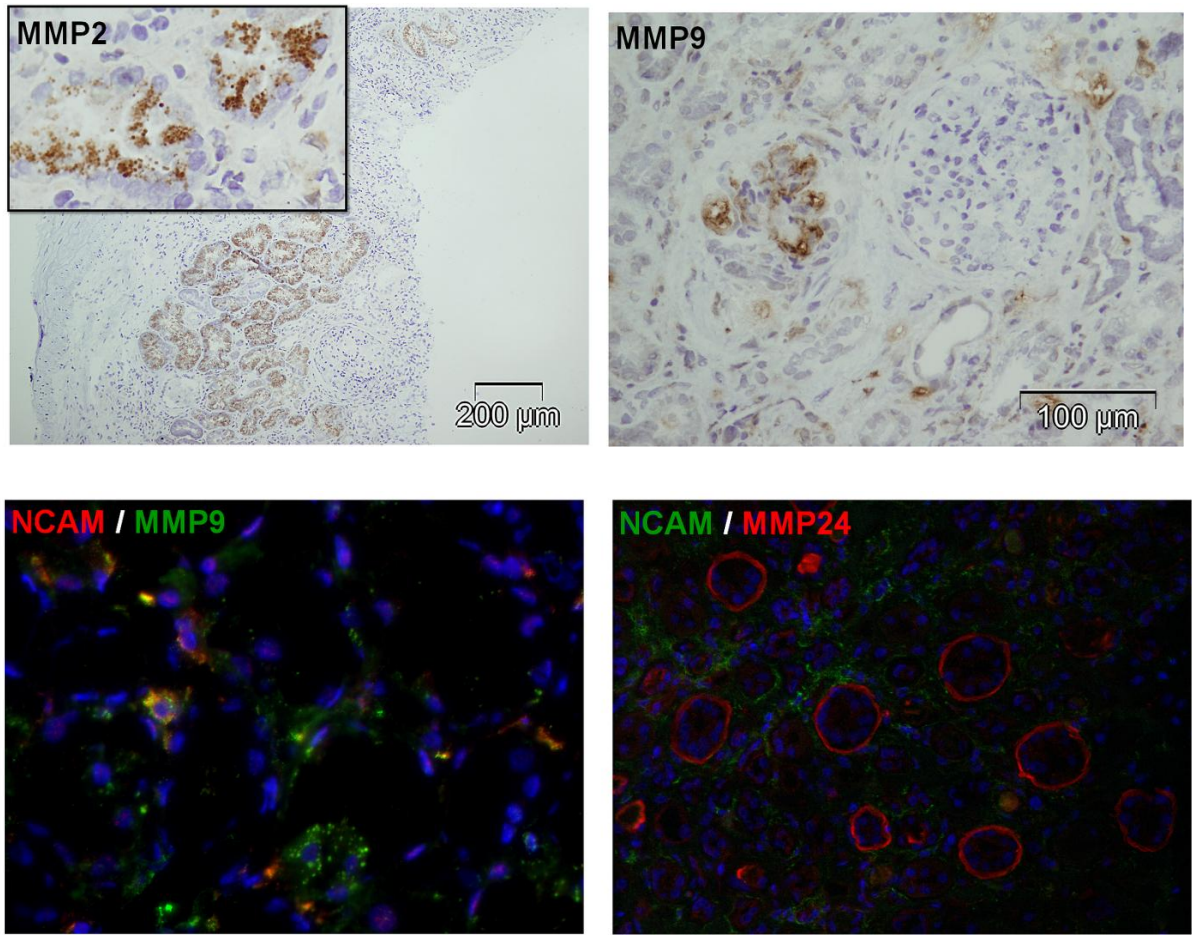

Figure 4.2.3. NCAM, MMP2, MMP9 and MMP24 immunolabeling.

At the beginning of our research, we found that increased interstitial NCAM positivity, appeared in incipient IRF, was independent of the underlying kidney diseases, although we cannot exclude

that increase in number of NCAM$^+$ interstitial cells was caused by hypoxia at least in some cases. In this setting, since erythropoietin (EPO) producing renal fibroblasts are expected to increase rapidly in response to tissue hypoxia [5, 21], double immunofluorescent labeling using EPO and NCAM antibodies was performed. Unfortunately, we were not able to detect any EPO and NCAM overlapping (Figs. 4.2.4. A-C). Since NCAM can be also expressed by natural killer (NK) cells of the innate immune system, double NCAM/granzyme B immunostaining was performed to clarify their relationship in incipient renal fibrosis. In the panel D, an area of diffuse NCAM interstitial staining is visible without any granzyme B positivity. Within the whole biopsy sample of the same case that belongs to FSGS with incipient IRF only a single interstitial cell expressed both NCAM and granzyme B (panel E). Among cases of lupus nephritises, overlapping between these two molecules has not been detected, even within areas of mononuclear interstitial infiltrates (panel F). Thus, there were interstitial NCAM$^+$ cells different from NK cells that were almost exclusively increased in incipient renal fibrosis.

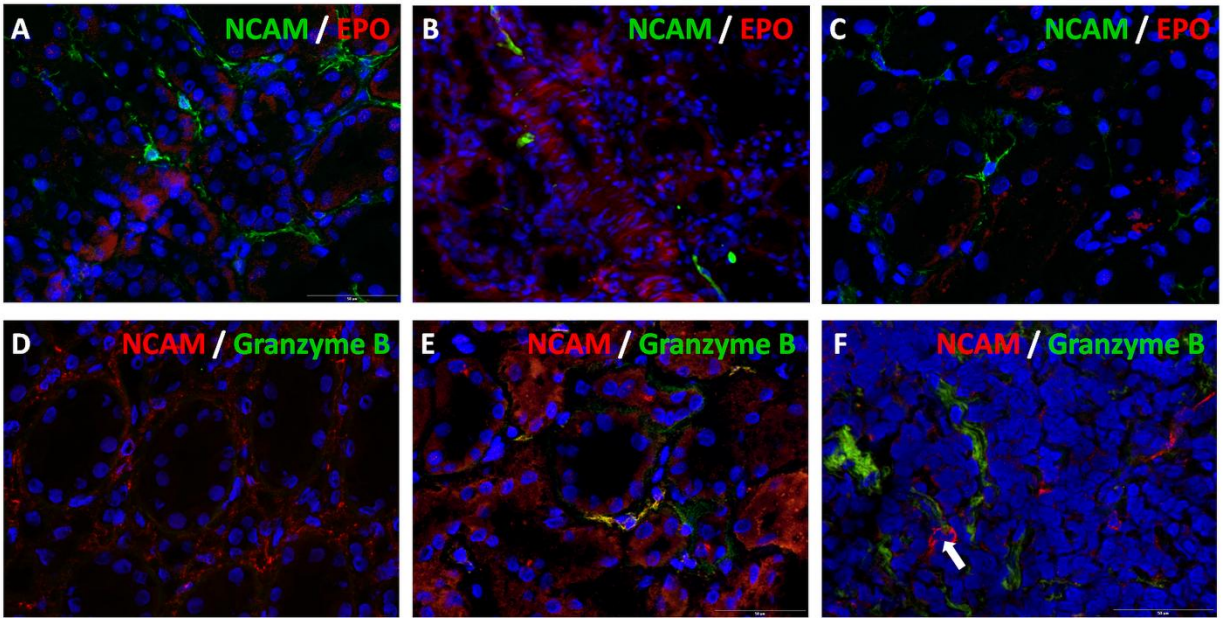

Figure 4.2.4. Double immunofluorescent labeling of NCAM with erythropoietin (EPO) and granzyme B.

Since tissue lysates could contain other NCAM expressing cells, not only the interstitial spindle shaped $NCAM^{+}$ cells which were within the focus of our study, we decided to perform laser capture microdissection (LCM) which allowed us to separate and collect pure cell populations of the relevant $NCAM^{+}$ cells out of tissue samples. Isolated pure $NCAM^{+}$ cell populations were the most suitable starting material for downstream quantitative real-time PCR (qRT-PCR). Fig. 4.2.5. (panels A and B) represents renal tissues stained with anti-NCAM antibody prior to LCM procedure, and illustrate widespread NCAM expression in incipient IRF (panel A) and scarce NCAM positivity in normal renal interstitium (panel B). Panels C-E illustrate tissues after LCM procedure. Statistically significant changes in the relative mRNA expression levels of NCAM isoforms have been revealed after applying qRT-PCR in the pure $NCAM^{+}$ cell population. $NCAM^{+}$ cells captured from incipient IRF significantly up-regulated $NCAM^{140kD}$ isoform compared to $NCAM^{+}$ cells in normal kidneys, p=0.004 (panel F). Nevertheless, mRNA expression levels of $NCAM^{120kD}$ and $NCAM^{180kD}$ isoforms were not changed significantly in comparison to normal kidneys (p=0.750; p=0.704; respectively), although both $NCAM^{120kD}$ and $NCAM^{180kD}$ were slightly up-regulated under fibrotic conditions. These findings implicate a specific NCAM isoform switch during fibrogenesis, thereby suggesting diverse roles of NCAM isoforms in homeostasis and during tissue repair.

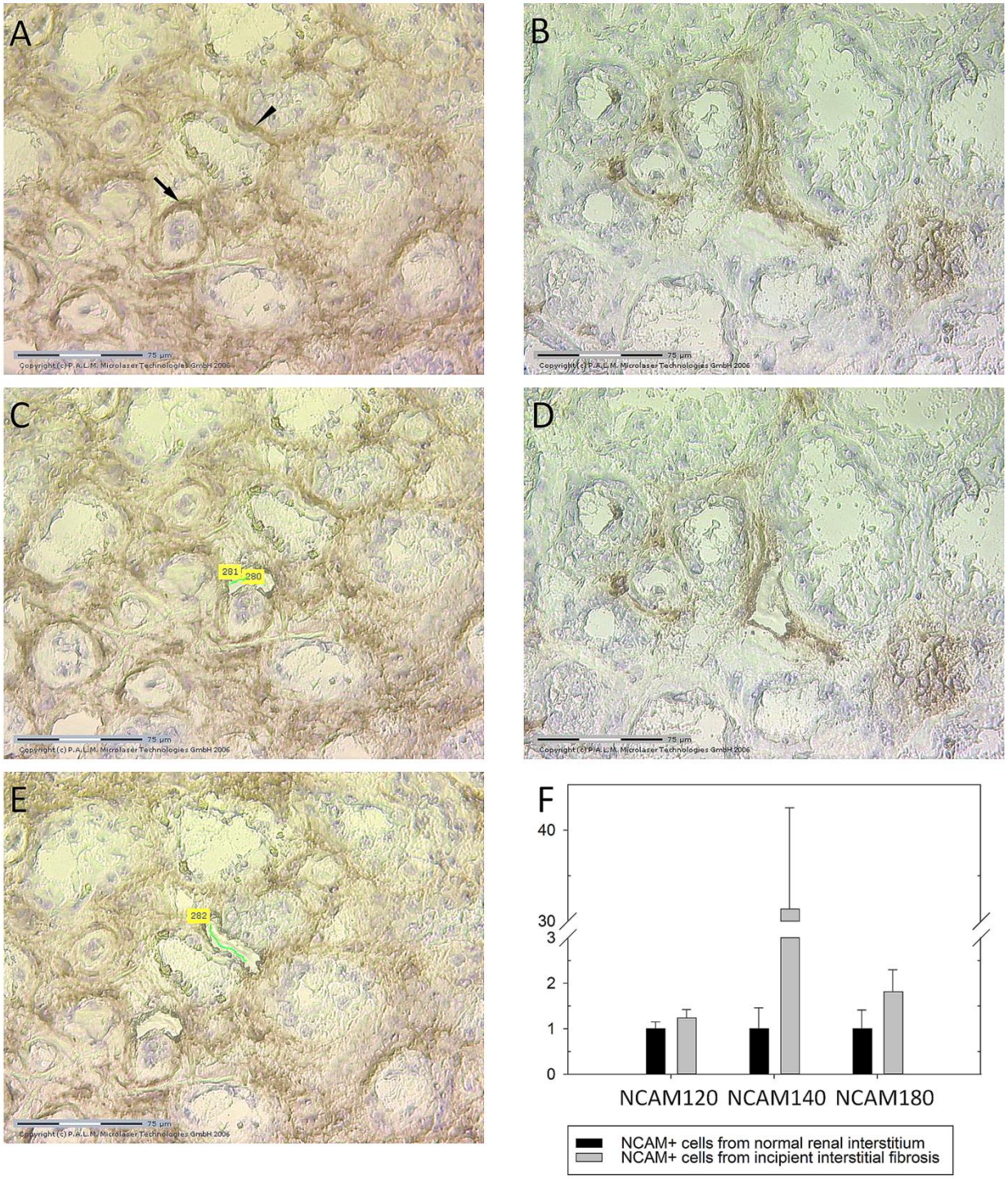

Figure 4.2.5. Isolation of NCAM positive renal interstitial cells by laser capture microdissection (LCM) and changes in relative mRNA NCAM isofroms expression levels in incipient renal fibrosis. (A) Slide performed on cryostat section and stained by NCAM, clone Eric-1, with widespread NCAM expression, prior laser capture microdissection (arrow indicates the first selected NCAM positive cell for further LCM, while arrowhead shows second selected area). **(B)** Slide with rare NCAM cells within normal interstitium prior LCM. **(C), (D)** and **(E)**

the same slides as Fig. (A) and (B) after LCM procedure. **(F)** Relative expression levels of NCAM mRNAs isoforms, determined by quantitative real-time PCR (qRT-PCR), in $NCAM^+$ cells captured by LCM from normal and from renal tissue with incipient IRF, data are presented with mean values and standard error bars; due to high variability of variables, exclusively in diseased kidneys, nonparametric Mann Whitney U test was applied to assess the difference in mRNA levels between controls and diseased kidneys; there were 6 samples (2 cases in triplicates) of control cases and 42 (14 cases in triplicates) samples of cases with incipient renal fibrosis.

4.3.Clinical relevance of NCAM expressing renal interstitial cells

NCAM expressing renal interstitial cells has been detected within 59.4% human kidney biopsy samples, independently of the underling pathohistological diagnosis (p=0.995). However, it has been confirmed that frequency of NCAM positivity was higher in early stage of renal interstitial fibrosis, compared to other stages (Table 4.3.1). There were no significant difference of the distribution of NCAM expressing cases with regard to CKD stage, neither at the time of biopsy (p=0.954) nor at the time of last medical examination (p=0.601), as shown in the Tables 4.3.2 and 4.3.3. However, it has been noticed that patients without NCAM expressing renal interstitial cell had higher serum creatinine values compared to patients with NCAM positivity (Table 4.3.2 and 4.3.3), although it did not reach statistical significance. Nevertheless, proteinuria was lower in patients whose biopsies revealed interstitial NCAM positivity (3.97 g/24h) than in patients without NCAM expressing renal interstitial cells (8.41 g/24h) (p=0.024).

These patients were also followed for 16 months (mean value). Pathohistological and clinical parameters were used in Kaplan-Meier survival analysis in order to define predictors of progression to advanced CKD stages. Among them, pathohistological diagnosis (p=0.026) and the degree of renal interstitial fibrosis (p=0.002) were marked as predictors of adverse outcome. Thus, patients with minimal change disease did not progress to advanced CKD stages, as illustrated on Fig.4.3.1.A. On the same Figure, panel B shows the impact of interstitial fibrosis degree on the CKD progression. Therefore, 90% of patients without fibrosis preserved kidney function during 3 years of follow-up, while patients with fibrosis exhibited deterioration of excretory kidney function with increasing incidence and faster appearance in advanced IRF stages (Fig.4.3.1.B). The presence of NCAM expressing renal interstitial cells (Fig.4.3.1.C) did not affect long-term patients outcome (with regard to CKD stages), p=0.273. Possibility of progression to advanced CKD stages depended on the clinical parameters, such as serum

creatinine (p<0.001) and urea (p=0.007) values. Kidney function was maintaining longer in patients with normal serum creatinine and urea values compared to the patients with elevated aforementioned values (Fig.4.3.1.D and E). Worse outcome was observed slightly faster in patients with proteinuria >3g/day (Fig.4.3.1.F), however without statistical significance (p=0.231).

Table 4.3.1. Distribution of patients with NCAM expressing renal interstitial cells with regard to pathohistological variables.

Pathohistological variables		*NCAM+ renal interstitial cells*		*p* value
		Present	Absent	
Diagnosis	FSGS	5 (38.8%)	8 (61.5%)	0.995
	Kidney graft	5 (71.4%)	2 (28.6%)	
	MGN	4 (33.3%)	8 (66.7%)	
	LN	5 (31.2%)	11 (68.8%)	
	MesPGN	0 (0.0%)	4 (100.0%)	
	MPGN	2 (33.3%)	4 (66.7%)	
	MCD	3 (100.0%)	0 (0.0%)	
	IgA nephropathy	2 (66.7%)	1 (33.3%)	
	RPGN	2 (40.0%)	3 (60.0)	
Stage of interstitial renal fibrosis (IRF)	*IRF* - 0	14 (70.0%)	6 (30.0%)	0.001*
	IRF - 1	4 (13.8%)	25 (86.2%)	
	IRF - 2	4 (44.4%)	5 (55.6%)	
	IRF - 3	6 (54.5%)	5 (45.5%)	

Table 4.3.2. Clinical and laboratory parameters recorded at the time of biopsy in patients with and without NCAM expressing renal interstitial cells.

Clinical and laboratory parameters recorded at the time of biopsy		NCAM expressing renal interstitial cells		*p* value
		Absent	Present	
CKD stage *n (%)*	*CKD* 1	12 (42.9%)	16 (57.1%)	0.954
	CKD 2	3 (33.3%)	6 (66.7%)	
	CKD 3	3 (50.0%)	3 (50.0%)	
	CKD 4	5 (55.6%)	4 (44.4%)	
	CKD 5	2 (28.6%)	5 (71.4%)	
Serum creatinine *[μmol/L]*		146.64 ± 136.28	200.07 ± 239.45	0.244
Creatinine clearance *[ml/min]*		77.56 ± 39.49	104.32 ± 70.19	0.199
eGFR [ml/min/1.73m^2]		73.80 ± 47.49	74.56 ± 47.21	0.952
Urea *[mmol/L]*		10.61 ± 8.66	11.037 ± 8.17	0.838
Glucose *[mmol/L]*		5.15 ± 1.11	4.76 ± 0.81	0.115
Eritrocyturia *n (%)*	absent	15(44.1%)	19 (55.9%)	0.585
	present	12 (37.5%)	20 (62.5%)	
Proteinuria *[g/24h]*		8.41 ± 9.45	3.97 ± 2.63	0.024*
Red blood cells *[×10^{12}/L]*		4.09 ± 0.66	4.09±0.76	0.999
Hemoglobin *[g/L]*		122.85 ± 16.77	121.61 ± 25.01	0.852
Hematocrit		0.35 ± 0.91	0.37 ±0.07	0.297
MCV [fL]		88.64 ± 52.45	90.56 ± 4.31	0.231

Table 4.3.3. Clinical and laboratory parameters recorded at the time of last medical examination in patients with and without NCAM expressing renal interstitial cells.

Clinical and laboratory parameters recorded at the time of last medical examination		*NCAM expressing renal interstitial cells*		*p* value
		Absent	Present	
CKD stage *n (%)*	*CKD 1*	9 (45.0%)	11 (55.0%)	0.601
	CKD 2	1 (14.3%)	6 (85.7%)	
	CKD 3	1 (25.0%)	3 (75.0%)	
	CKD 4	4 (100.0%)	0 (0.0%)	
	CKD 5	2 (22.2%)	7 (77.8%)	
Serum creatinine *[μmol/L]*		183.95 ± 242.20	183.95 ± 242.20	0.560
Creatinine clearance *[ml/min]*		86.75 ± 46.34	86.75 ± 46.34	0.334
eGFR [ml/min/1.73m^2]		74.59 ± 51.60	74.59 ± 51.60	0.744
Urea *[mmol/L]*		12.24 ± 11.64	12.00 ± 10.50	0.938
Glucose *[mmol/L]*		5.27 ±2.24	5.27 ±2.24	0.175
Eritrocyturia *n (%)*	absent	10 (34.5%)	19 (65.5%)	0.547
	present	9 (42.9%)	12 (57.1%)	
Proteinuria *[g/24h]*		2.58 ± 2.36	2.58 ± 2.36	0.993
Red blood cells *[×10^{12}/L]*		3.43 ± 1.43	4.14 ±0.78	0.962
Hemoglobin *[g/L]*		120.20 ± 17.1	123.71 ± 18.54	0.63
Hematocrit		0.34 ± 0.05	0.39 ± 0.10	0.211
MCV [fL]		93.52 ± 4.30	82.97 ± 29.32	0.248

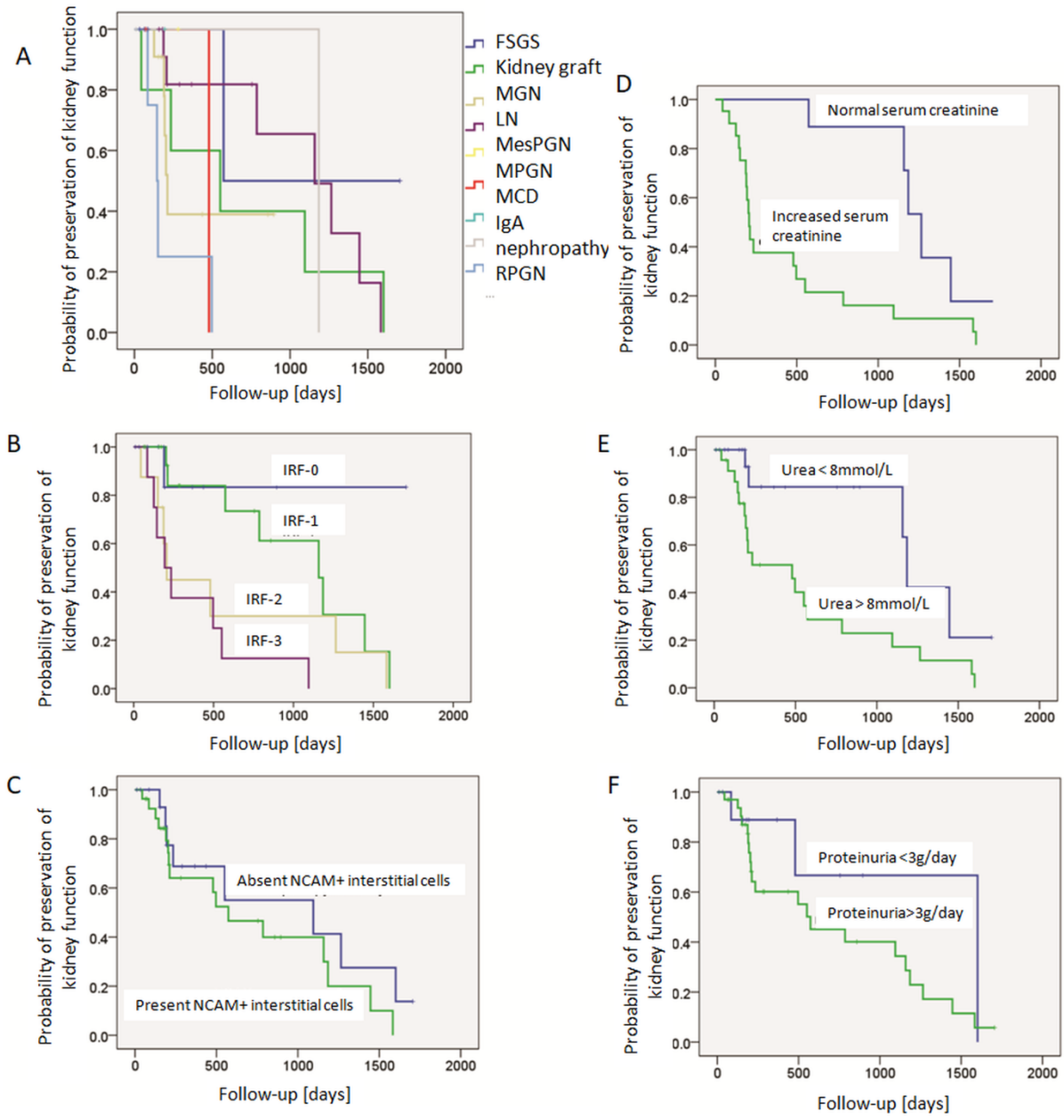

Figure 4.3.1. Probability of preservation of kidney function depending on the pathohistological and clinical parameters.

Since it has been previously shown in animal models that NCAM interstitial detection could be transiently observed following hypoxic kidney injury (88), we felt encouraged to investigate NCAM relations to HIF molecules, as well as their relations to EPO productions. NCAM and HIF-2α were rarely co-expressed on the same cell, and expression pattern of HIF-2α in these cells included only cytoplasmic localization (Fig.4.3.2). However, NCAM expressing renal interstitial cells did not express EPO, as we already showed, but sometimes rare cells in the glomerular tuft exhibited NCAM/EPO co-localization (Fig.4.3.2).

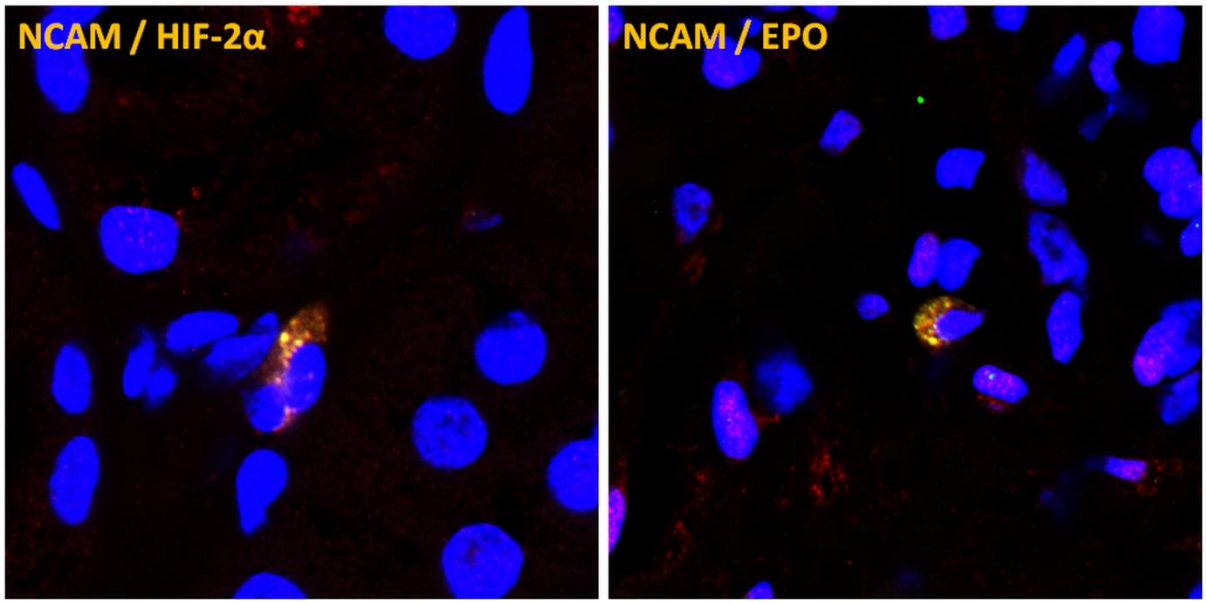

Figure 4.3.2. NCAM co-expression with HIF-2α in renal interstitial cell and NCAM/EPO co-expression in the cell of glomerular tuft.

Furthermore, HIF-2α was found to be widely expressed in the nuclei both in interstitial cells and tubular epithelial cells, but strongly associated with some signs of chronic renal parenchymal damage, such as renal interstitial fibrosis (Fig.4.3.3.). However, HIF-1α was rarely detectable in the human kidney biopsy samples and was mainly found in almost normal interstitial compartment, sometimes associated with cells capable of EPO production (Fig.4.3.4.).

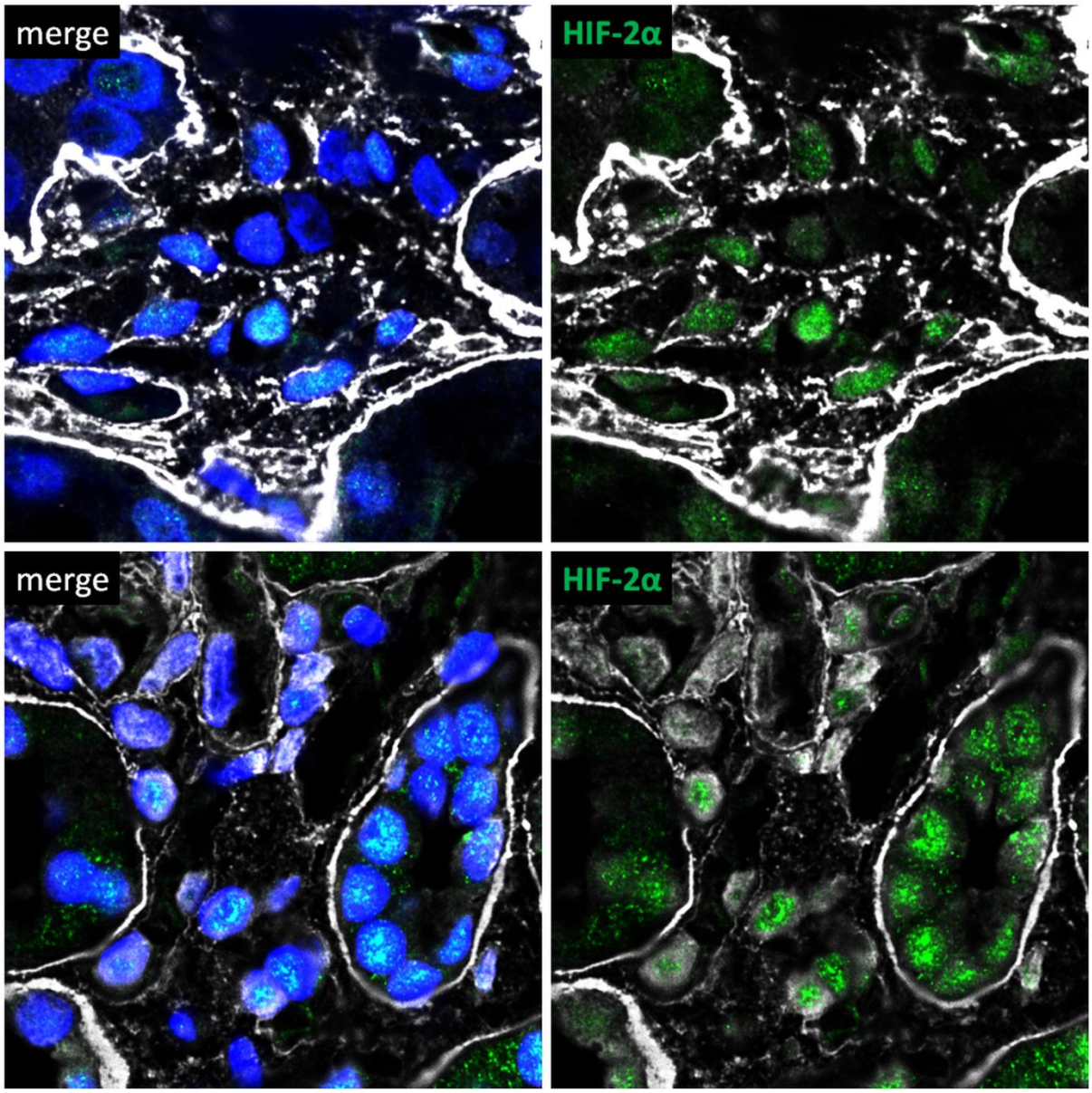

Figure 4.3.3. HIF-2α nuclear expressions (green) in renal interstitial cell within widened and fibrotic interstitial compartment and the same expression pattern in tubular epithelial cells of the tubuli surrounded by affected interstitium.

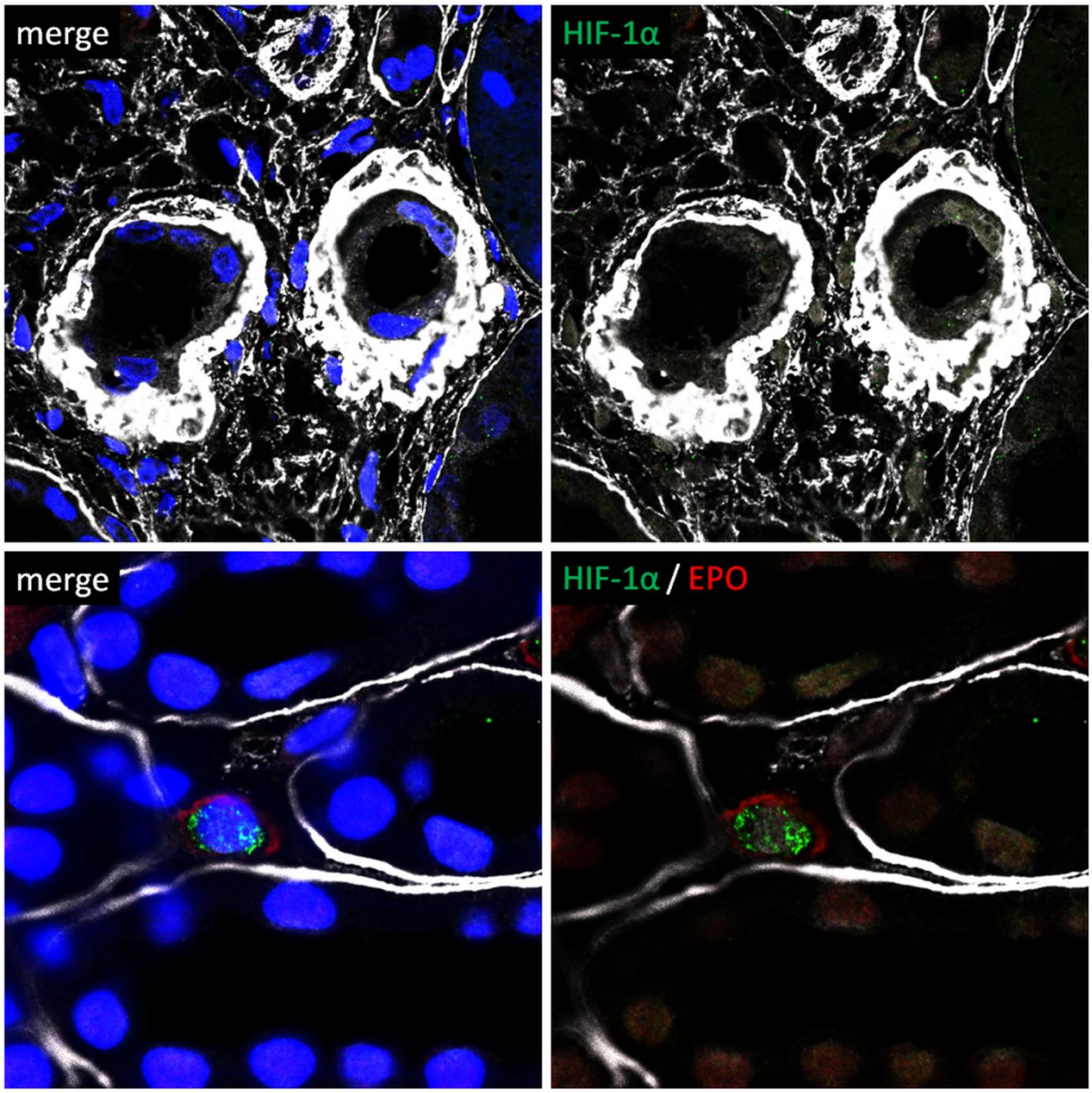

Figure 4.3.4. HIF-1α (green) nuclear expressions in renal interstitial cell could not be observed neither within cells of the widened and fibrotic interstitial compartment nor within atrophic tubular epithelial cells, whereas rare EPO producing cells (red) situated peritubularly in the area without fibrosis expressed HIF-1α (green) in the nuclei.

4.4.TGF-β down-stream effectors in kidney biopsy samples

4.4.1. SMAD2 SMAD3 and SNAIL – immunohistochemistry

Among 47 biopsy samples of patients presented with proteinuria (alone or as a part of nephrotic syndrome), SMAD3 was detected in all cases exhibiting constitutive expression in distal tubules and collecting ducts with cytoplasmic and membranous expression pattern (Fig.4.4.1.1.). Proximal tubular epithelial cells and atrophic tubuli did not express SMAD3, as shown on (Fig.4.4.1.1.B and D).

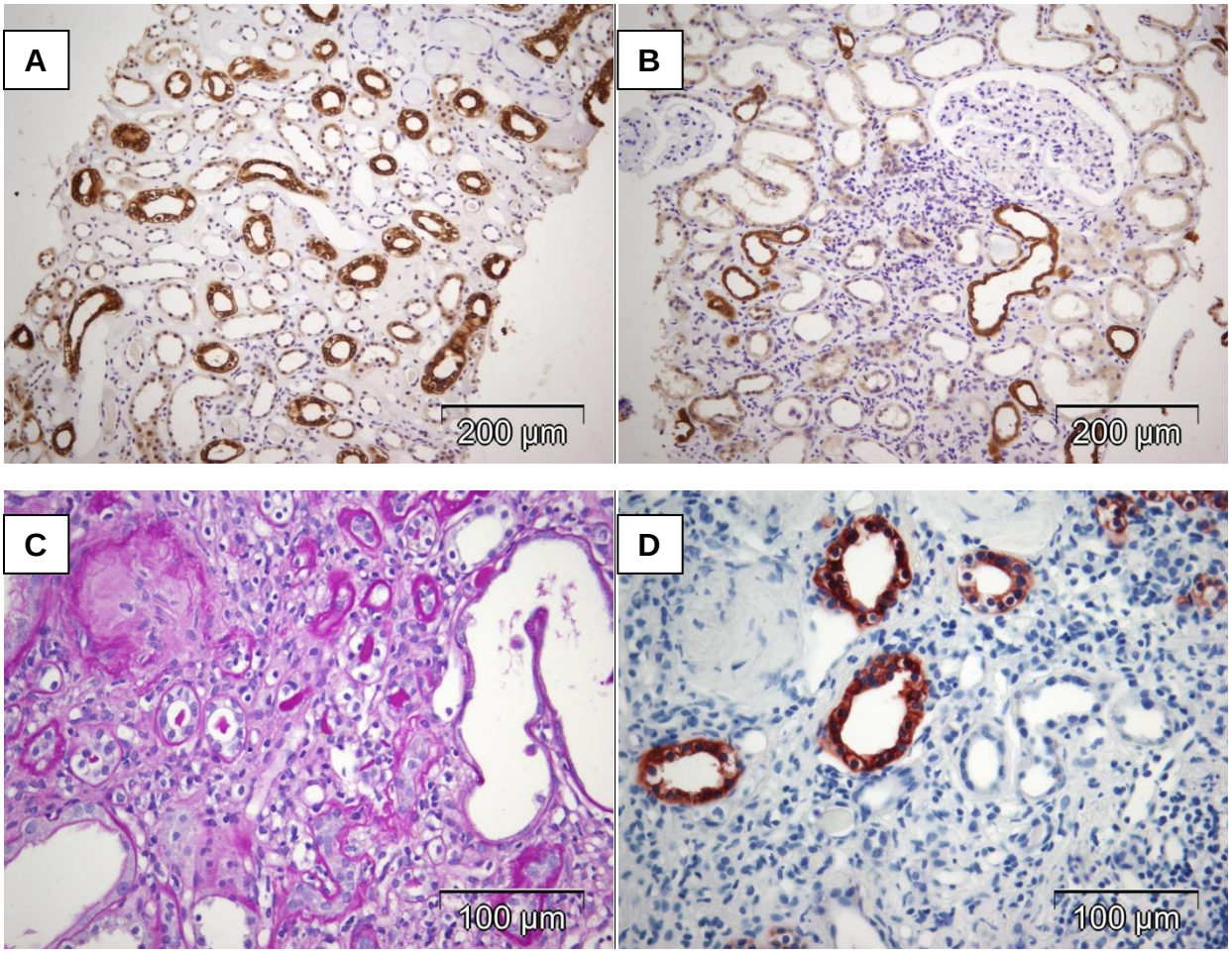

Fig 4.4.1.1. SMAD3 expression in kidney biopsies. (A) Immunopositivity of collecting ducts in renal medulla; (B) Immunopositivity of distal tubules in renal cortex; (C) Abundant interstitial fibrosis and tubular atrophy with global glomerulosclerosis in patient with end-stage kidney disease, *PAS* ×400; (D) Immunopositivity of collecting ducts in renal cortex and the absence of SMAD3 in atrophic tubuli.

Therefore, SMAD3 immunoreactivity was characteristic of morphologically preserved cortical and medullar distal tubules and collecting ducts and was not related to chronic renal parenchymal damages (interstitial fibrosis and tubular atrophy). On the other hand, SMAD2 protein was expressed in nuclei of many epithelial structures of nephron. This spectrum included distal tubules, collecting ducts and parietal cells of Bowman's capsule. Moreover, in contrast to SMAD3, SMAD2 was present diffusely in nuclei of all atrophic tubules surrounded by interstitial fibrosis (Figure 4.4.1.2.A), whereby morphologically preserved proximal tubules were devoid of SMAD2 immunoreactivity.

SNAIL transcription factor had almost identical distribution and pattern of expressions as SMAD2. Thus, all atrophic tubules with SMAD2 presence in nuclei displayed also expression of SNAIL (Figure 4.4.1.2.B). Furthermore, we showed statistically significant correlation of SMAD2 and SNAIL expression in tubular epithelial cells with interstitial fibrosis ($p<0.001$) and tubular atrophy ($p<0.001$), as presented in Figure 4.4.1.3. Additionally, variable frequency of SNAIL expression was observed in glomerular podocytes. We have noticed that patients with neprhotic range proteinuria expressed SNAIL in podocytes (Figure 4.4.1.2.C), while in those with sub-nephrotic proteinuria values SNAIL could not be detected (Figure 4.4.1.2.D).

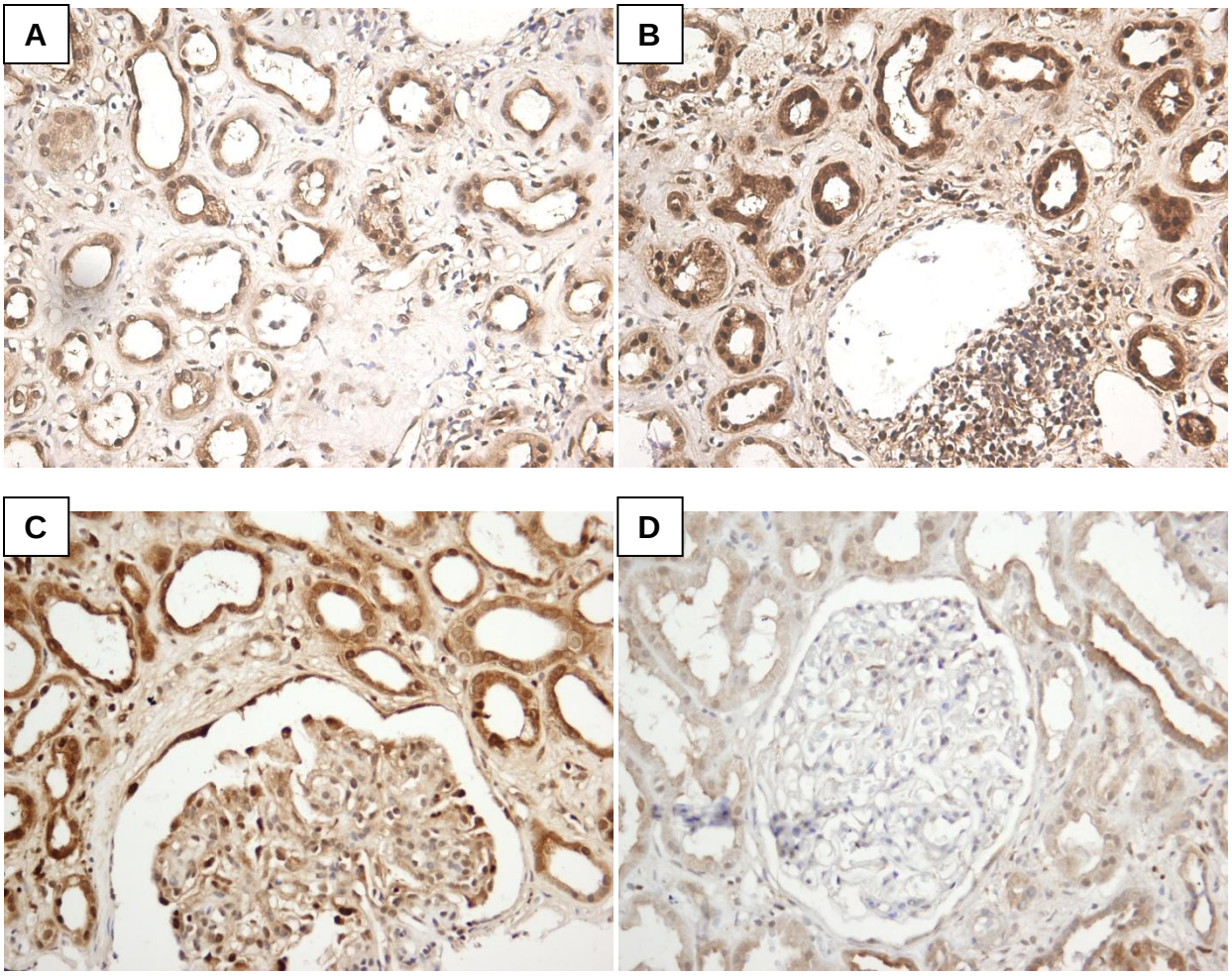

Figure 4.4.1.3. SMAD2 and SNAIL expressions in kidney biopsy samples (A) Immunopositivity of atrophic tubules surrounded with interstitial fibrosis, *SMAD2* ×400; (B) Immunopositivity of atrophic tubules surrounded with interstitial fibrosis, *SNAIL* ×400; (C) *SNAIL* expression in podocytes in patient with nephrotic range proteinuria, ×400; (D) The absence of SNAIL expression in podocytes in patient with sub-nephrotic proteinuria value, ×400.

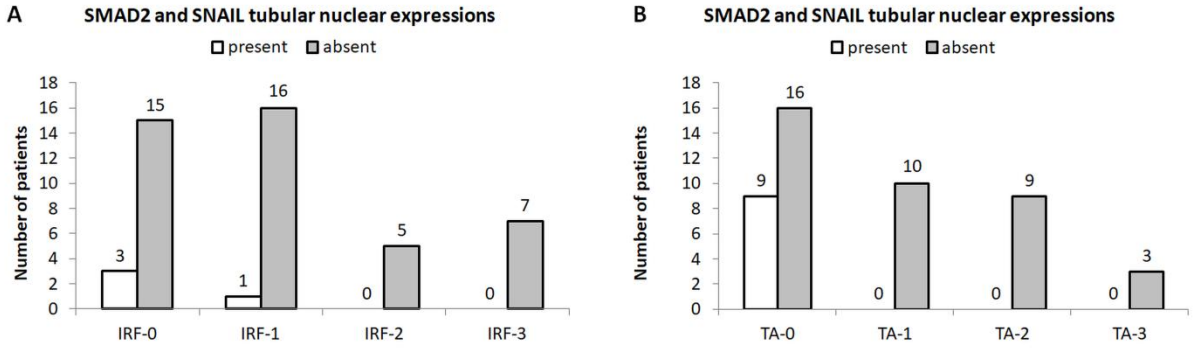

Figure 4.4.1.3. Distribution of SMAD2 and SNAIL tubular nuclear expressions with regard to presence and degrees of interstitial fibrosis (IRF) and tubular atrophy (TA).

4.4.2. SMAD2, SMAD3 and SNAIL - clinico-immunomorphological correlations

It has been statistically confirmed that patients who expressed SMAD2 in nuclei of proximal tubule cells (i.e. all atrophic tubuli) had significantly higher urea and creatinine levels, as well as significantly reduced eGFR (Table 4.4.2.1). Furthermore, there were statistically significant more SMAD2 and SNAIL positive cases (with regard to nuclear tubular expression) with each increase in CKD stage, as shown in Table 4.4.2.1.

Table 4.4.2.1. Clinical and laboratory parameters recorded at the time of biopsy in patients with and without SMAD2 and SNAIL expressing tubular epithelial cells.

Clinical and laboratory parameters		SMAD2 and SNAIL expressing tubular epithelial cells		*p* value
		Absent	Present	
Age (years)		40.0±17.6	44.9±14.8	0.354
	CKD1	9 (69.2%)	4 (30.8%)	
	CKD2	3 (30.0%)	7 (70.0%)	
CKD stage *n (%)*	*CKD3*	2 (16.7%)	10 (83.3%)	0.001*
	CKD4	0 (0.0%)	4 (100%)	
	CKD5	0 (0.0%)	1 (100%)	
Serum creatinine *[μmol/L]*		84.5±29.3	129.7±68.3	0.006*
eGFR [ml/min/1.73m^2]		95.9±33.3	61.7±38.1	0.007*
Urea *[mmol/L]*		7.3±1.9	9.8±4.9	0.026*
Glucose *[mmol/L]*		5.0±0.6	4.9±0.9	0.795
Proteinuria *[g/24h]*		4.2±2.3	6.2±4.5	0.072

SNAIL expression in podocytes was clinically followed with higher proteinuria values. The average level of proteinuria in patients with SNAIL expression in podocytes was 7,4±3,5 g/24h, while in patients without SNAIL positivity in podocytes was only 1,6±0,97 g/24h ($p<0.001$).

4.4.3. Immunofluorescent detection of TWIST, activated form of SMAD proteins and SNAIL protein

TWIST has been considered to be involved in EMT events and could be induced by TGF-β ligand. In the analyzed human kidney biopsy samples, TWIST was occasionally detected in proximal tubular epithelial cells (as labeled with N-cadherin) even in the absence of chronical tubulointerstitial damages (right panel on Fig.4.4.3.1.). However, normal proximal tubuli were usually labeled only with N-cadherin but not with TWIST (left panel on Fig.4.4.3.1.).

Since immunohistochemistry gave useful hint for further investigations but provided immunolabeling with a lot of background staining, we further wanted to explore the presence of activated SMAD forms (phosphorylated) and to check SNAIL and TWIST expression using imunofluorescent labeling. Surprisingly, we found variable pSMAD2 and pSMAD3 immunofluorescent staining among cases. Thus, pSMAD2 was expressed focally in tubular epithelial cells and sometimes was associated with MMP2 immunopositivity, as illustrated on Figure 4.3.3.1.A. The same pattern in tubular compartment was observed with pSMAD3 and MMP9 (Figure 4.3.3.1.B). However, pSMAD2, but not pSMAD3, was visible in renal interstitial cells closely packed between tubuli (Figure 4.3.3.1.C), as well as in glomerular tuft of the case with diabetic glomerolopathy (Figure 4.3.3.1.D). SNAIL was expressed exclusively in podocytes of patients with nephrotic range proteinuria and could not be detected in any other compartment by immunofluorescence (Figure 4.3.3.1E and F).

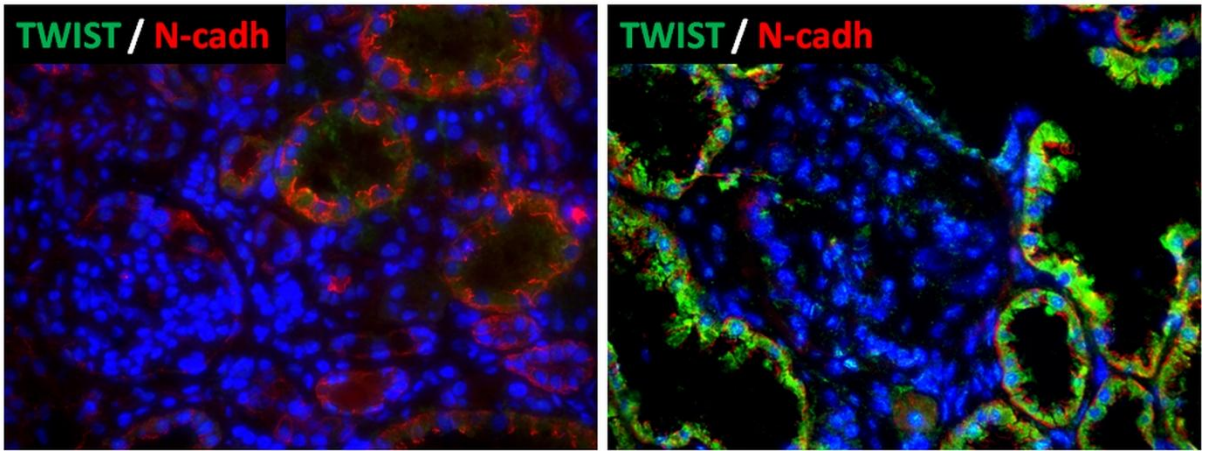

Figure 4.4.3.1. TWIST/N-cadherin double immunofluorescent labeling.

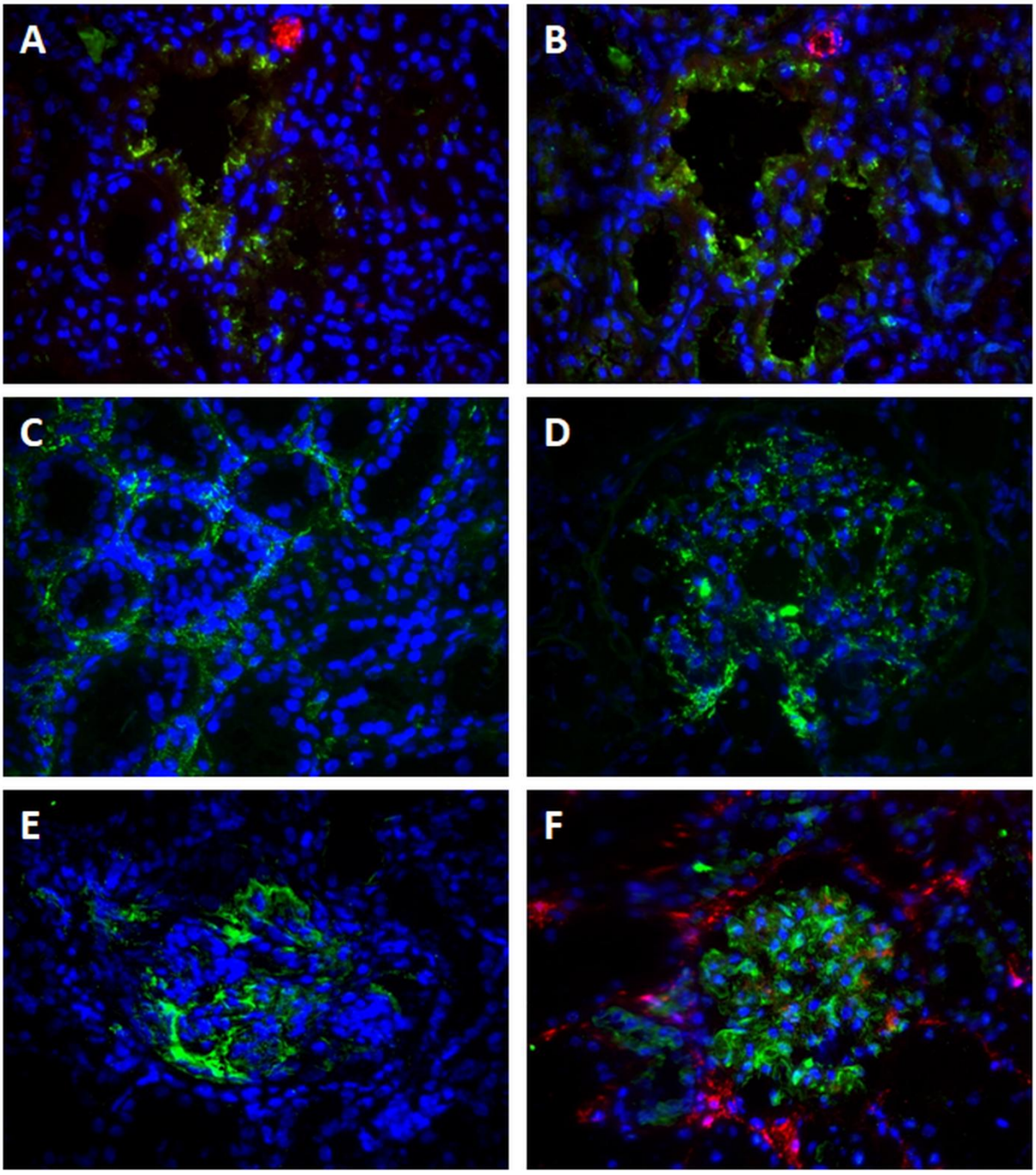

Figure 4.4.3.2. pSMAD2, pSMAD3 and SNAIL immunofluorescent labeling with additional double staining with MMP2, MMP9 and α-SMA in human kidney biopsies. A) pSMAD2 (green) and MMP2 (red)**; B)** pSMAD3 (green) and MMP9 (red); **C)** pSMAD2 widespread interstitial expression in the case of diabetic nephropathy; D) pSMAD2 glomerular expression in the same case of diabetic nephropathy**; E)** SNAIL expression in glomerulus of patient clinically presented with nephrotic range proteinuria**; F)** Glomerular SNAIL (green) and interstitial α-SMA (red) expressions in patient clinically presented with nephrotic range proteinuria.

4.5.Gene expression levels - kidney biopsy samples of renal fibrosis

It has been observed that NCAM-140 became higher expressed in advanced IRF stages, and FGFR1 has been shown similar trend, as shown on Fig. 4.5.1.

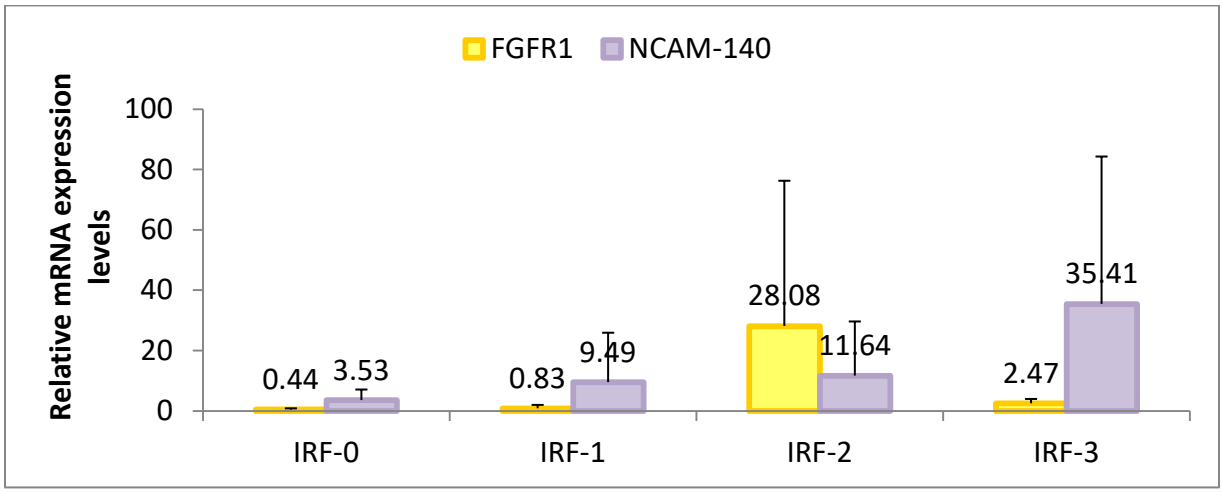

Figure 4.5.1. NCAM-140 and FGFR1 mRNA expression levels among different IRF degrees.

The most prominent changes within various stages of renal interstitial fibrosis were detected in mRNA expression levels of ITGA5 and ITGB1. Fig. 4.5.2 illustartes extremely high ITGA5 expression in the most severe IRF stage.

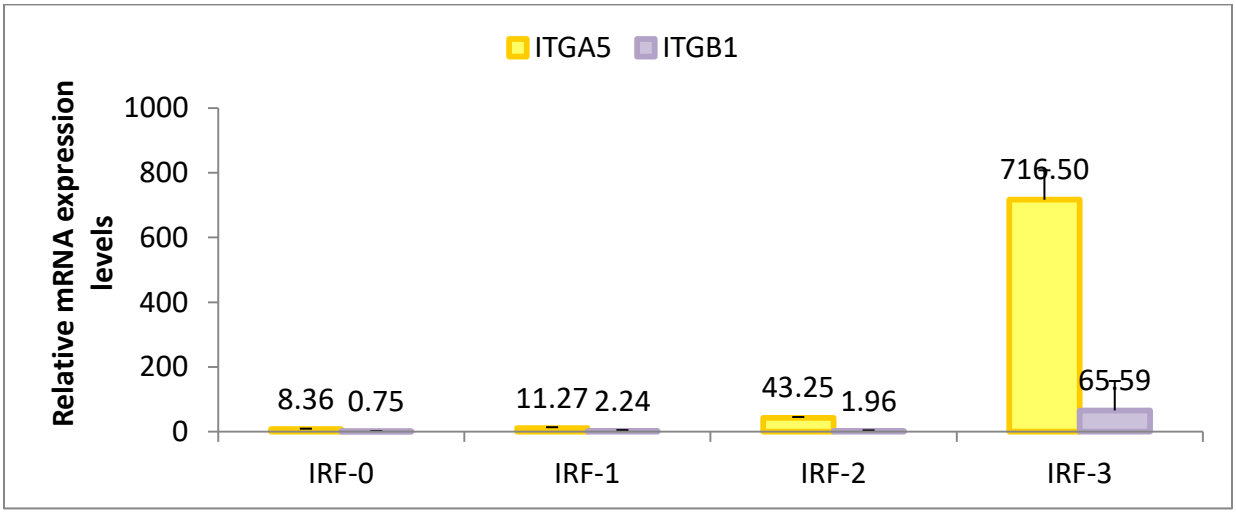

Figure 4.5.2. ITGA5 and ITGB1 mRNA expression levels among different IRF degrees.

FSP1 was the most prominent in the earliest stage of fibrosis (IRF-1), while α-SMA mRNA was the highest in the most advanced stage (IRF-3), as shoen on the Fig.4.5.3.

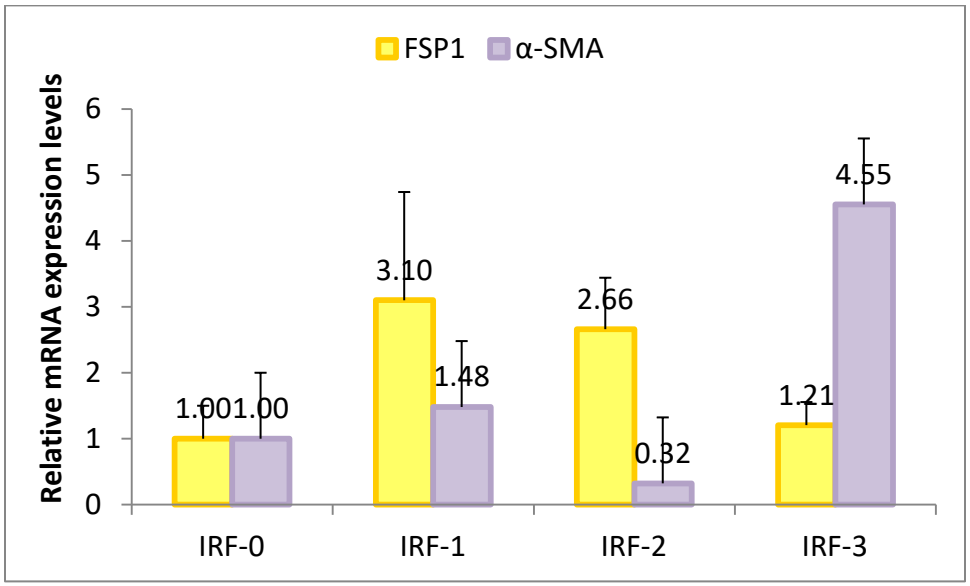

Figure 4.5.3. FSP1 and α-SMA mRNA expression levels among different IRF degrees.

RUNX1, RUNX1T1 and PRMT1 showed increased expressions in higher IRF stages. (Fig.4.5.4)

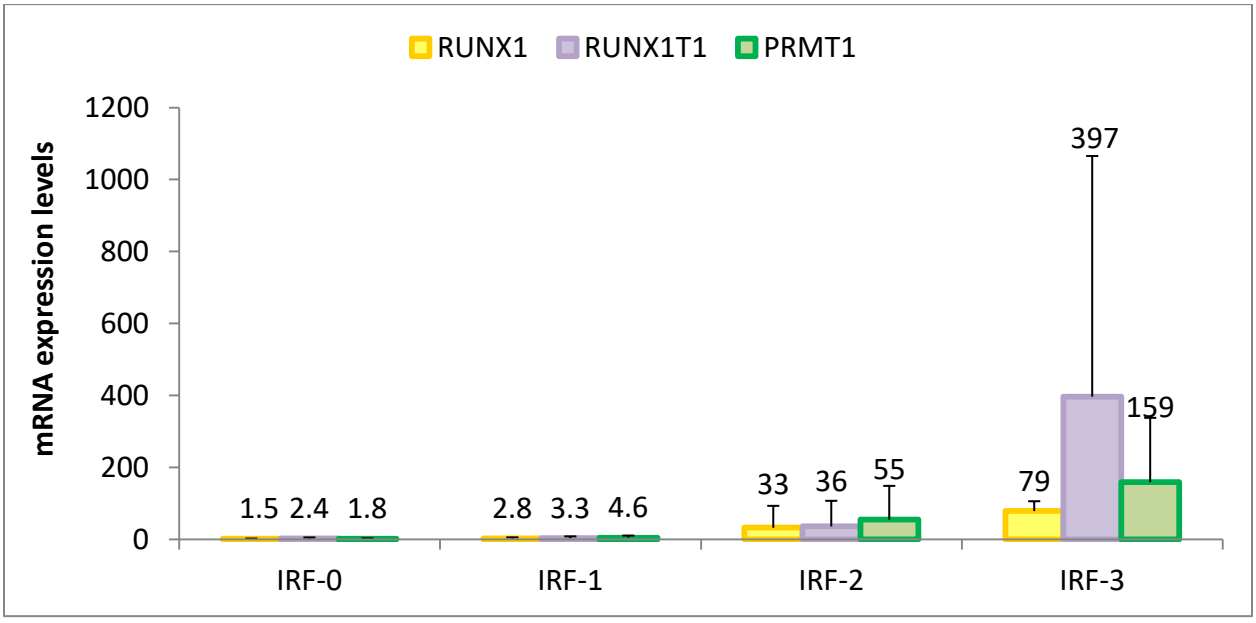

Figure 4.5.4. RUNX1, RUNX1T1 and PRMT1 mRNA expression levels among different IRF degrees.

Considering increased expressions of aforementioned genes with each increase in severity of renal interstitial fibrosis, regardless of the underlying kidney diseases, we further explored their correlations with RUNX1 transcription factor since RUNX1 is one of known transcriptional inducers of NCAM expression (89). Considering also that RUNX1 activity can be stimulated by PRMT1 induced methylation (90) and suppressed by RUNX1T1 (91), we have been searched thir possible relations, as illustrated on Fig.4.5.5 and Fig.4.5.6.

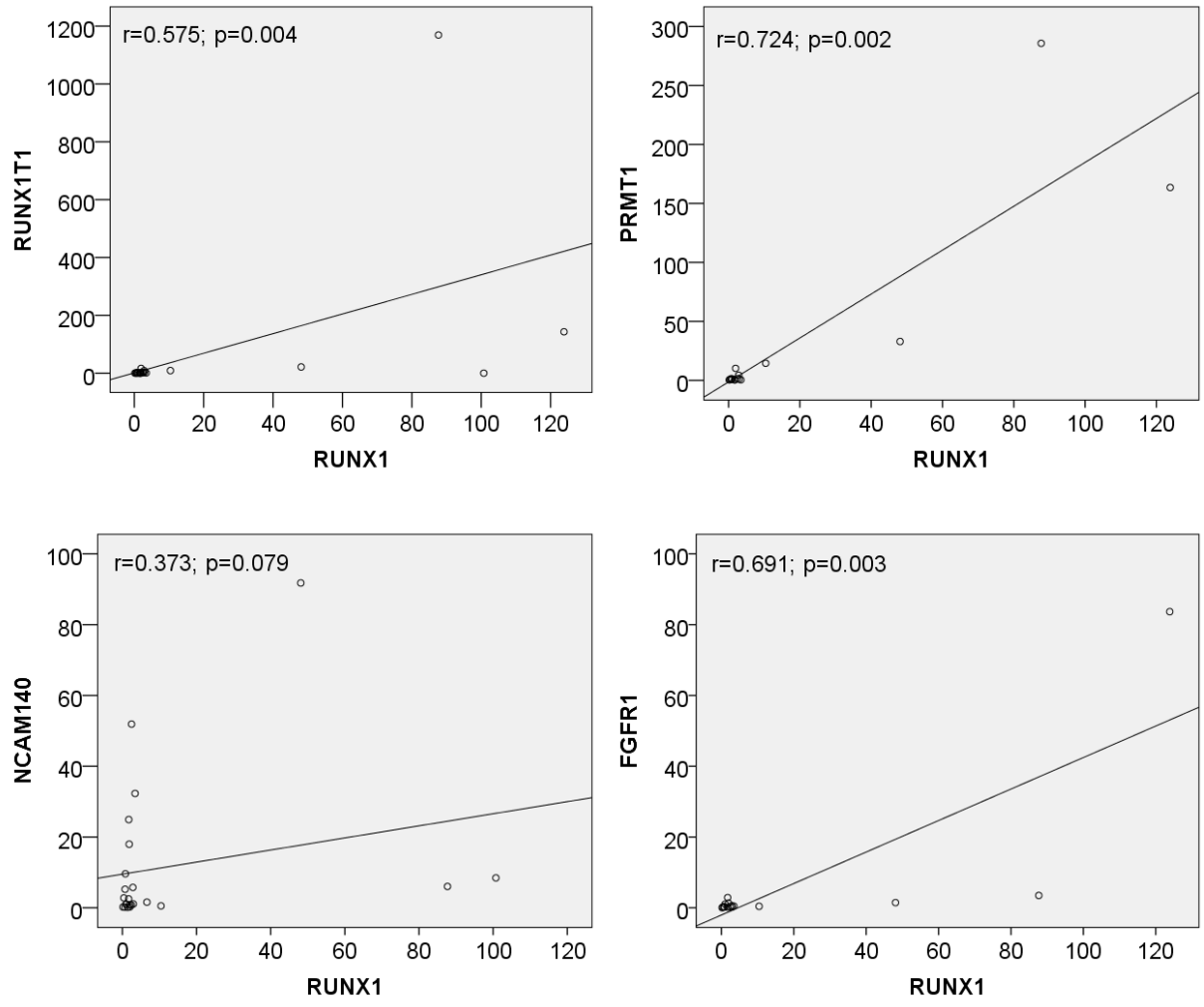

Figure 4.5.5. Spearman's correlations of RUNX1 with RUNX1T1, PRMT1, NCAM-140 and FGFR1.

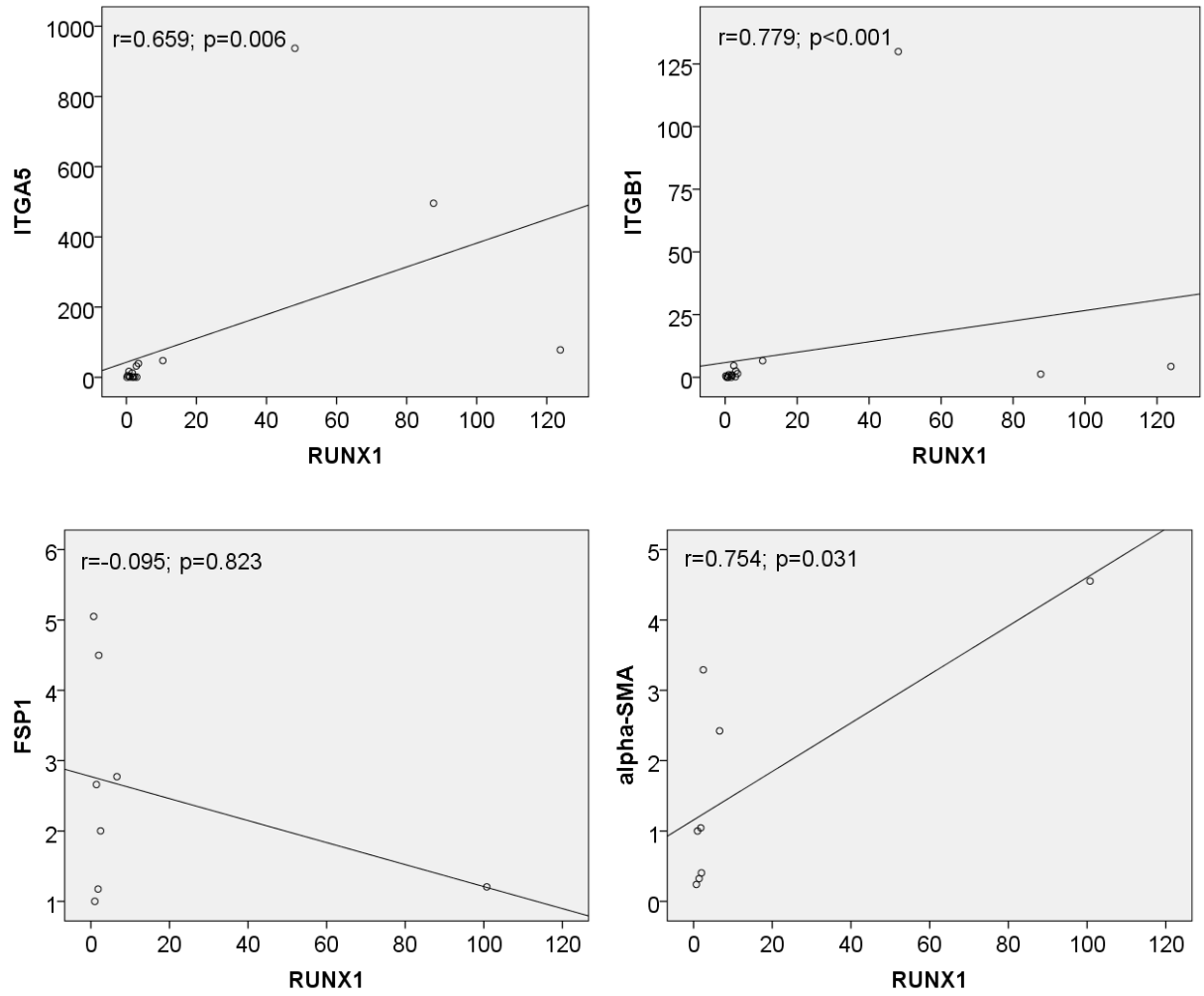

Figure 4.5.6. Pearson's correlations of RUNX1 with FSP1, α-SMA, ITGA5 and ITGB1.

4.6.The effects of TGF-β on kidney tubular epithelial cells (HK-2 cells) and modulation of these effects by FGFR inhibitor

4.6.1. Time-dependant morphological changes of HK-2 cells

Based on the cell morphology, clear influence of TGF-β1 was detected 72h after stimulation. As shown in the Fig.4.6.1.1, cells were spindle-shaped and acquired fibroblast-like morphology. PD173074 completely prevented such morphological changes under the TGF-β1 influence, leading to preservation of normal epithelial shape of HK-2 cells.

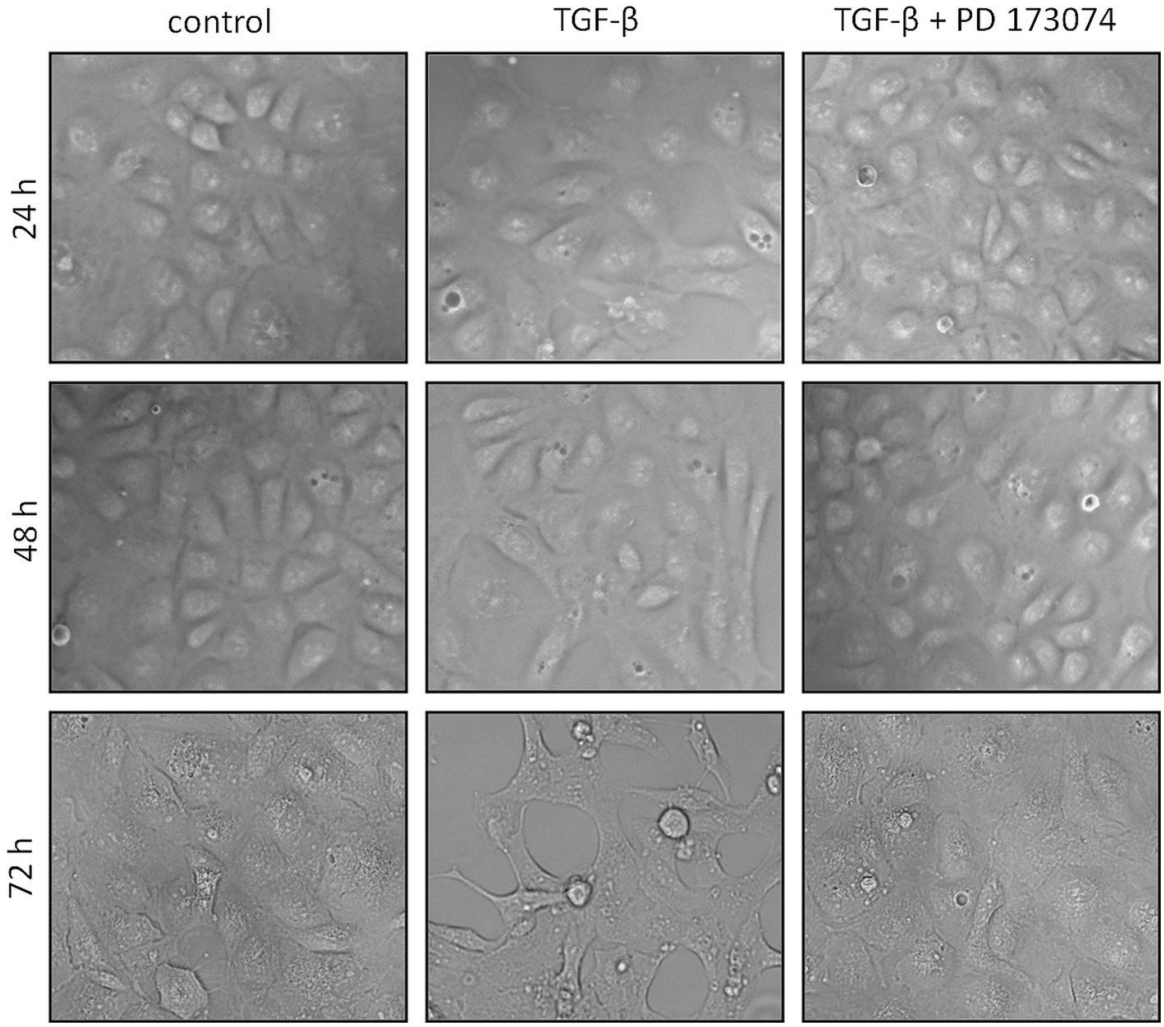

Figure 4.6.1.1. Time dependant morphological changes induced by TGF-β1 and modulated with PD173074.

4.6.2. Migration sctratch assay

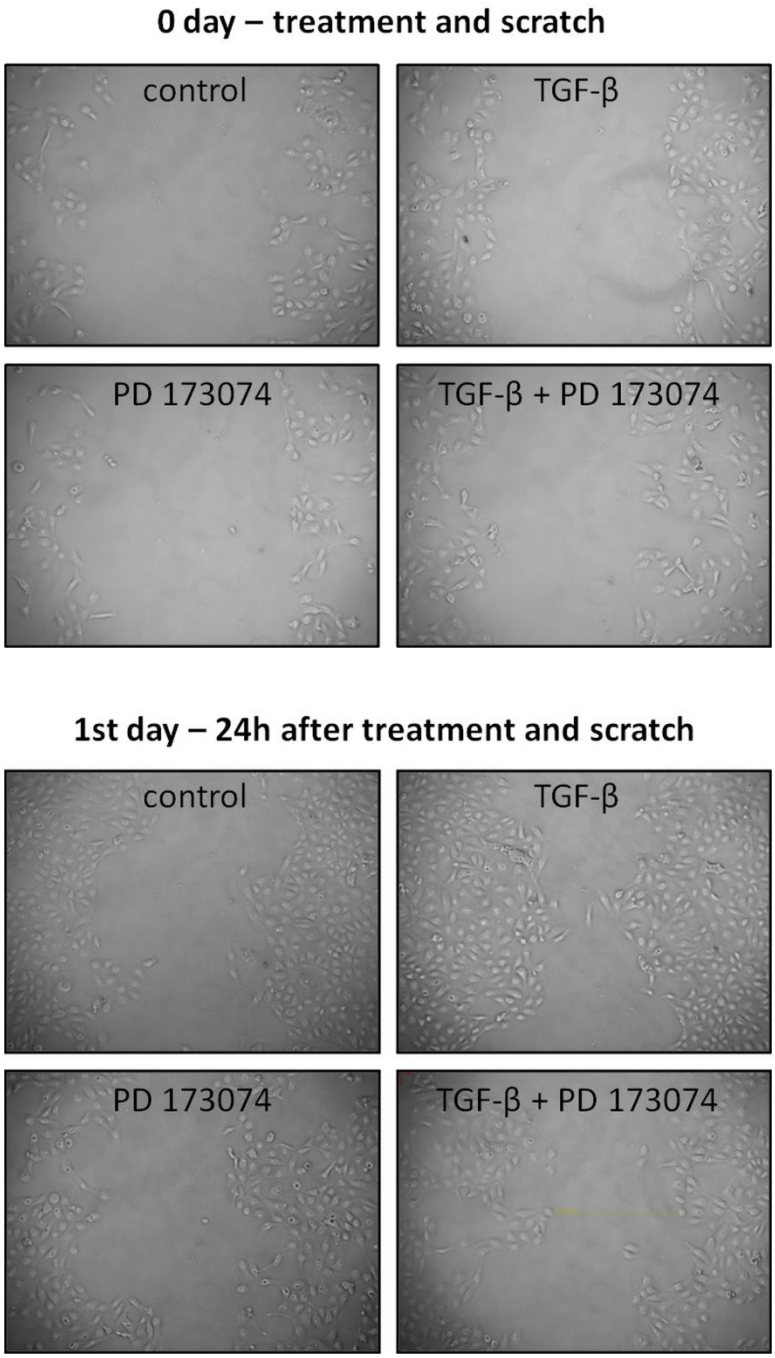

Figure 4.6.2.1. Pictures captured at the time of treatment and scratch (0 day) and next experimental day (1st day).

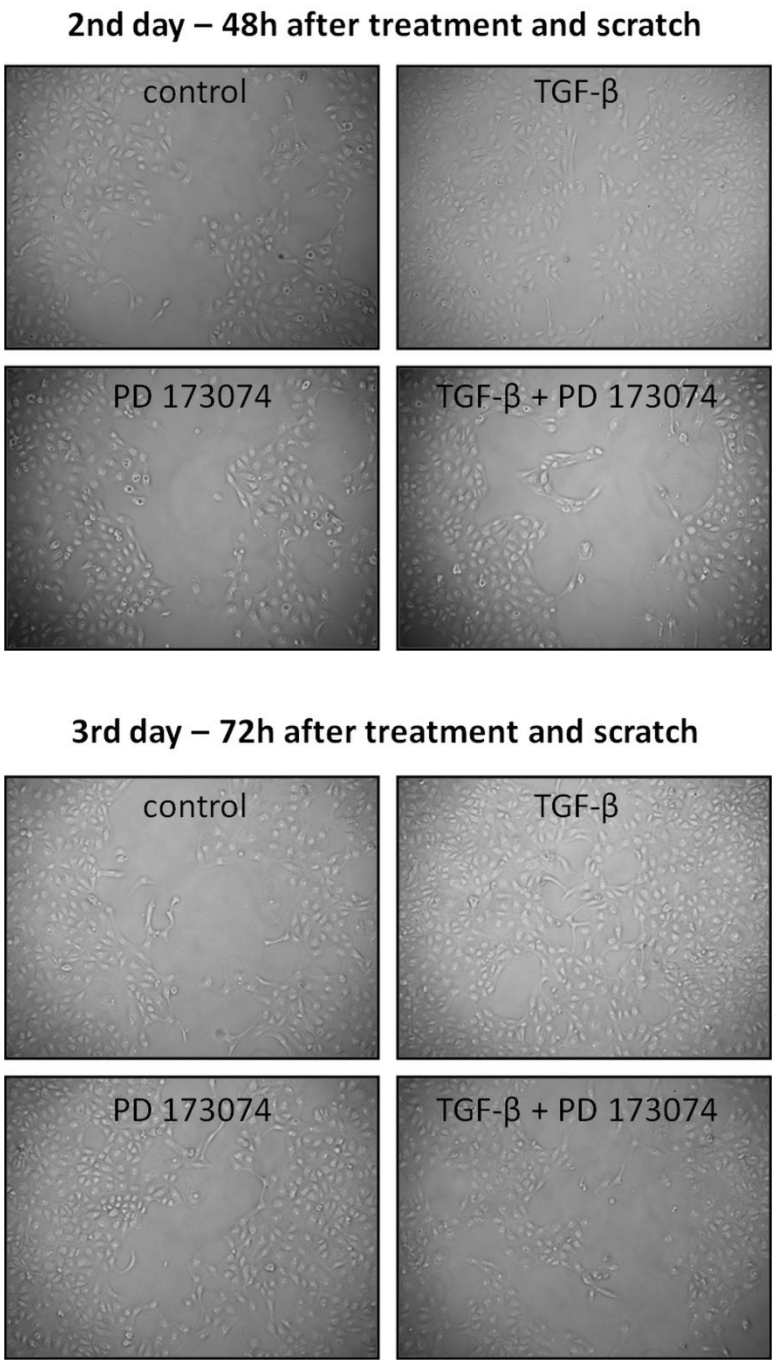

Figure 4.6.2.2. Pictures captured on the second and third experimental days.

As shown in the Fig.4.6.2.1 and 4.6.2.2., TGF-β1 treated cells migrated faster, and PD173074 suppressed TGF-β1 induced potential of enhanced cell migration.

Using scratch assay analysis, TGF-β1 treated cells migrated faster than control HK-2 cells, PD173074 treated, as well as TGF-β1+PD173074 treated cells. Thus, 24h after TGF-β1

stimulation, around 55% of scratch distance was visible, whereby in three other groups almost 90% of initial scratch distance could be observed (Fig.4.6.2.3.). The same cell migration patterns were detected during the next two experimental days. Illustrations in the Fig.4.6.2.3 show clear difference in the migration capacity of cells treated with TGF-β1 compared to the cells stimulated with TGF-β1 in addition to PD173074 within three days.

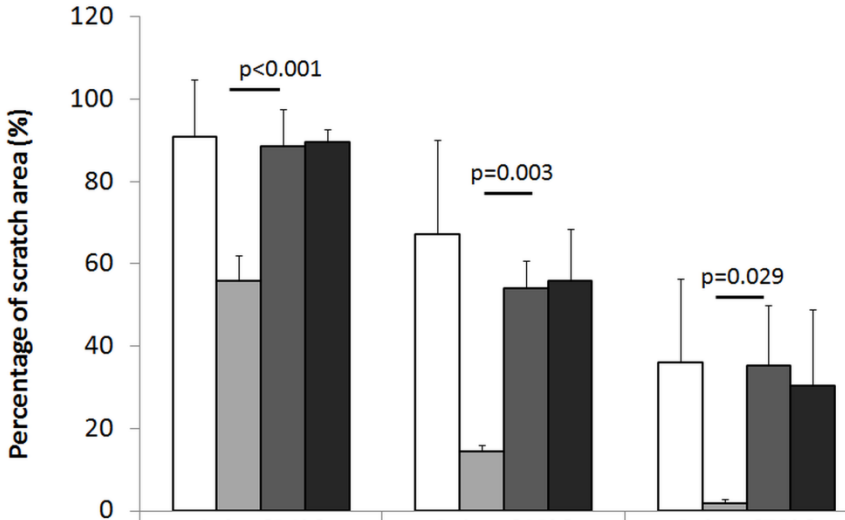

	1 day [24h]	2 days [48h]	3 days [72h]
control	91.01	67.16	35.99
TGF-β	55.91	14.50	1.72
TGF-β + PD173074	88.67	54.20	35.37
PD173074	89.72	55.75	30.38

Figure 4.6.2.3. Scratch assay analysis within three experimental days.

4.6.3. Gene expression analysis

Initially, HK-2 cells were tested for the relative mRNA expression levels of NCAM (three isoforms: NCAM-120, NCAM-140, NCAM-180) and FGFR1 within control and TGF-β1 (10ng/µl) treated group. qRT-PCR analysis revealed over-expression picks of both NCAMs and FGFR1 24h after TGF-β1 stimulation (Fig. 4.6.3.1 A), whereby morphological difference was not observed among these two group using light microscopy (Fig. 4.6.3.1 C).

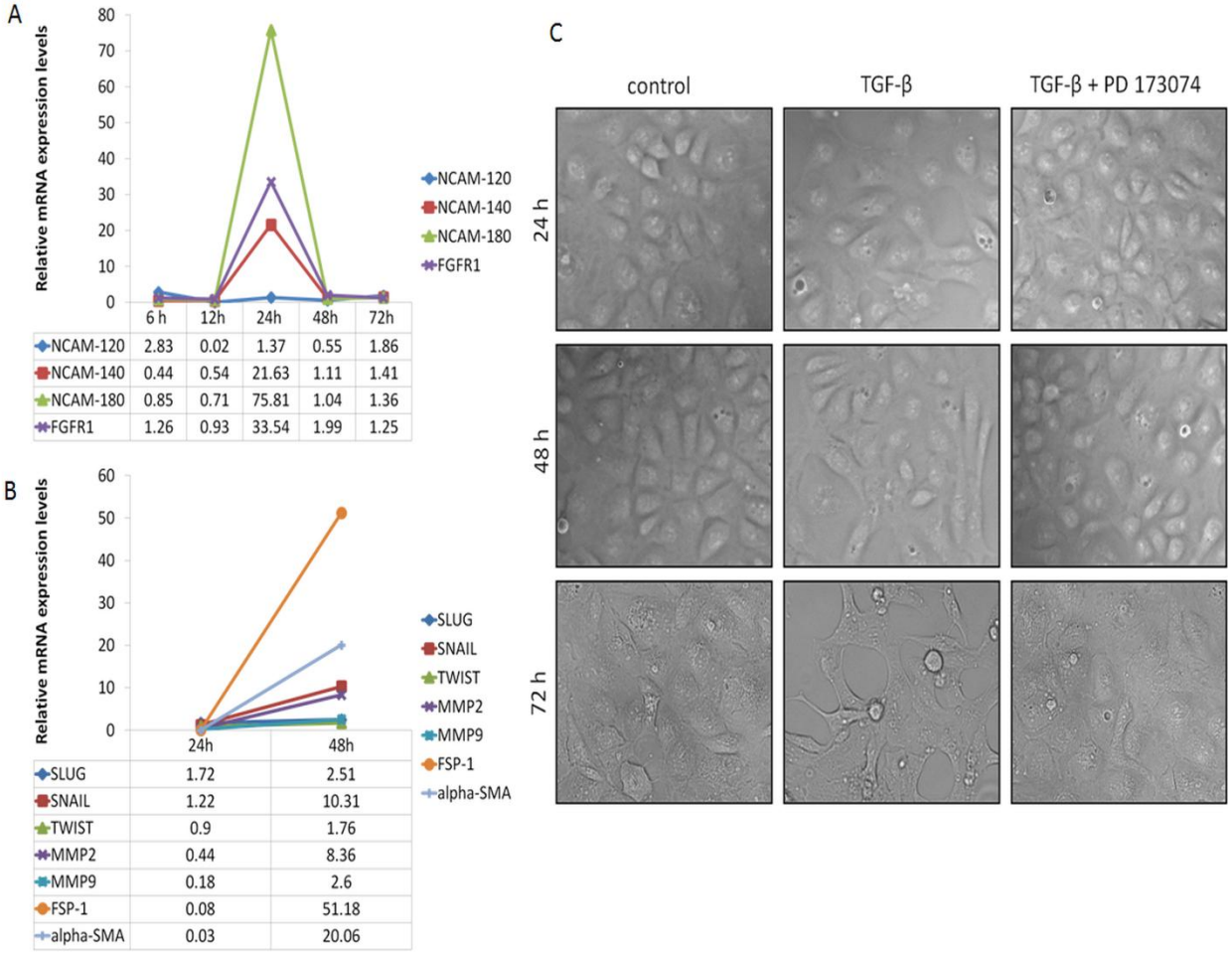

	6 h	12h	24h	48h	72h
NCAM-120	2.83	0.02	1.37	0.55	1.86
NCAM-140	0.44	0.54	21.63	1.11	1.41
NCAM-180	0.85	0.71	75.81	1.04	1.36
FGFR1	1.26	0.93	33.54	1.99	1.25

	24h	48h
SLUG	1.72	2.51
SNAIL	1.22	10.31
TWIST	0.9	1.76
MMP2	0.44	8.36
MMP9	0.18	2.6
FSP-1	0.08	51.18
alpha-SMA	0.03	20.06

Figure 4.6.3.1. Time-dependant morphological and molecular changes upon TGF-β1 stimulation of proximal tubular epithelial cells (HK2-cells). A) relative mRNA expression levels of NCAM isoforms and FGFR1 at 5 different time points (6h, 12h, 24h, 48h, 72h) after TGF-β1 treatment; **B)** relative mRNA expression levels of genes known to be affected during TGF-β1 stimulation measured 24h and 48h after TGF-β1 treatment of HK2-cells; **C)** cell morphology observed at three time points (24h, 48h, 72h) optico-microscopically in control group, as well as in groups treated with TGF-β1 alone and in addition to PD173074.

However, 48h upon TGF-β1 administration HK-2 cells started to change their phenotype acquiring somewhat spindle shape appearance, but still many of them resemble normal epithelial morphology (Fig. 4.6.3.1 C). At that time point, rapid decrement of NCAMs and FGFR1 mRNA levels was observed (Fig. 4.6.3.1 A). Furthermore, genes known to be affected in TGF-β1 induced fibrosis were highly over-expressed 48h after stimulation, whilst their expressions were low the day before (24h after TGF-β1) as illustrated in Fig. 4.6.3.1 B. Since it seemed that over-expression picks of NCAMs and FGFR1 were the earliest changes observed upon TGF-β1 stimulation, and appreciating rapid decline of their mRNA levels even next day that were followed by increased expression of SLUG, SNAIL, TWIST, MMP2, MMP9, FSP-1 and α-SMA, we hypothesized that at least FGFR1 could have an important role in the initiation of renal fibrosis *in vitro*. Thus, we further wanted to explore effects of FGFR1 inhibitor (PD173074) on TGF-β1 induced fibrosis, following cell morphology, cell migration, gene expressions and relevant protein expressions and localizations.

Since the picks of genes up-regulations upon TGF-β1 stimulation were detected 48h after such treatment, we further followed gene expression levels under the impact of both PD173074 and TGF-β1 in order to clarify ability of PD173074 to modulate aforementioned transcriptional events.

SLUG, SNAIL and TWIST

Thus, 48h after TGF-β1 and PD173074 stimulation SLUG, SNAIL and TWIST were expressed at significantly lower levels compared to their expression under the influence of TGF-β1 alone (Fig. 4.6.3.2 A), achieving the levels similar to those observed in control HK-2 cells. At 72h SLUG mRNA (Fig. 4.6.3.2 B) was lower than 48h after experimental procedure. Although PD173074 suppressed SLUG up-regulation, the difference was not significant (Fig. 4.6.3.2 B). However, SNAIL remained up-regulated 72h after TGF-β1 stimulation, but unfortunately PD173074 could not significantly resist powerful TGF-β1 influence (Fig. 4.6.3.2 B). Furthermore, TWIST reached over-expression pick 72h upon TGF-β1 treatment, whereby such effect was remarkably reduced by PD173074 administration (panel B).

FSP-1 and α-SMA

Both FSP-1 and α-SMA are considered as key contributors to tissue fibrosis. Consequently, it was not surprising that their relative mRNA expression levels were highly over-expressed in *in vitro* model of TGF-β1 induced renal fibrosis (Fig. 4.6.3.2 C and D). However, PD173074 successfully suppressed extremely extensive up-regulation of either FSP-1 or α-SMA, as shown in Fig. 4.6.3.2 C and D.

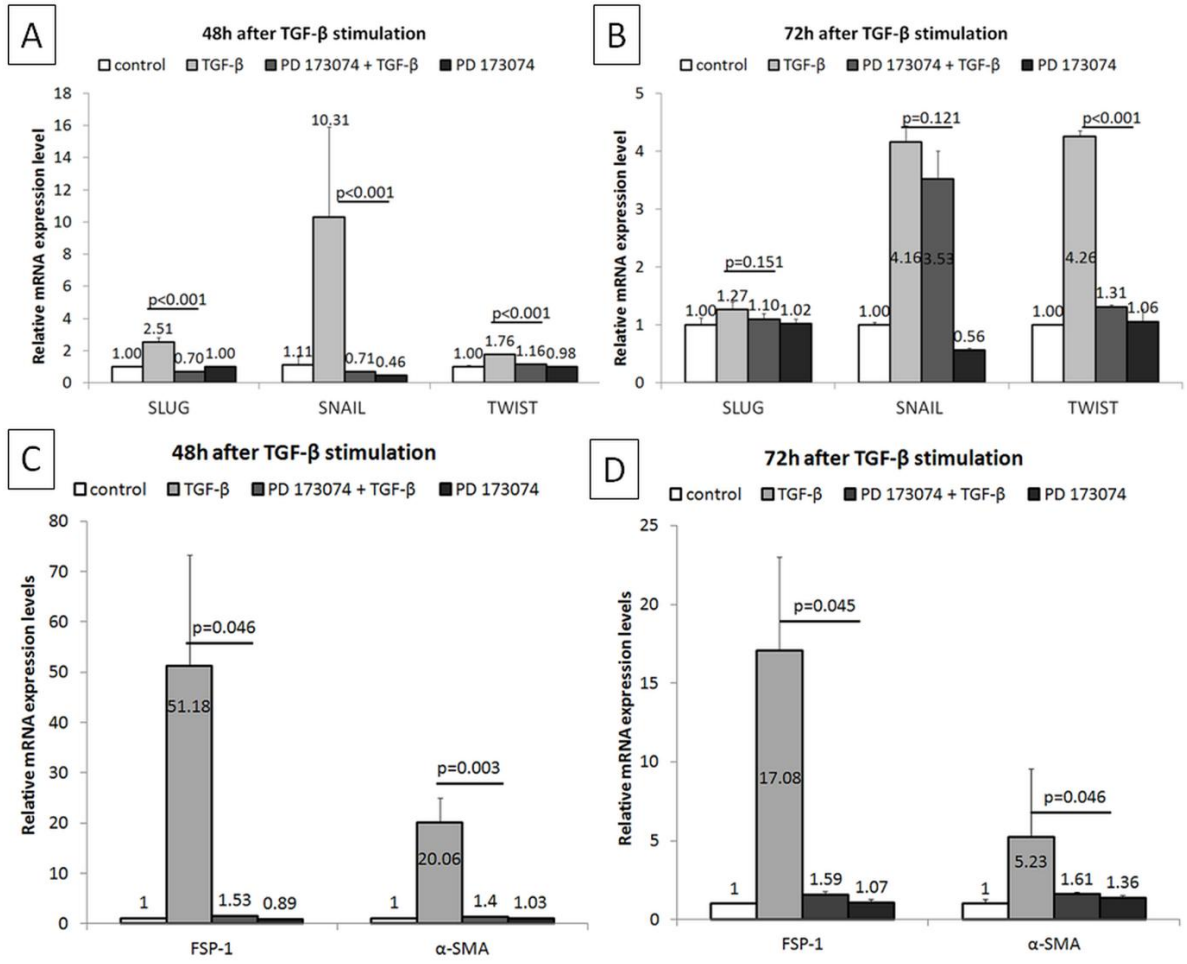

Figure 4.6.3.2. Modulation of gene expressions by PD173074 in TGF-β1 stimulated HK-2 cells – SLUG, SNAIL, TWIST, FSP-1 and α-SMA (48h and 72h).

E-cadherin and N-cadherin

It has been shown that switch of cadherins appeared 48h after TGF-β1 application, persisting also the next day (Fig.4.6.3.3). Thus, a remarkable molecular trait of TGF-β1 influence on HK-2 cells was E-cadherin down-regulation followed by up-regulation of N-cadherin. The effect of PD173074 on modulation of cadherin expressions was not too strong at the beginning (48h), but became striking on the third day (72h). Indeed, the third experimental day was accompanied by almost complete restoration of cadherin expression.

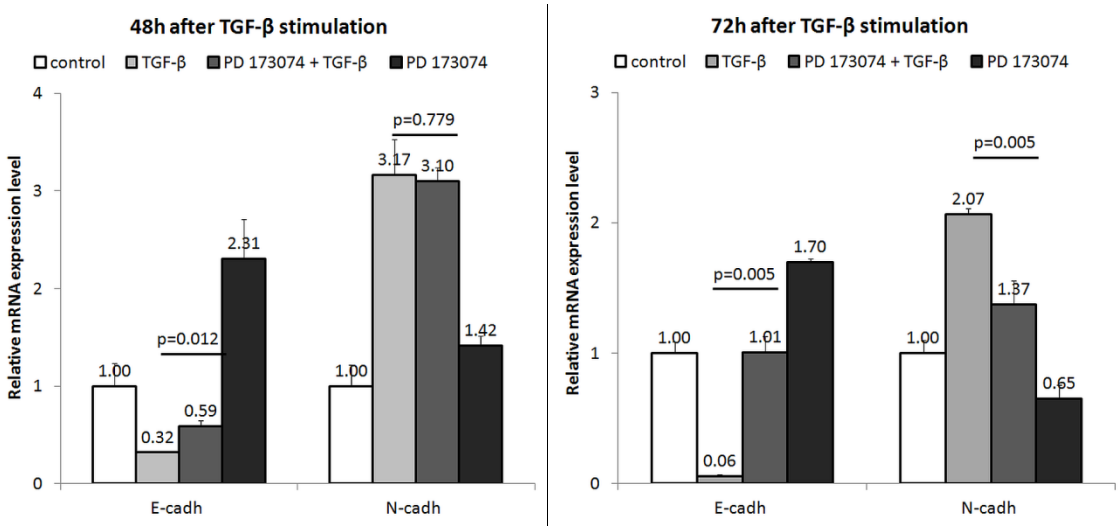

Figure 4.6.3.3. Modulation of gene expressions by PD173074 in TGF-β1 stimulated HK-2 cells: E-cadherin and N-cadherin relative mRNA expression levels.

MMP2 and MMP9

MMP2 responded stronger than MMP9 during TGF-β1 stimulation (Fig. 4.6.3.4). PD173074 succeeded to prevent high over-expressions of both MMPs, but still MMP2 remained up-regulated in comparison to control HK-2 cells.

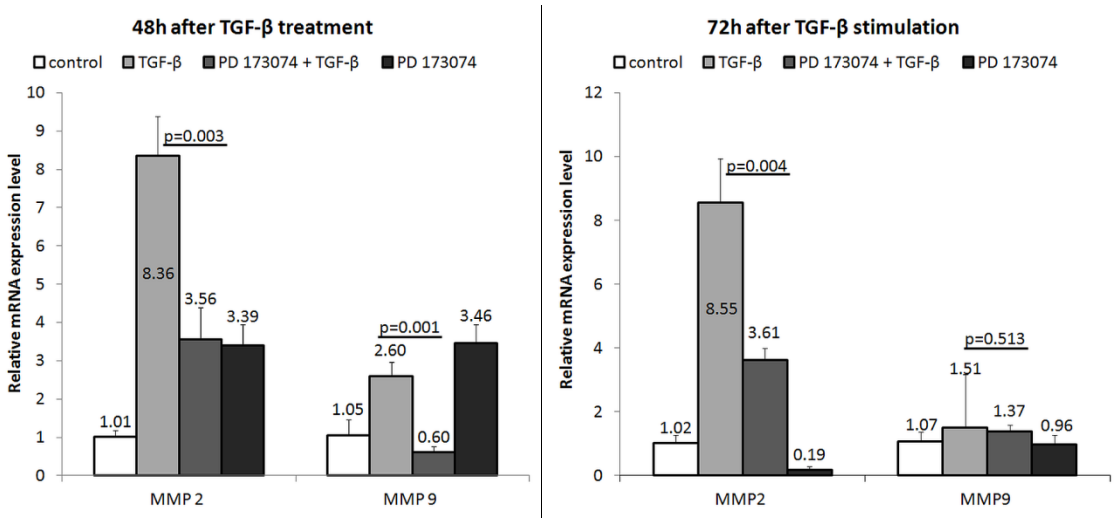

Figure 4.6.3.4. Modulation of gene expressions by PD173074 in TGF-β1 stimulated HK-2 cells: MMP2 and MMP9 relative mRNA expression levels.

Integrins (ITGA5 and ITGB1)

In response to TGF-β1 stimulation, HK-2 cells upregulated expressions of both ITGA5 and ITGB1, whereby ITGB1 mRNA levels were slightly higher compared to ITGA5. Statistically significant down-regulation of both ITGA5 and ITGB1 was observed upon PD173074 treatment in the cells stimulated with TGF-β1 (Fig. 4.6.3.5). Although ITGA5 was still overexpressed 48h after treatment, an observed downregulation was significant, and it became confident next experimental day (72h).

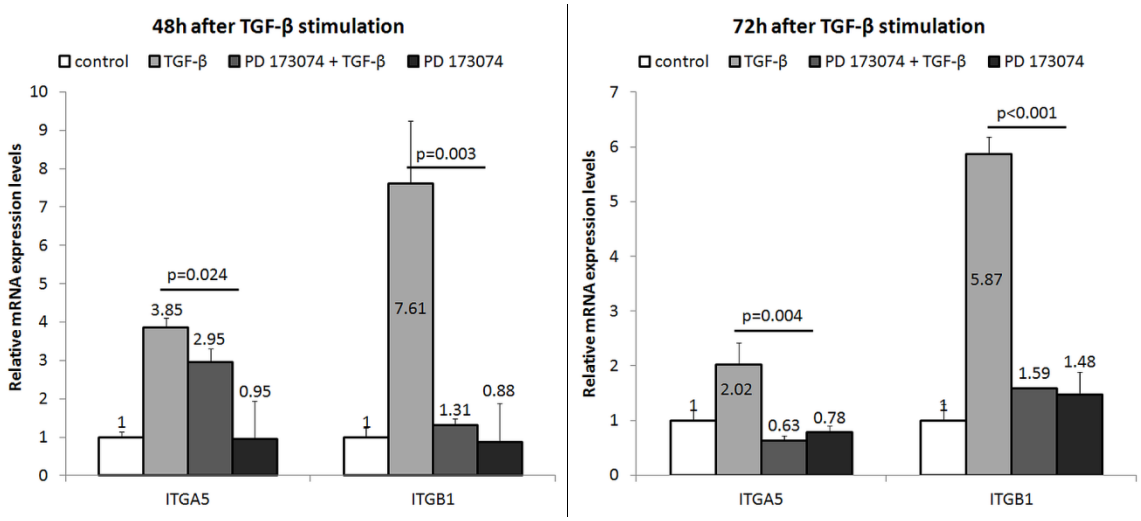

Figure 4.6.3.5. Modulation of gene expressions by PD173074 in TGF-β1 stimulated HK-2 cells: ITGA5 and ITGB1 relative mRNA expression levels.

FGFR1 and FGFR2 isoforms (IIIb and IIIc)

qRT-PCR primers for FGFR1 and FGFR2 IIIb and IIIc isoforms were not good enough to get strong conclusions. As illustrated below (Fig. 4.6.3.6), on the amplification plots GAPDH was excellent, while FGFR1 IIIb and FGFR2 IIIc were not satisfying but not so bad. Moreover, FGFR1 IIIc and FGFR2 IIIb could not be used for gene expression analysis.

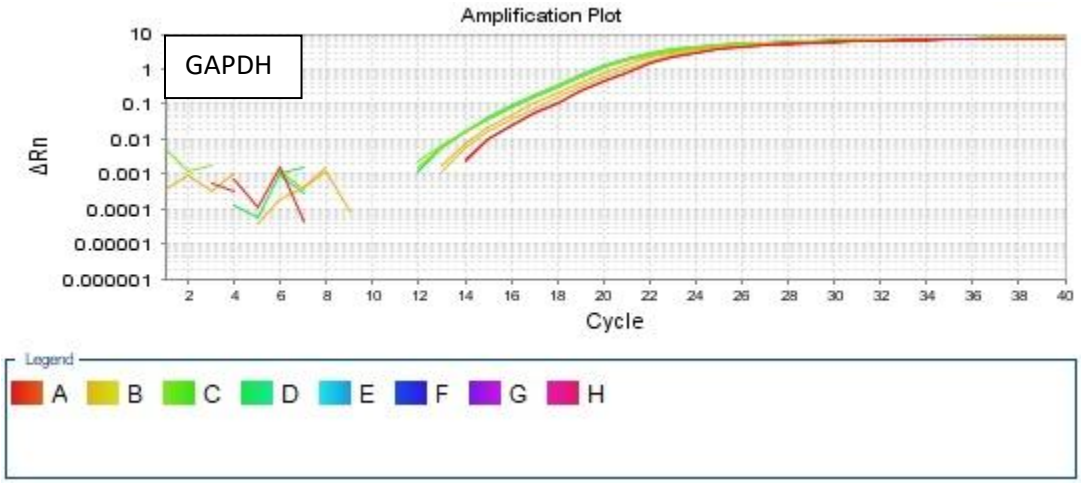

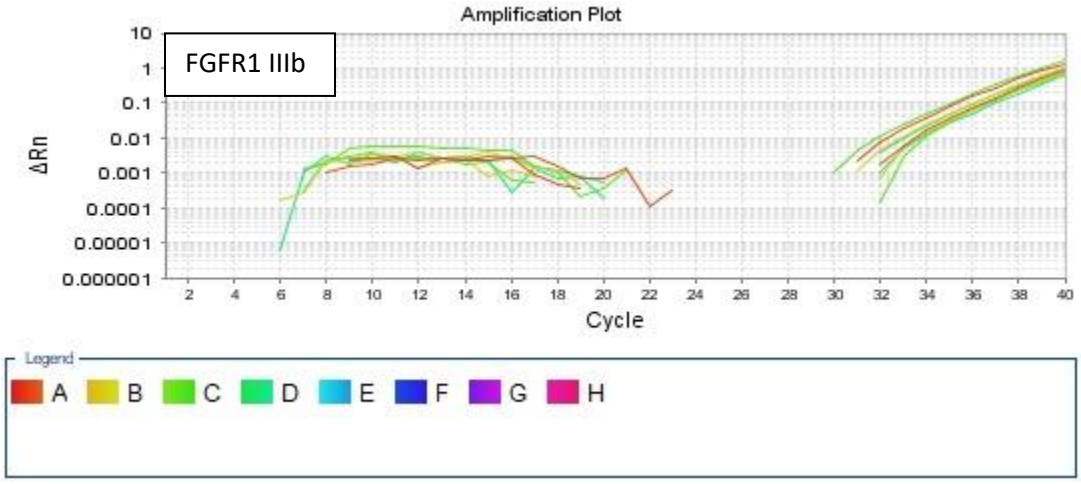

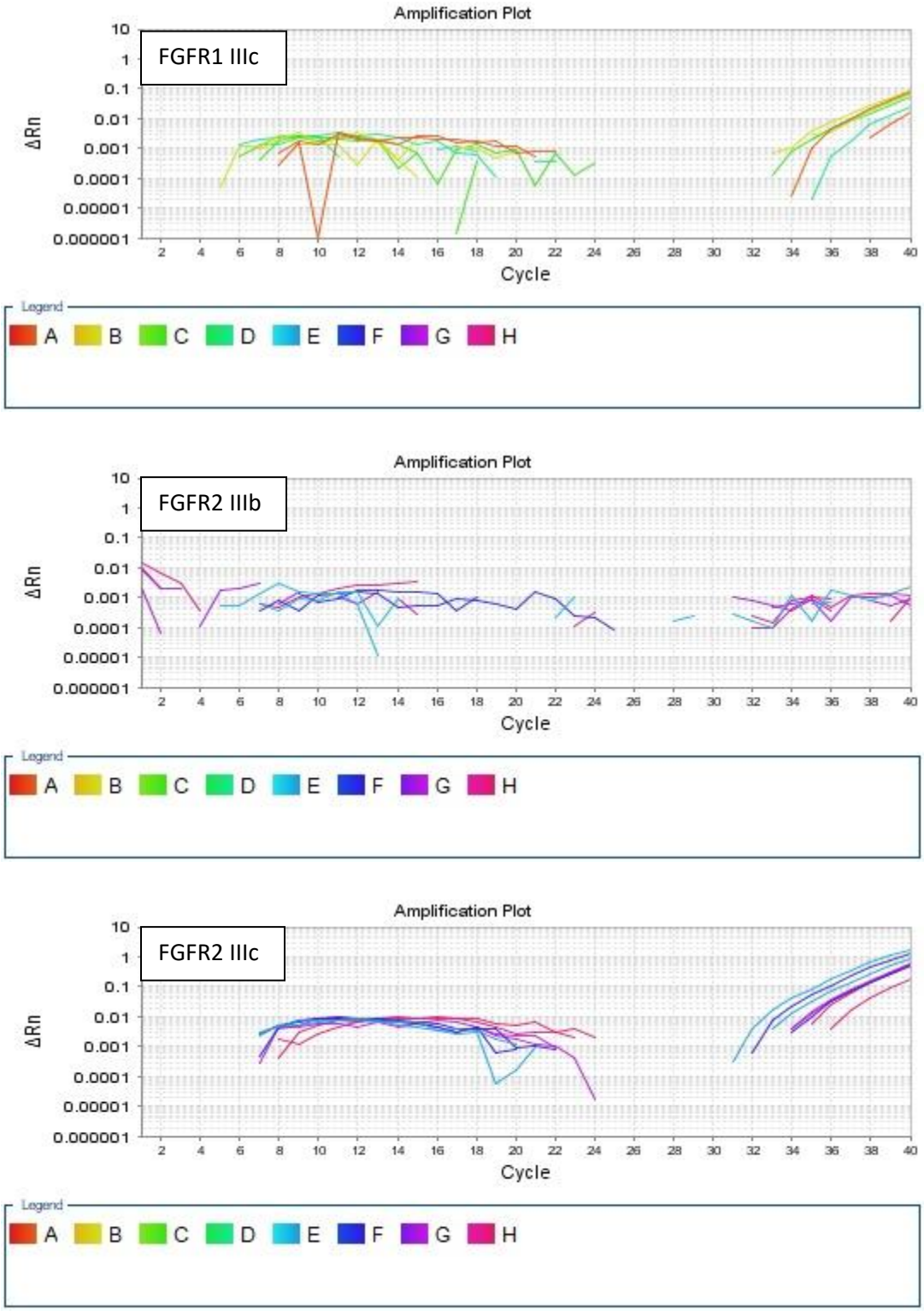

Figure 4.6.3.6. Amplification plots of GAPDH and FGFR1 and FGFR2 (IIIb and IIIc isoforms).

Thus, we presented on the Fig. 4.6.3.7 total FGFR1 and FGFR2, as well as mRNA levels of FGFR1 IIIb and FGFR2 IIIc isoforms. Despite over-expression of total FGFR1 and FGFR2, both FGFR1 IIIb and FGFR2 IIIc isoforms were downregulated upon TGF-β stimulation and were restored after PD173074 administration (Fig. 4.6.3.7).

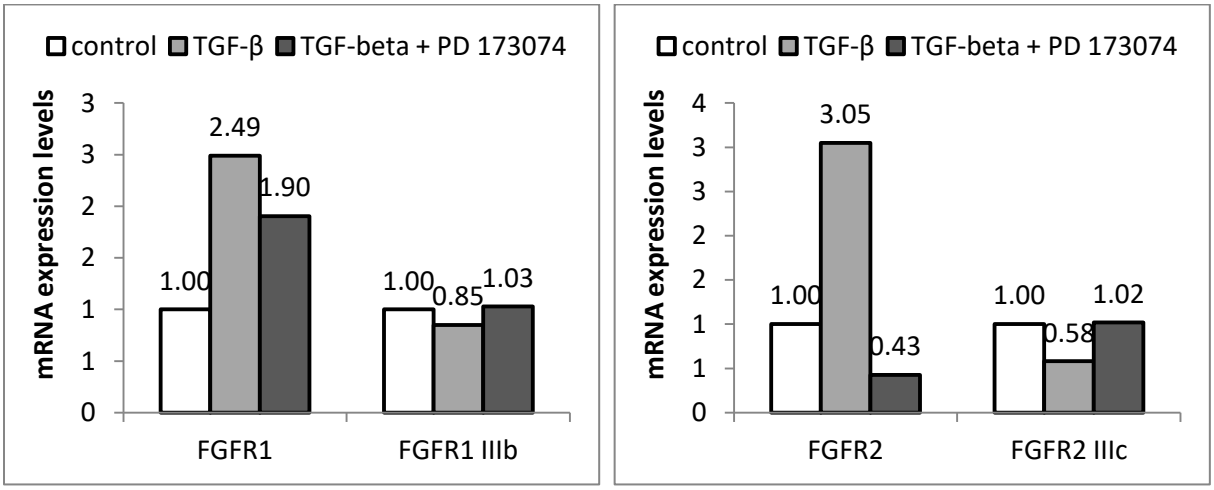

Figure 4.6.3.7. Modulation of gene expressions by PD173074 in TGF-β1 stimulated HK-2 cells: total FGFR1 and FGFR1 IIIb isoform and total FGFR2 and FGFR2 IIIc isoform - relative mRNA expression levels 48h after treatment.

4.6.4. Protein expression detected by double immunofluorecent labeling

Since previous results (with regard to cell morphology, their migration capacity and gene expressions estimated by qRT-PCR) suggested potential of FGFR inhibitor (PD173074) to suppress TGF-β1 effects on HK-2 cells, we further wanted to evaluate presence and localization of TGF-β1 down-stream effectors, such as SMAD proteins, as well as transcription factors up-regulated in response to TGF-β1/SMAD signaling (SNAIL and TWIST). Considering α-SMA and N-cadherin up-regulation upon TGF-β1 treatment and their decrement after PD173074 application in TGF-β1 treated HK-2 cells, we performed immunolabeling using these two antibodies in the experimental groups. Moreover, vimentin as an intermediate filament protein characteristic for mesenchymal cells, and Ki-67 as marker of proliferation were also explored by immunofluorescent staining.

PD173074 prevented pSMAD2 and pSMAD3 appearance in the nuclei

SMAD2 and SMAD3 proteins became phosphorylated upon TGF-β1 and were detected in the nuclear compartment as pSMAD2 and pSMAD3 either 48 (Fig. 4.6.4.1) or 72h (Fig. 4.6.4.2) after stimulation (panels on the left side).

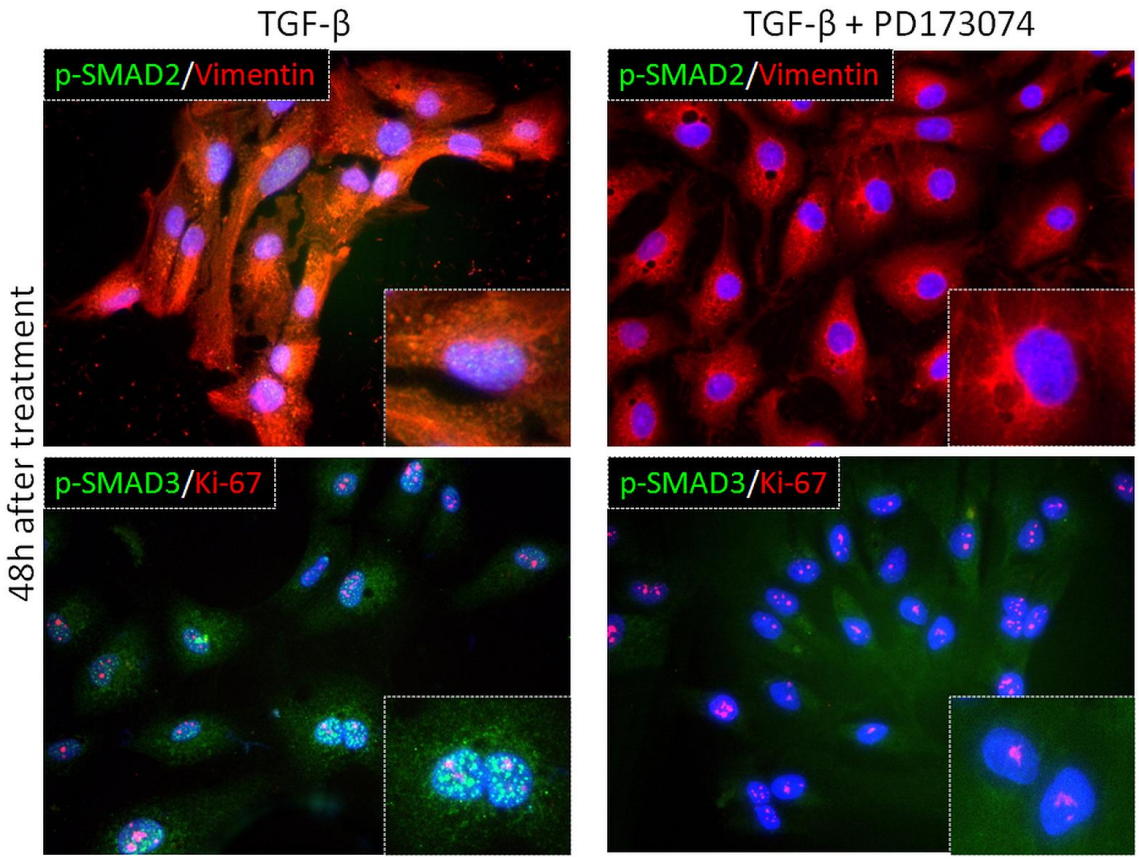

Figure 4.6.4.1. Double immunofluorescent labeling: pSMAD2/Vimentin and pSMAD3/Ki-67 – 48h after treatment.

These green fluorescent dots representing aforementioned pSMAD proteins could not be visible in the TGF-β1+PD173074 treated cells (Fig. 4.6.4.1 and Fig. 4.6.4.2, panels on the right side), suggesting that PD173074 (known as FGFR inhibitor) suppressed TGF-β1 signaling through inhibition of SMAD dependent downstream actions.

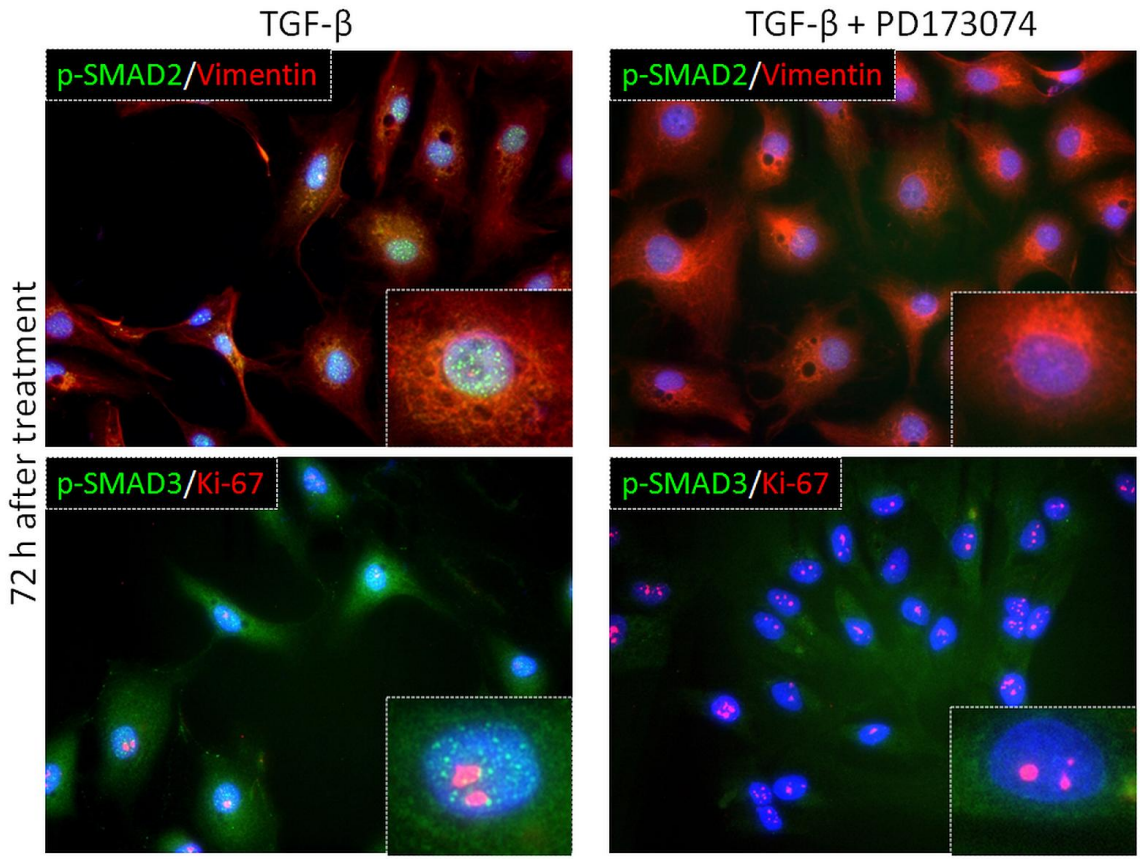

Figure 4.6.4.2. Double immunofluorescent labeling: pSMAD2/Vimentin and pSMAD3/Ki-67 – 72h after treatment.

Since PD173074 acts as small ATP competitive inhibitor of tyrosine/kinase receptors it was not clear why serine/threonine dependant phosphorylation of SMAD proteins was affected by administration of PD173074. Thus, we decided to look at even earlier time point and performed immunolabeling 24h after stimulation with TGF-β1 alone and with TGF-β1+PD173074. Surprisingly, pSMAD3 was detected in the cytosol, but not in the nuclei, in both experimental groups (Fig. 4.6.4.3), indirectly implicating that PD173074 did not cross-react with serine/threonine dependent SMAD phosphorylation. Possible explanation for later disappearance of pSMAD3 from the cells treated with TGF-β1+PD173074 could be that prolonged effect of PD173074 prevents nuclear translocation of pSMAD3 and stimulates its degradation in the cytosol.

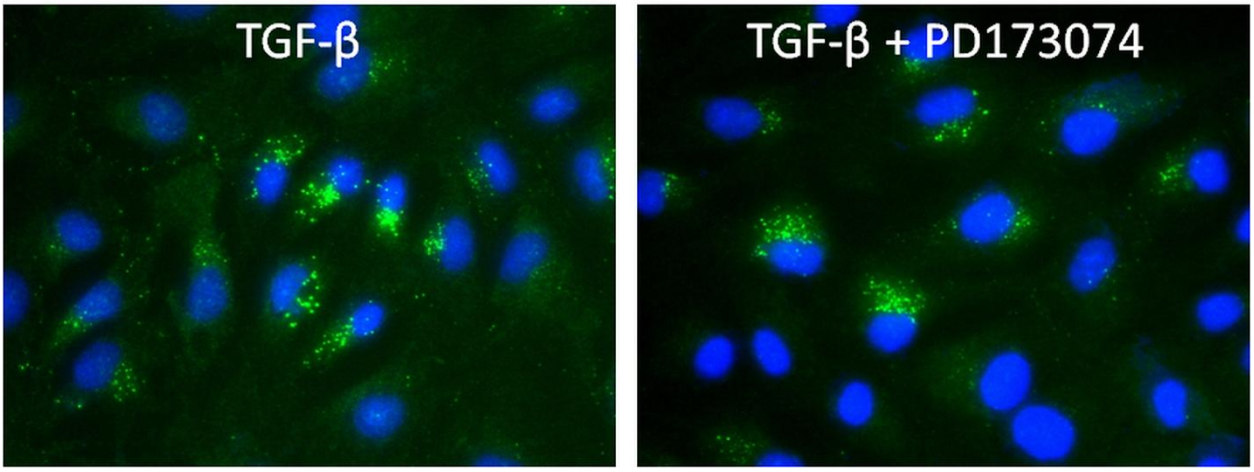

Figure 4.6.4.3. Immunofluorescent labeling of pSMAD3 in HK-2 cells 24h after treatment with TGF-β1 alone and in addition to PD173074.

PD173074 preserved vimentin expression and did not affect cell proliferation capacity

Although vimentin is known as intermediate filament protein of mesenchymal cells, it is constitutively expressed in normal human proximal epithelial cells. As shown on Fig. 4.6.4.1 and Fig. 4.6.4.2, vimentin (red) is expressed upon exposure to TGF-β1 (diffusely), as well as upon additional stimulation with PD173074 (perinuclearly).

Based on immunofluorescent staining, nuclear detection of Ki-67 (red) was observed in each cell, thus there was no influence of PD173074 on the cell proliferation (Fig. 4.6.4.1 and Fig. 4.6.4.2), although migration capacity was reduced (Fig. 4.6.2.3).

Influence of PD73074 on the presence and localization of SNAIL and TWIST

TGF-β1 stimulation caused widespread SNAIL protein expression (Fig. 4.6.4.4 and Fig. 4.6.4.5), beside its effects on significant transcriptional up-regulation of SNAL mRNA (Fig. 4.6.3.2 A and B). At 48h experimental time point, SNAIL was detected both in cytoplasm and nuclei (Fig. 4.6.4.4).

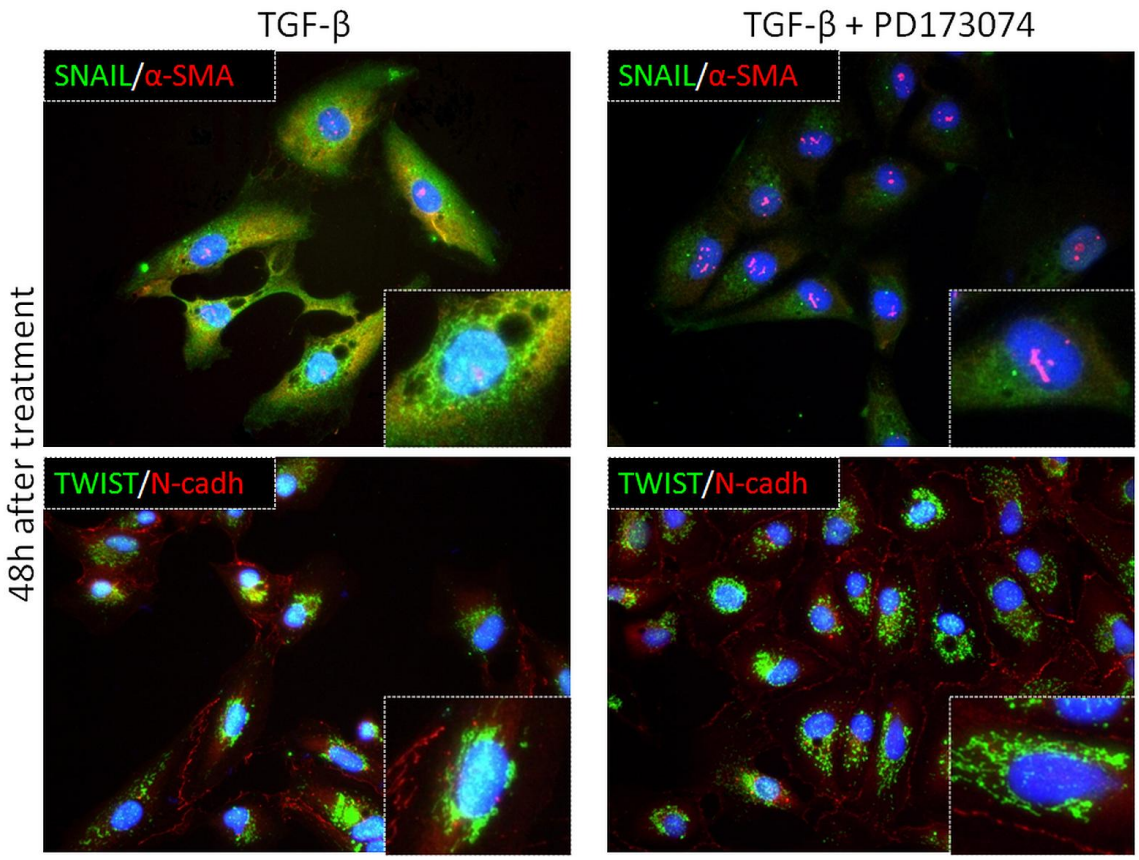

Figure 4.6.4.4. Double immunofluorescent labeling: SNAIL/α-SMA and TWIST/N-cadh – 48h after treatment.

These findings were confirmed the next day (72h), whereby an immunofluorescent signal (green) became even stronger in the nuclear compartment (Fig. 4.6.4.5). Treatment with PD173074 succeeded to prevent SNAIL protein appearance either in cytoplasm or nuclei during 48h of experimental procedures (Fig. 4.6.4.4) and that was in accordance with highly down-regulated SNAIL mRNA expression as shown on Fig. 4.6.3.2 A. However, 72h upon treatment together with TGF-β1 and PD173074, SNAIL became slightly detectable in nuclei of few HK-2 cells (Fig. 4.6.4.5) but still more than significantly less compared to TGF-β1 treated group.

TWIST was significantly over-expressed in TGF-β1 treated group both on mRNA (Fig. 4.6.3.2) and protein level (Fig.4.6.4.4 and Fig. 4.6.4.5). Although PD173074 reduced TWIST mRNA level (Fig. 4.6.3.2, panels A and B), TWIST protein was still visible in the cells. However, it is very important to notice that at 48h TWIST was mainly detected in cytoplasm, whereby its

protein expression was also detected in nuclei of some HK-2 cells stimulated with PD173074 and TGF-β1.

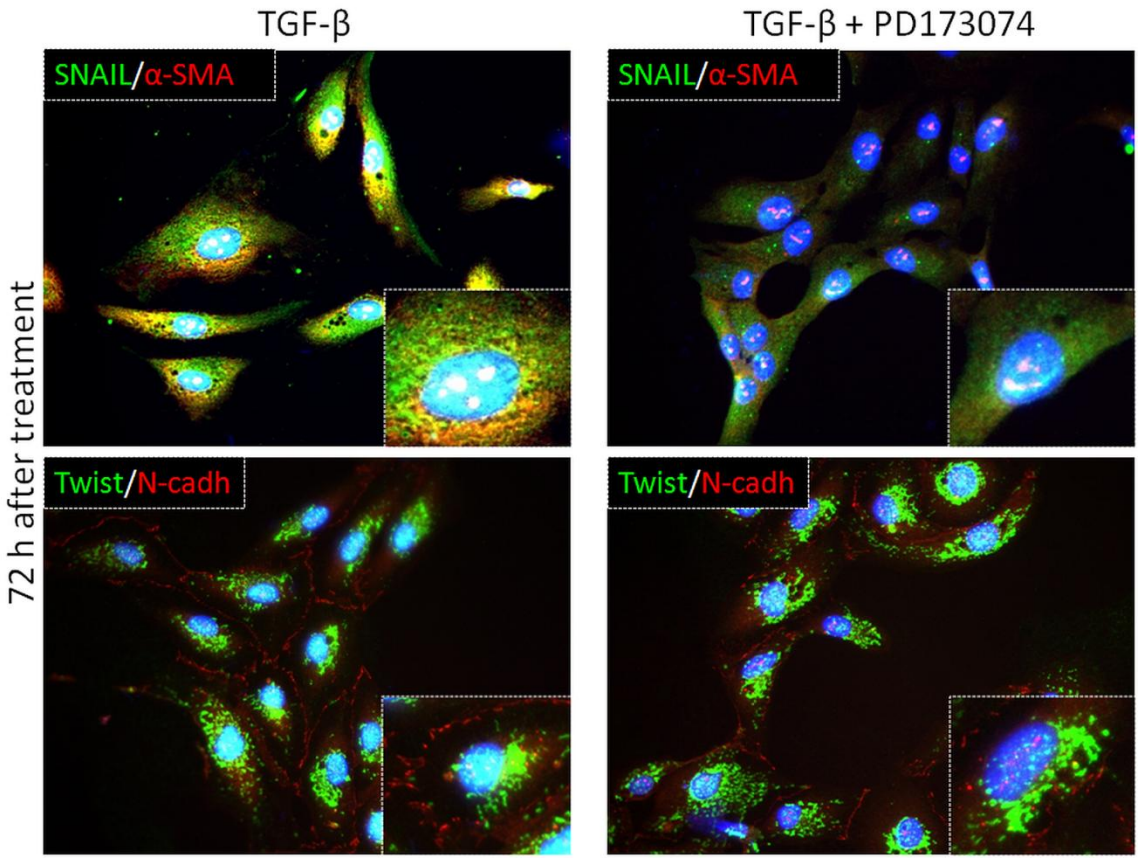

Figure 4.6.4.5. Double immunofluorescent labeling: SNAIL/α-SMA and TWIST/N-cadh – 72h after treatment.

PD173074 completely prevented α-SMA protein expression upon TGF-β1 stimulation, but did not influence N-cadherin

α-SMA, as a crucial protein expressed upon TGF-β1 stimulation, was observed in cytoplasm of HK-2 cells both 48h and 72h after TGF-β1 treatment (Fig. 4.6.4.4 and 4.6.4.5). This phenotype was not detected in the group stimulated with PD173074 and TGF-β1 together, since α-SMA was not visible on the protein level in any cell (Fig. 4.6.4.4 and 4.6.4.5). These results obtained by immunofluorescent labeling were in accordance with qRT-PCR data (Fig. 4.6.3.2 C and D).

Despite significant changes of N-cadherin mRNA observed among control, TGF-β1 and TGF-β1-PD173074 treated groups of HK-2 cells (Fig.4.6.3.3), immunolabeling discovered the presence of N-cadherin (cell surface red immunofluorecent signal) in all groups (Fig. 4.6.4.4 and 4.6.4.5), including control (not shown).

5. DISCUSSION

Progression of chronic kidney disease (CKD) remains an unsolved problem in clinical nephrology since approaches to reverse or repair chronic renal injury are not yet available (92). Independent of the underlying disease, loss of functional kidney parenchyma and tubulo-interstitial fibrogenesis are commonly observed when kidney injury progresses towards CKD (9). In this regard, epithelial-to-mesenchymal transition (EMT) in tubular epithelial cells (TECs) and consecutive G2/M arrest have been shown to determine maladaptive kidney repair in response to injury, ultimately associated with renal fibrogenesis and progression into CKD (40, 93, 94). Persistent effort to modulate CKD progression has led scientists to better understand molecular mechanisms driving renal fibrosis (95). TGF-β1 is considered as a key mediator of intrarenal EMT program and renal fibrosis (10, 96, 97). Preclinical studies found many effective strategies to attenuate EMT program in rodents (11-13), but only a few of them are applicable in humans (10). Moreover, some of the proposed therapy strategies were efficient to reduce fibrosis, but unfortunately it stimulated inflammation (98). Thus, further investigations to develop new strategies to modulate EMT program should be focused on down-stream effectors of TGF-β1 signaling pathway.

NCAM and FGFR signaling during EMT program have already been described and it has been noticed that both molecules are fundamental for EMT program *in vitro* (99-102; 24-26, 14). Moreover, their up-regulations in response to TGF- β have been also previously detected (103-107). Thus, it encouraged us to investigate aforementioned molecules in human kidneys and to evaluate their significance in fibrotic response within the renal interstitial compartment.

NCAM and renal fibrosis: its isoforms and possible transcriptional regulation

Here we presented that NCAM cells were really scarce in the normal interstitial compartment of the kidney and were almost exclusively increased at the beginning of renal interstitial fibrosis, independently of the underling diagnosis. Looking deeper at the molecular background, NCAM-140 isoform appeared to be a hallmark of these NCAM+ cells in incipient renal fibrosis since it was specifically over-expressed in those kidneys compared to NCAM+ cells found in normal interstitium. Furthermore, it has been observed that NCAM-140 isoform is also over-expressed focally in the cardiomiocytes as reaction to local scar formation in ischemic cardiomyopathy (89,

108). Since molecular characterization of NCAM expressing renal interstitial cells revealed their heterogeneity, we enrolled series of experimental procedure in order to see whether these cells could further contribute to progression of renal fibrosis or they could serve as counteracting mechanisms preventing/ameliorating such disease progression.

Taking into account that NCAM is widely expressed during embryonic kidney development in metanephric mesenchyme and its derivates and progressively disappears during maturation of structures which further forms nephron unit in the kidney through the process of mesenchymal-to-epithelial transformation (MET) (86, 109), we thought that rare interstitial NCAM expressing cells in mature adult kidney could represent population of resident metanephric mesenchymal cells with self-renewing and stem like properties. However, it was hard to perceive possible origin of increased NCAM+ cell population within the diseases kidneys with early interstitial fibrosis. Thus, there were several possible explanations for this phenomenon. I might be that an increased number of NCAM+ renal interstitial cells arise from enhanced proliferation of resident NCAM+ cells, however the question is whether these resident cell have such high proliferation capacity to fill abundantly the interstitial compartment as observed in early stages of renal fibrosis. The second possibility is that NCAM molecule appears on the surface of some kind of fibroblasts, such heterogeneous within the fibrotic interstitium, during the course of renal fibrosis. It could be supported by the presence of HE4 protein in some NCAM+ cells, since HE4 is newly labeled as marker of activated fibroblasts (28). However, the most interesting question for us was whether an increased number of NCAM+ interstitial cells could represent transient phenotype of tubular epithelial cells undergoing EMT and serve as an evidence of *in vivo* EMT process within the kidney following tubular injury. This question looks the most exciting, but this answer is the most difficult to be given. Although EMT is widely investigated by numerous researchers in *in vitro* studies (17), there is a lacking of evidence that such process contribute to fibrogenesis *in vivo*. This hypothesis made controversies and polemics in science (110, 111). Despite these controversial opinions with regard to existence of EMT driving fibrosis *in vivo* (110, 111), *in vitro* studies could be helpful in determination of molecular function and could provide more conclusive and confident data in order to clarify significance of previously observed phenomenon.

Here we used an established *in vitro* model of EMT induced renal fibrosis, applying TGF-β1 as a major trigger of EMT program in cultured proximal tubular epithelial cells of the kidney (HK-2 cells). We followed various EMT events at several time points during 96 hours and carefully monitored changes, including gene expression levels. Thus, the robust induction of all three NCAM isoforms was observed with the highest mRNA levels 24h after EMT program stimulation. In accordance with our results are the findings arisen from the study of Lehembre et al (14). Moreover, it has been also previously reported that TGF-β is involved in modulation of NCAM expression, inducing up-regulation of all three major NCAM isoforms, mainly NCAM-140, but also in a lesser extent two others (NCAM-120 and NCAM-180) (103-105).

TGF-β, the major activator of EMT program, seems to act by stimulating the transcriptional activity of the NCAM gene (104). There are several transcription factors with potential binding site to NCAM promoter region (NF-kappa B, PAX, HOX, RUNX1). However, it seemed that RUNX1 could be directly involved in the stimulation of aberrant NCAM expression, since other known transcription factors are usually constitutively expressed, while RUNX1 follows the trend of NCAM-140 up-regulation (89). Thus we proceeded to the next investigation step and performed kidney tissue lysates of the 16 patients suffered from various glomerulonephritides and glomerulopathies whose biopsies revealed different degrees of interstitial fibrosis. Here we examined expression of NCAM-140 isoform, as well its potential transcription factor RUNX1. qRT-PCR analysis discovered increasing relative mRNA expressions of both NCAM-140 and RUNX1 with increasing IRF stages, implicating that NCAM-140 up-regulation in severely affected kidneys with IRF can be result of over-expression of RUNX1 gene. Furthermore, PRMT1 as a known epigenetic positive regulator of RUNX1 is also highly expressed in advanced IRF stages following the same dynamics of both NCAM-140 and RUNX1 mRNA expressions. Unfortunately, these observations with regard to NCAM-140 expression levels are not in accordance with the finding of immunolabeling using NCAM antibody, since in morphologically NCAM+ cells were most numerous in the less severe IRF in the kidney biopsy samples. In order to try to explain this inconsistency between NCAM mRNA levels and protein detection among various IRF stages, afterward one more gene is explored on the mRNA level – RUNX1T1 as a putative repressor of RUNX1. Surprisingly we found nearly 400 times fold increase in RUNX1T1 in the most advanced IRF stage. Despite obvious increase in PRMT1 (159 times fold increase) and RUNX1 (79 times fold increase), it is very likely that huge RUNX1T1

over-expression overcomes the possible effects of NCAM-140 inducers. Although RUNX1T1 has not been well studied alone yet, its function is usually considered through the roles of RUNX1/RUNX1T1fusion oncoprotein. Nevertheless, these findings have to be further explored and it is possible that distinct explanations for currently acquired data in our study would be available.

NCAM signaling pathways

NCAM is not a simple adhesion molecule, but it is rather involved in signaling cascades essential for many physiological processes and could be also aberrantly activated during variable pathological conditions (89, 101, 108).

Since NCAM was apparently up-regulated early upon response to TGF-β1 and considering its potential signaling not only by NCAM-NCAM homophilic bindings but also its signaling through the activation of FGFR signaling pathway, we tried to find any potential relationship between NCAM and FGFR during fibrotic response in kidney and their association with EMT program. Indeed, here we present that both NCAM and FGFR1 are rapidly over-expressed after EMT program induction, implicating their role in the initiation of EMT in proximal tubular epithelial cells (TECs). Although all three NCAM isoforms were up-regulated during EMT program in TECs, the most prominent was the expression of NCAM-140. Furthermore, applying qRT-PCR we also revealed significant increase of NCAM-140 and FGFR1 mRNAs with progression of renal fibrosis in human biopsy samples. Lehembre et al. also showed that upon TGF-β EMT induction, NCAM starts to be more expressed, specifically its 140kDa isofrom (14). These findings were the triggers for subsequent investigation steps stimulating us to further clarify their relation to other molecules known to be involved during NCAM and FGFR signaling. Beside heterophilic NCAM interaction with FGFR (cell-cell interaction), it is also involved in cell-matrix interactions through the interactions with integrins. Thus, ITGB1 (integrin β1) was found to be important for neuroblastoma cell migration through the interplay with NCAM-140 (112). Furthermore, it has been illustrated that this process depends on MAPK/ERK activation. Since ERK is the point of convergence of NCAM-NCAM and NCAM-FGFR pathways, the investigator applied MAPK and FGFR (50 nM PD173074) inhibitors. They found that NCAM/integrin β1dependant cell migration was FGFR independent, although requires MAPK/ERK signaling cascade that might be induced through the other mechanisms

including NCAM-NCAM interactions (112). However, in our experiments it has been shown enhanced HK-2 cell migration toward TGF-β1 could be significantly suppressed by PD173074, thus leading us to conclude that FGFR signaling play an important role in cell migration during EMT program induced in HK-2 cells. Since in the absence of FGF ligands, a highly over-expressed FGFR1 could be stimulated only by interaction with NCAM (up-regulated in the same manner, after TGF-β1 induction), we concluded that forced migration of HK2-cells undergoing TGF-β1 induced EMT is highly dependent on NCAM/FGFR1 signaling pathway. In parallel, performed qRT-PCR analysis shows also significant decrease of ITGB1 upon FGFR signaling blockade. In human biopsy samples, ITGB1 follows the same trend of expression as NCAM-140 and was highly expressed in the most advance fibrosis stage. Beside, stimulation of cell migration undergoing EMT, integrity of NCAM/FGFR1 signaling appeared to be important for the induction and maintenance of mesenchymal morphological and molecular traits, and will be further discussed. Since β1 usually makes a complex with α5 subunit of integrin (113), and considering an involvement of α5 integrin in fibroblast activation and contribution to progression of renal fibrosis (5), we became encouraged to assess α5 integrin mRNA expression during EMT in vitro and renal fibrosis in human biopsy samples. It has been found here that ITGA5 mRNA expression levels increase during EMT program and could be sufficiently down-regulated by inhibition of NCAM/FGFR signaling. Moreover, in human kidneys, mRNA levels of ITGA5 correlate with the degree of interstitial fibrosis. Thus, in the interstitium widely affected with fibrosis the levels of ITGA5 were the highest. Integrin α5 is already found to be significantly up-regulated in response to TGF-β in murine tubular epithelial cells (114). Since α5 subunit defines binding site to ECM components of α5β1 integrin, it has been proposed that it has high affinity to fibronectin (15, 113).

Moreover, several studies also suggested that both NCAM and FGFR are fundamental for EMT in vitro. However, it has been also indicated that alternative splicing of FGFRs' Ig3 (D3) domain generates IIIb and IIIc isoforms influencing distinct affinity of FGFRs to their FGF and other ligands (83). NCAM specifically binds by its second FNIII domain to Ig2 and Ig3 FGFRs domains (24, 26). However, since FGFR isoforms differ in Ig3 domain, researchers further found the NCAM interacts with IIIc FGFR isoforms (24, 26, 115).

FGFRs IIIb isoforms are characteristically found in epithelial cells, whereas IIIc isoforms are known to be expressed by mesenchymal cells and during carcinogenesis, leading to disease progression (116, 117). Thus, it was reasonable to further consider expressions of specific FGFR isoforms during EMT program. It has been noticed TGF-β1 induced switches from IIIb to IIIc isoform (116). However, they found that FGFR2 IIIb isoform is characteristically expressed by NMuMG cells, and EMT induced acquisition of FGFR1 IIIc isoform. It indicates that not only alternative splicing changes during EMT, but also FGF receptor type could be affected. Accordingly, in our study we have tried to explore the influence of TGF-β1 on the expression levels of alternatively spliced FGFR1 and FGFR2 isoforms (IIIb and IIIc). However, we have not been able to make strong conclusions because the lacking of evidence for mRNA expressions of FGFR1 IIIc and FGFR2 IIIb isoforms, but we suggested that both FGFR1 IIIb and FGFR2 IIIc isoforms could be down-regulated in response to the EMT program induction. Nevertheless, since we observed over-expression of both total FGFR1 and FGFR2 mRNAs, it could be indirectly concluded that these over-expressions resulted from FGFR1 IIIc and FGFR2 IIIb isoforms up-regulation (since the second isoform of both FGFRs were down-regulated). Moreover, these changes were almost completely restored by inhibition of NCAM/FGFR signaling (by PD173074), implicating that specific FGFR isoforms are required for the interaction with NCAM and consecutive signaling during EMT of HK-2 cells.

Molecular background of renal fibrosis in human kidneys: an involvement of TGF-β signaling pathway

TGF-β1 has been widely investigated in many *in vitro* and *in vivo* models of organ fibrosis, including those in kidneys. However, the morphological evidence of the existence and contribution of this signaling pathway to human kidney fibrosis *in vivo* have not been completely clarified yet. Hence, here we were able to present that major down-stream signaling effectors of TGF-β1 are expressed in many epithelial structures in human kidneys either morphologically preserved or damaged. An abundant constitutive expression of pSMAD2/3 is already found in distal tubules and collecting ducts in human kidneys (118). However, they found co-localization of pSMAD2/3 and SNAIL with vimentin in tubules exhibiting EMT like features in human kidney transplants (118). Beside constitutive expressions of SMADs and SNAIL, our study revealed similar expression patterns of both SMAD2 and SNAIL as found in kidney grafts, and

they were significantly related to chronic renal parenchymal damages (tubular atrophy and interstitial fibrosis) influencing excretory renal functions with impaired response and leading to acquisition of more advanced CKD stages. It has been also shown that SNAIL is not simply related to morphological EMT features in kidney transplants (fibrosis), but was found to be significantly related to graft dysfunction (low eGFR levels) (118). Our study also revealed that activated SMADs (pSMAD2/SMAD3) are expressed in lesser extent than non-phosphorylated SMADs. Indeed, we did not find constitutive expression of pSMAD2/SMAD3 in human kidneys (by immunofluorescent labeling), but rather observed them in epithelial cells of some tubuli within the core biopsy. These tubuli also expressed MMP2 and MMP9, implicating an early disturbance that would probably lead to further tubular damage involving degradation of tubular basement membrane and providing access of transforming epithelial cells to the interstitial compartment, suggesting their potential to contribute fibrogenesis (an active process of ECM remodeling/production). An induction of MMP2 and MMP9 has been already found in epithelial cells as reaction to FGF-2 stimuli (119).

SNAIL shares the same pattern of expression as SMAD2 in human kidney tubulointerstitial compartment, but also has an additional involvement in glomerular damage. Indeed, in parallel with affection of excretory function of the human kidney, SNAIL also contributes to impaired podocyte function. Thus, SNAIL expression by podocytes leads to appearance of nephrotic range proteinuria values. These findings did not surprise us since it has been previously shown that in nephrotic rats Snail is highly expressed in podocytes either on protein or in mRNA levels (120).

The underling mechanism considers Snail induced repression of nephrin synthesis, as one of the important protein constituent of slit-diaphragm between glomerular podocytes. Additionally, there are evidences that also high glucose levels in mice are able to induce podocytes' Snail over-expression, subsequently leading to down-regulation of both nephrin and podocin (121). However, both studies found that Wnt/β-Catenin pathway act up-stream of Snail induction in podocytes (120, 121), although is known that SNAIL can be induced by TGF-β as well (122). Induction of Snail is sufficient to induce renal fibrosis in animals, and high mRNA SNAIL levels are found in fibrotic human kidneys (123, 124). For the first time here we detected morphological evidence of the SNAIL involvement in chronic tubulointerstitial damages and

approved that aberrant SNAIL expression by podocytes could be responsible for nephrotic range proteinuria in patients.

Our results that came from experimental induction of EMT program in tubular epithelial cells of the human kidney and that were confirmed in human biopsy samples suggested an involvement of both NCAM and FGFR in initiation step of renal fibrosis. In the same setting, other molecules that are known to be affected in fibrotic response were also examined. Thus, undoubtedly we found significant increase in mRNA levels of ITGA5 (encoding integrin α5) and ITGB1 (encoding integrin β1) both after EMT program induction *in vitro* and in the whole human kidney tissue lysates. By increased severity of renal interstitial fibrosis, a gradual increment of both integrins' mRNA was observed. α5β1 integrin is known marker of *in vitro* EMT (4), and is also previously detected in fibrotic kidneys (5, 85). α5β1 integrin cooperates in cell adhesion, proliferation and differentiation and plays a role in extracellular matrix assembly. When expressed by fibroblasts, α5β1 integrin promotes acquisition of a myofibroblastic phenotype with typical α-SMA expression pattern (5, 15, 14; 112). In EMT model, it has been shown that α5 integrin knock-down results in attenuation of α-SMA (induced by TGF-β) but does not affect cells morphology (114), suggesting that α5 integrin could be involved in fibroblast activation. It has been shown that TWIST, acts up-stream of the α5 integrin induction during EMT program (125).

Interstitial fibrosis and tubular atrophy are morphological hallmarks of CKD. The degree of affected tubulointerstitial compartment directly influences kidney function and serves as prognostic marker for renal failure. Fibroblasts are thought to be the main effectors cells in renal fibrogenesis. They reside within kidney cortex, as well as in perivascular area. However, fibroblasts do not have unique molecular traits but rather represent highly heterogeneous population situated within fibrotic area. Their activation leads to excessive production of ECM components. During activation some of these fibroblasts start to express α-SMA, a prototypic characteristic for myofibroblast. Some other fibroblasts could express FSP-1 and they are considered to be important in early phase of fibrogenesis (119, 126). FSP-1 is a cytoskeletal protein that belongs to calmodulin-S100-troponin C superfamily of intracellular calcium binding proteins, and is known to be expressed by mesenchymal cells influencing cell motility (127). FSP-1 stimulates fibronectin and collagen production. Numerous experimental procedures

demonstrated an induction of α-SMA and FSP-1 towards TGF-β1 stimulation. Our findings revealed up-regulation of both α-SMA and FSP-1 in human kidney samples with various degree of renal interstitial fibrosis. However, the highest over-expression of FSP-1 was found in early fibrosis stage (IRF-1), whereas α-SMA showed the highest relative mRNA level in the most severe fibrosis stage (IRF-3).

Modulation of NCAM/FGFR signaling – relevance for renal fibrosis and implication for therapy

NCAM induced FGFR signaling has been widely studied, mainly in neural tissues and cancer cells (14, 24-27, 99, 100, 115). However, there is a lacking of evidence for the contribution of their interplay to fibrogenesis, although several studies confirmed that both molecules can be separately involved such process (88, 106, 128). Thus, FGFR is widely studied in many fields of research, including fibrosis. Nevertheless, according to available data and our knowledge, involvement of NCAM expressing cells in renal fibrosis is only considered by our research group and also by Vansthertem and co-workers (85, 88, 129). Thus, for the first time, here we present a functional significance of NCAM and FGFR co-operation in the induction of renal fibrosis, mediated by TGF-β1.

Hence, based on the previously discussed results from the beginning of our research we further suspected that modulation of NCAM/FGFR1 signaling can suppress EMT of human tubular epithelial cells (TECs), currently used as an established in vitro model of renal fibrosis and a good starting point for experiments that can be able to clarify molecular pathway underling such process.

Firstly, we observed that morphologically TECs do not develop mesenchymal traits (spindle shape morphology) when treated with FGFR inhibitor (PD173074), despite an influence of TGF-β1. This observation implicates an important role of NCAM/FGFR signaling in acquisition of mesenchymal characteristic of epithelial cells. Thus, we decided to explore important molecules that influence cell morphology such as intermediate filaments (vimentin and α-SMA - characteristic for mesenchymal cells and activated fibroblasts) and those involved in tight-junction formation (E-cadherin and N-cadherin) (130-132).

However, HK-2 cells (human proximal tubular epithelial cells) share many features characteristic for the majority of epithelial cells, but also exhibit many differences, especially with regard to expression of vimentin, E-cadherin and N-cadherin.

Vimentin

Normal HK-2 cells express vimentin that is usually considered to be characteristic for mesenchymal cells. However, normal HK-2 cells makes perinuclear aggregation of vimentin intermediate filaments, while upon injury vimentin filaments spread through the whole cytoplasmic compartment making a fine network appearance (133). Thus, in order to follow vimentin expression during EMT changes in HK-2 cells, careful consideration should be done. Indeed, appearance of vimentin in cells is not a sign of EMT because normal cells also have this filament protein, but the pattern of its expression could suggest cell injury and the widespread appearance in the cytoplasm should be considered as mesenchymal characteristic. In our experiments, vimentin was found to be abundantly expressed in HK-2 cells towards TGF-β1 stimulation. However, FGFR inhibitor restored the pattern of vimentin expression to perinuclear localization, as also observed in control.

E-cadherin and N-cadherin

Moreover, tubular epithelial cells in humans have several specificities with regard to expression of cadherins. It is widely accepted that switch from E-cadherin to N-cadherin culminates toward EMT. However, normal proximal tubular epithelial cells in human and rats already express N-cadherin, instead of E-cadherin that makes tight-junctions in many epithelial structures including proximal tubuli in mice. According to our results, mRNA level of N-cadherin was up-regulated upon EMT program induction and was normalized by FGFR inhibitor application, whereas immunofluorescence did not show any difference with regard to expression patterns. Thus, N-cadherin was almost identically visible on the cell membranes of HK-2 cells in all experimental groups. On the other hand, E-cadherin mRNA levels were repressed by TGF-β1 stimulation, while inhibition of NCAM/FGFR signaling in these cells normalized E-cadherin mRNA levels. These results could support the findings in the literature that upon EMT induction epithelial cells switch their cadherin phenotype by increased expression of N-cadherin and decreased E-cadherin levels. Moreover, it has been shown that loss of E-cadherin induces NCAM up-regulation (14).

However, here we present that NCAM up-regulation in response to TGF-β1 precedes E-cadherin down-regulation.

SNAIL, SLUG and TWIST

SNAIL superfamily (including SNAIL and SLUG) and TWIST transcription factors are fundamental in the induction of EMT. They regulate gene expression, stimulating those characteristic for mesenchymal cells and suppressing genes defined to be characteristic for epithelial cells. These transcription factors can be induced by several up-stream factors, including TGF-β1 (134, 135). However, transcriptional induction of SNAIL upon TGF-β1 stimulation is direct consequence of SMAD2/3 phosphorylation which making a complex with SMAD4 translocate in the nuclear compartment stimulating SNAIL transcription. On the other hand, induction of TWIST transcription towards TGF-β1 is also regulated by STAT3 (134). Down-stream targets of TWIST and SNAIL family are numerous, but in the EMT context the most important is repression of E-cadherin. This repression is a direct consequence of SNAIL phosphorylation, whereby TWIST acts through the SLUG up-regulation which than in turns suppress E-cadherin (136). Altogether, it becomes apparent that SNAIL family of transcription factors are key point convergence during EMT that further induce changes in cells phenotype influencing their behavior.

In our investigation, all aforementioned transcription factors were induced by TGF-β1 and afterwards significantly down-regulated by inhibition of NCAM induced FGFR signaling, as obtained by qRT-PCR. Moreover, applying double imunofluorescence we found vary prominent SNAIL and TWIST expression both in cytoplasm and nuclei of TECs undergoing EMT, as previously also detected for SNAIL protein upon TGF-β induced EMT of mammary epithelial cells (137). However, administration of PD173074 succeeded to almost completely prevent SNAIL expression, while TWIST appeared to less sensitive to the NCAM/FGFR inhibition. Thus, despite inhibition of FGFR signaling TWIST was still visible on the protein levels, but its subcellular localization was mainly detected within cytoplasm, indirectly implicating a functional inhibition of TWIST putative roles during EMT.

Beside TGF-β1, SNAIL can be also induced in response to receptor tyrosine kinases (RTKs) signaling, activated by HGF, FGF, or EGF, acting through the RAS-MAPK or PI3K-Akt

pathways (135). It further expands our findings, suggesting a following putative axis of gene regulation: TGF-β1/NCAM/FGFR1/SNAIL, meaning that upon TGF-β stimulation SNAIL can be induced through the pSMAD2/3/4 manner and additionally by the induction of RTKs signaling (NCAM/FGFR1 signaling). The impotence of our findings can be supported with previous report where it has been shown that signaling via MAPK or PI3K are necessary and sufficient to regulate EMT in collaboration with TGF-β (138).

α-SMA and FSP-1

Both α-SMA and FSP-1 are considered as EMT markers and can be induced by TGF-β1 (23). Robust induction of both molecules was observed upon TGF-β1 simulation and was successfully suppressed by inhibition of NCAM/FGFR signaling in TECs. Furthermore, FSP-1 is found to be involved in the regulation of cell migration (127). Thus, beside ITGB1 modulation by PD173074, it might be that FSP-1 down-regulation is also one of the underling mechanisms of reduced cell capacity to migrate upon FGFR1 inhibition. Morphologically, α-SMA diffusely occupied cytoplasmic compartment upon induction of EMT program and could not be detected on the protein level in any cell treated with PD173074, implicating an important role of NCAM/FGFR signaling in the rearmament of cell cytoskeletal structure. Considering that α-SMA is apparently expressed during fibroblast activation, as well as an important role of FGFR signaling in the same way (139), NCAM signaling through FGFR activation appears to be mechanisms driving acquisition of mesenchymal traits of tubular epithelial cells.

Matrix-metalloproteinases (MMP2 and MMP9)

MMPs, especially gelatinases MMP2 and MMP9 are up-regulated in response to tubular injury. Functionally, they promote degradation of basement membrane, thus providing an access of injured tubular cells to the interstitium, thereby facilitating cell migration (119, 140). Restoration of MMP2 an MMP9 mRNA levels after treatment with PD173074, could be also a background feature of reduced cell motility in this experimental group, compared to cells treated with TGF-β1 alone.

Integrins (ITGA5 and ITGB1)

Inhibition of NCAM/FGFR signaling leads to significant modulation of integrins' expression initially induced by TGF-β1. However, ITGA5 responded slowly to such signaling modulation, since during the first two days mRNA levels were still higher than in controls but the third day after treatment it also normalized mRNA, similar to ITGB1 response. Since these integrins are considered to be hallmarks of EMT, their down-regulation which was also followed by cell morphology changes (reversal of spindle shaped to epithelial) and reduced migration capacity could be accepted as signs of MET (mesenchymal to epithelial transformation) observed upon inhibition of NCAM/FGFR signaling.

Furthermore, it has been previously shown that ITGB1 is involved in the regulation cell migration behavior. It is known that NCAM induce cell migration through the interaction with ITGB1 (112). Moreover, an induction of ITGB1-FAK/ILK signaling axis is found to be underling mechanism of enhanced cell migration undergoing EMT induced by TWIST transcription factor (141). Thus, it might be that reduced cell migration observed upon PD173074 treatment appeared due to down-regulation of ITGB1, previously up-regulated in response to TGF-β.

SMADs

The main down-stream effectors of TGF-β are SMAD proteins. Among them, R-SMADs are fundamental for the EMT program induction. Both SMAD2 and SMAD3 phosphorylitaion induce cascade of gene reprogramming. When aberrant induction of TGF-β appears, intracellular signaling cross-talk becomes affected changing the cell fate. Thus, during EMT program, pSMAD2 and pSMAD3 translocate into nuclear compartment modulating gene expressions. These effects are manly induced by stimulation of SNAIL transcription which then triggers a wide range of gene expression changes.

SMAD phosphorylation appears upon TGF-β1 to its receptor on the cell surface. Here we detected by immunofluorescent staining the presence of pSMAD2/3 in cytoplasmic compartment 24h after TGF-β1 stimulation and found them in the nuclei next two days. Suppression of NCAM/FGFR signaling by small ATP inhibitor (PD173074) does not influence SMAD phosphorylation, as we observed pSMAD2 and pSMAD3 in the cylosol one day after treatment.

However, even next experimental day (48h) and also 72h after NCAM/FGFR signaling inhibition in cells stimulated with TGF-β1, neither pSMAD2 nor SMAD3 could be observed in cells. This finding has to be further clarified, since it is not clear why inhibition of FGFR signaling results in disappearance of pSMAD2/3. It might be this inhibition promotes ubiquitination and degradation of activated SMADs, but underling mechanisms has to be resolved.

Plasticity of EMT and opportunity for managements

Although TGF signaling triggers robust EMT activation in epithelial cells, either during wound healing and tissue repair or during carcinogenesis, a reversal of the EMT phenotype could also appear at some time point, indicating natural termination of EMT and subsequent acquisition of epithelial traits again or effects of induced pharmacological inhibition, indicating a high degree of plasticity in the EMT process (136).

TGF-β1, a major inducer of EMT program and fibrosis, has been previously shown that induces over-expression of FGFR family members and stimulates NCAM up-regulation (88, 105). Our previous research revealed increased NCAM expression in interstitial kidney compartment in the initial renal fibrosis with consecutive disappearance in later fibrosis stages in human kidneys (85). These observations encouraged us to further consider possible role of NCAM molecule in kidney fibrosis, especially during the initiation of such process. Despite controversial opinions with regard to existence of EMT driving fibrosis *in vivo* (110, 111), *in vitro* studies could be helpful in determination of molecular function and could provide more conclusive and confident data in order to clarify significance of previously observed phenomenon. Since we also detected that NCAM expressing renal interstitial cells in human kidneys occasionally express FGFR molecule (129), and considering their potential cross-talk with subsequent signaling stimulation (24-26, 99-101), we here explored for the first time significance and involvement of NCAM/FGFR interplay during EMT program in cultured TECs.

NCAM and FGFR signaling alone have already been described during EMT program and it has been noticed that both molecules are fundamental for EMT *in vitro* (14, 25, 99, 100, 102). However, relevance of their interplay during EMT program in kidney has not been evaluated yet, although cross reactions of NCAM and FGFR are known to be significant in oncology researches

(101). It is well known that functional cooperation between these two molecules results in induction of FGFR signaling directly stimulated by NCAM molecule (14, 25, 26). However, FGFR signaling induced by NCAM stimulation differs from the pathway initiated by other ligands such as FGF. In the absence of FGF, activation of FGFR by NCAM specifically promotes characteristic FGF receptor cellular trafficking and recycling that results in sustained FGFR signaling (14, 27), leading to enhanced cell migration with invasive and aggressive biological behavior (99, 101, 142).

Since we observed early induction of NCAM and FGFR1 upon exposure to TGF-β1, as proto-typical mediator of intrarenal EMT program, even before EMT hallmarks became apparent, it was reasonable to consider an opportunity to modulate or even prevent EMT program by modulation of NCAM/FGFR signaling responses, especially considering that TGF- β1 plays an important role in development renal fibrosis in humans influencing excretory kidney function. The majority of morphological and molecular TGF-β1 induced changes of TECs were obviously suppressed by inhibition of NCAM induced FGFR signaling, afterwards confirmed as acting through SMAD dependant manner. Altogether, it becomes apparent that NCAM and FGFR1 are the earliest up-regulated molecules upon TGF- β1 stimulated EMT program whose mechanistic co-operation can be effectively suppressed by FGFR inhibitor (PD173074) administration. An efficiency of PD73074 to modulate EMT events during carcinogenesis has been already investigated, as well as its therapeutical potential to reduce hearth fibrosis (143-147).

Considering renal fibrosis as a common consequence of many kidney diseases, requirements for novel anti-fibrotic therapies are growing (92). For the first time, we here provide evidence for a direct mechanistic link between NCAM and FGFR signaling in initiation of EMT program TECs, and also explore clinical relevance of TGF-β1 downstream effectors detection in human kidney biopsies revealing their association with impaired renal excretory function and chronic kidney disease development. Since aberrant NCAM/FGFR signaling is equally present among various human renal diseases especially at the beginning of renal interstitial fibrosis (129), and TGF-β1 is considered as master inducer of fibrogenic response in the kidney, our current findings could have significant translational implications. Finally, modulation of such NCAM/FGFR signaling as established by PD173074 effectively blocks EMT program in cultured TECs, offering new insights into aberrant EMT program during renal fibrosis and new

therapeutical targets for such EMT program. Since therapeutic efficacy of PD173074 has been investigated and proven in various cancers but also non-cancerous diseases and already entered clinical testing, our findings expand our knowledge of a putative role of NCAM/FGFR in EMT program initiation and renal fibrosis and it is attractive to speculate that specific modulation of such NCAM/FGFR signaling could be equally effective in the treatment of renal disease associated with aberrant EMT program.

The substance explored in this investigation (PD173074) belongs to receptor tyrosine kinases (RTKs) inhibitors (TKIs). Since RTKs signaling pathway a crucial in various pathological processes, including malignancies and fibrosis, numerous TKIs are widely studied and many of them are already in clinical use or are subjected to clinical trials (148, 149). However, among proposed therapies selective inhibitors are scarce, but rather involve inhibition of several RTKs. Thus, controversies about application of non-selective therapy still exist. Considering that in many pathological states an aberrant induction of several signaling pathways appear and can also involve signaling by several RTKs, therapy with non-selective TKIs could be more promising and with extended benefits. However, this opportunity could be retained only for management of malignancies and appears to be unsuitable for non-malignant conditions, such as fibrosis (150).

Many TKIs are already explored in animal models of renal fibrosis, focusing mainly on the inhibition of platelet-derived growth factor receptor (PDGFR), epidermal growth factor receptor (EGFR) and vascular endothelial growth factor receptor (VEGFR). With regard to FGFR signaling in pathogenesis of renal diseases, it has been only proven that FGFR1 and its ligand FGF2 (basic FGF) are involved in the induction of renal fibrosis and contribution to renal damage in immune-mediated injury (149). Moreover, using fibroblast cell line, it has been shown that TGF-β1 induced fibroblast proliferation through the up-regulation of FGF2 synthesis, implicating a significant role of FGFR1 signaling (151). Thus, FGFR signaling is already known to be activated by TGF-β1 in fibroblasts. However, here we present an involvement of FGFR signaling in epithelial cells and induction of EMT program induced by non-FGF ligand (NCAM). This finding confirms again that FGFR acts down-stream of TGF- β1 and provides a novel mechanism of its induction, as shown – stimulated with aberrant NCAM expression rapidly induced upon TGF- β1 and in line with FGFR1 over-expression. Considering that low dose of PD73074 is found to be FGFR selective, mostly affected FGFR1 activity, it could

designate this substance to be a choice for management of early fibrosis, thus preventing a widespread fibrogenesis in kidney and terminal renal fibrosis with end-stage kidney disease (ESKD) occurrence.

Kidney diseases are important problem worldwide. They are defined as impaired kidney structure or function, influencing global health of those individuals. Any kidney disease can occur abruptly and afterwards either resolve or become chronic. Chronic kidney disease (CKD) is a general term that considers heterogeneous disorders affecting renal function and kidney morphology with wide range of clinical presentation patterns. Clinical presentations could be related to cause of disease, its severity and the progression rate. Impairment of renal excretory function is considered as the most serious outcome of CKD. Earlier stages of kidney disease could be asymptomatic and are usually detected during routine comorbid evaluations. These stages could be reversible, while more severe presentation often have progressive disease course.

Patients with pathohistologicaly revealed underlying kidney damage are considered to have CKD. Depending on the estimated glomerular filtration rate (eGFR) and albuminuria levels, patients are classified in four CKD prognostic/risk categories: low, moderate, high and vary high risk. According to KDIGO recommendations (3), all patients have to be carefully monitored and management of progression and CKD complications is still challenging. All people with CKD are risk to develop acute kidney injury, and all of them with disease progression could develop complications such as anemia, metabolic bone disease including laboratory abnormalities, acidosis, cardiovascular and cerebrovascular diseases. Targeted therapies could provide better balance between beneficial and adverse effects. Thus, defining the main signaling pathway and discovering the major inducer underling fibrogenesis with individual approach might not be cost-effective option, but could be the most appropriate choice for patients and clinicians in the future.

6. CONCLUSIONS

NCAM expressing cells do not only increase during fibrogenesis but also switch the isoforms. Compared to NCAM expressing in normal human kidneys, these cell under fibrotic microenvironment highly express NCAM-140 isoform. NCAM expression in renal interstitial compartment is disease independent, representing a trait of early fibrogenesis in the human kidney. These cells are highly heterogeneous, whereby sub-populations share some markers involved in fibrosis. Moreover, relative gene expression levels involved in fibrosis, assessed by qRT-PCR, were higher in advanced stages and NCAM followed that trend. However, interstitial NCAM expression does not have long term impact on disease outcome and could not be used as predictor for the impairment of kidney function. Moreover, NCAM interstitial positivity is frequently found in patients with lower range proteinuria values.

Since TGF-β is the main cytokine involved the fibrogenic response, here we underline the influence of this signaling pathway on morphology of renal tubulointerstitial compartment suggesting its signaling cascade is visible in chronic parenchymal damage (tubular atrophy and interstitial fibrosis), resulting in impaired renal excretory function and CDK development and progression. Beside SMAD2 influence on morphology of renal tubulointerstitial compartment and patients' outcome, SNAIL expression in podocytes is associated with nephrotic range proteinuria.

Collectively, the most important finding in our study reflects a robust induction of NCAM expression in incipient renal fibrosis and an important role of NCAM/FGFR interplay in the initiation step of fibrogenic response that could be effectively suppressed by inhibition of their cross-talk applying FGFR inhibitor (PD173074). Despite clear morphological and molecular evidence that PD173074 reduced TGF-β1 effects on proximal tubular epithelial cells *in vitro* through switch from EMT to MET like phenotype, great ambiguity still persists with regard to the precise background molecular mechanism and cross-talk between these two pathways, requiring profound clarification. Moreover, although it has been also previously observed that both NCAM and FGFR could be up-regulated in response to TGF-β1 stimulation, there is still gap in between since NCAM/FGFR up-stream inducers are not identified in response to TGF-β1 signaling. TGF-β signaling can also induce non-SMAD dependant cellular response and it is

clear that the co-operation between SMAD and non-SMAD signaling pathways determines the final outcome of cellular response to TGF-β. Since both NCAM and FGFR1 are up-regulated rapidly after TGF-β1 stimulation and before morphological evidence of nuclear localization of pSMAD2/3, it might be that regulation of NCAM and FGFR1 gene expressions under the influence of TGF-β1 involves non-SMAD pathways. Nevertheless, since inhibition of NCAM/FGFR signaling pathway by administration of PD173074 results in suppression of nuclear translocation of SMAD2/3 and promotes their degradation in cytosol, it looks that TGF-β1 reduced responses by PD173074 were highly SMAD dependant.

Unequivocally, FGFR inhibitor could be a promising anti-fibrotic strategy for kidney diseases and has to be further explored at least on animal models, since investigations in the field of molecular background of renal interstitial fibrosis and signaling pathways driving initiation, maintenance and progression of such process could contribute to better understanding of the complex network involved in renal fibrosis and permit development of new potential strategies to treat renal fibrosis in humans. There is no cure for CKD that affects more than million lives each year, but researcher may now be one step closer.

7. REFFERENCES

1. Zeisberg M, Kalluri R. Physiology of the renal interstitium. Clin J Am Soc Nephrol. 2015.

2. Kurt B, Kurtz A. Plasticity of renal endocrine function. Am J Physiol Regul Integr Comp Physiol. 2015; 308(6): R455-466.

3. KDIGO 2012 Clinical Practice Guideline for the Evaluation and Management of Chronic Kidney Disease. Kidney Disease: Improving Global Outcomes (KDIGO) CKD Work Group. Kidney inter. Suppl. 2013; 3: 1–150.

4. Zeisberg M, Kalluri R. Cellular mechanisms of tissue fibrosis. 1. Common and organ-specific mechanisms associated with tissue fibrosis. Am J Physiol Cell Physiol. 2013; 304: C216–225.

5. Norman JT, Fine LG. Progressive renal disease: fibroblasts, extracellular matrix, and integrins. Exp Nephrol. 1999; 7: 167-177.

6. Zeisberg M, Neilson EG. Mechanisms of Tubulointerstitial Fibrosis. J Am Soc Nephrol. 2010; 21: 1819–1834.

7. Tampe B, Zeisberg M. Contribution of genetics and epigenetics to progression of kidney fibrosis. Nephrol Dial Transplant. 2014; 29: 72-79.

8. Liu Y. Renal fibrosis: New insights into the pathogenesis and therapeutics. Kidney Int. 2006; 69(2): 213-217.

9. Genovese F, Manresa AA, Leeming DJ, et al. The extracellular matrix in the kidney: a source of novel non-invasive biomarkers of kidney fibrosis? Fibrogenesis Tissue Repair. 2014; 7(1): 4.

10. Meng XM, Tang PM, Li J, et al. TGF-b/Smad signaling in renal fibrosis. Front Physiol. 2015; 6: 82.

11. Zeisberg M, Hanai J, Sugimoto H, et al. BMP-7 counteracts BMP-7 counteracts TGF-beta1-induced epithelial-to-mesenchymal transition and reverses chronic renal injury. Nat Med. 2003; 9(7): 964-968.

12. Shima H, Sasaki K, Suzuki T et al. A novel indole compound MA-35 attenuates renal fibrosis by inhibiting both TNF-α and TGF-β1 pathways. 2017; Sci Rep. 7(1): 1884.

13. Sun X, Liu Y, Li C et al. Recent Advances of Curcumin in the Prevention and Treatment of Renal Fibrosis. Biomed Res Int. 2017; 2017: 2418671.

14. Lehembre F, Yilmaz M, Wicki A, et al. NCAM-induced focal adhesion assembly: a functional switch upon loss of E-cadherin. EMBO J. 2008; 27: 2603-2615.

15. Takagi J, Strokovich K, Springer TA, et al. Structure of integrin α5β1 in complex with fibronectin. EMBO J. 2003; 22: 4607–4615.

16. Meran S, Steadman R. Fibroblasts and myiofibroblasts in renal fibrosis. Int J Exp Path. 2011; 92: 158-167.

17. Lee KA, Nelson CM. New Insights into the Regulation of Epithelial–Mesenchymal Transition and Tissue Fibrosis. International Review of Cell and Molecular Biology. Elsevier, 2012; 294: 173-206.

18. LeBleu VS, Taduri G, O'Connell J, et al. Origin and function of myofibroblasts in kidney fibrosis. Nat Med. 2013; 19(8): 1047-1053.

19. Xiao HB, Liu RH, Ling GH, et al. HSP47 regulates ECM accumulation in renal proximal tubular cells induced by TGF-β1 through ERK1/2 and JNK MAPK pathways. Am J Physiol Renal Physiol. 2012; 303(5): F757-765.

20. Hinz B, Phan SH, Thannickal VJ, et al. The myofibroblast: one function, multiple origins. Am J Pathol. 2007; 170: 1807-1816.

21. Strutz F, Müller GA. Renal fibrosis and the origin of the renal fibroblast. Nephrol Dial Transplant. 2006; 21: 3368–3370.

22. Boor P, Floege J. The renal (myo-)fibroblast: a heterogeneous group of cells. Nephrol Dial Transplant. 2012; 27: 3027–3036.

23. Strutz F, Zeisberg M, Hemmerlein B et al. Basic fibroblast growth factor (FGF-2) expression is increased in human renal fibrogenesis and may mediate autocrine fibroblast proliferation. Kidney Int. 2000; 57: 1521–1538.

24. Kiselyov VV, Soroka V, Berezin V, et al. Structural biology of NCAM homophilic binding and activation of FGFR. J Neurochem. 2005; 94: 1169–1179.

25. Kochoyan A, Poulsen FM, Berezin V, et al. Structural basis for the activation of FGFR by NCAM. Protein Sci. 2008; 17: 1698-1705.

26. Kiselyov VV, Skladchikova G, Hinsby AM, et al. Structural basis for a direct interaction between FGFR1 and NCAM and evidence for a regulatory role of ATP. Structure. 2003; 11: 691-701.

27. Francavilla C, Cattaneo P, Berezin V, et al. The binding of NCAM to FGFR1 induces a specific cellular response mediated by receptor trafficking. J Cell Biol. 2009; 187: 1101-1116.

28. LeBleu VS, Teng Y, O'Connell JT, et al. Identification of human epididymisprotein-4 as a fibroblast-derived mediator of fibrosis. Nat Med. 2013; 19: 227-231.

29. Chhikara N, Saraswat M, Tomar AK, et al. Human epididymis protein-4 (HE-4): a novel cross-class protease inhibitor. PloS One. 2012; 7: e47672.

30. Chen G, Lin SC, Chen J, et al. CXCL16 recruits bone marrow-derived fibroblast precursors in renal fibrosis. J Am Soc Nephrol. 2011; 22(10): 1876-1886.

31. Yan J, Zhang Z, Jia L, Wang Y. Role of Bone Marrow-Derived Fibroblasts in Renal Fibrosis. Front Physiol. 2016; 7: 61.

32. Lin SL, Kisseleva T, Brenner DA, Duffield JS. Pericytes and perivascular fibroblasts are the primary source of collagen-producing cells in obstructive fibrosis of the kidney. Am J Pathol. 2008; 173(6): 1617-1627.

33. Lamouille S, Xu J, Derynck R. Molecular mechanisms of epithelial–mesenchymal transition. Nat Rev Mol Cell Biol. 2014; 15(3): 178–196.

34. Fustaino V, Presutti D, Colombo T et al. Characterization of epithelial-mesenchymal transition intermediate/hybrid phenotypes associated to resistance to EGFR inhibitors in non-small cell lung cancer cell lines. Oncotarget. 2017; 8: 103340-103363.

35. Thomasova D, Anders HJ. Cell cycle control in the kidney. Nephrol Dial Transplant. 2015; 30: 1622–1630.

36. Venkatachalam MA, Weinberg JM, Kriz W, Bidani AK. Failed tubule recovery, AKI-CKD transition, and kidney disease progression. J Am Soc Nephrol. 2015; 26: 1765–1776.

37. Hodgkins KS, Schnaper HW. Tubulointerstitial injury and the progression of chronic kidney disease. Pediatr Nephrol. 2012; 27(6): 901–909.

38. Wang N, Deng Y, Liu A, et al. Novel Mechanism of the Pericyte-Myofibroblast Transition in Renal Interstitial Fibrosis: Core Fucosylation Regulation. Sci Rep. 2017; 7(1): 16914.

39. Lipphardt M, Song JW, Matsumoto K, et al. The third path of tubulointerstitial fibrosis: aberrant endothelial secretome. Kidney Int. 2017; 92(3): 558-568.

40. Zeisberg EM, Potenta SE, Sugimoto H, et al. Fibroblasts in Kidney Fibrosis Emerge via Endothelial-to-Mesenchymal Transition. J Am Soc Nephrol. 2008; 19(12): 2282–2287.

41. Curci C, Castellano G, Stasi A. Endothelial-to-mesenchymal transition and renal fibrosis in ischaemia/reperfusion injury are mediated by complement anaphylatoxins and Akt pathway. Nephrol Dial Transplant. 2014; 29(4): 799–808.

42. Chang Y, Li H, Guo Z. Mesenchymal Stem Cell-Like Properties in Fibroblasts. Cell Physiol Biochem. 2014; 34: 703-714.

43. Gilles C, Newgreen DF, Sato H, Thompson EW. Matrix Metalloproteases and Epithelial-to-Mesenchymal Transition: Implications for Carcinoma Metastasis. Madame Curie Bioscience Database. 2000-2013; Austin (TX): Landes Bioscience.

44. Fadnes B, Hadler-Olsen E, Sylte I, et al. Matrix metalloproteinase complexes and their biological signifance. In: Extracellular martix: pathobiology and signaling. Ed: Karamanos NK. 2012; 291-308.

45. Guiteras R, Flaquer M, Cruzado JM. Macrophage in chronic kidney disease. Clinical Kidney Journal. 2016; 9(6): 765–771.

46. Zeidel ML, Hoenig MP,Palevsky PM. A New CJASN Series: Renal Physiology for the Clinician. Clin J Am Soc Nephrol. 2014; 9: 1272–1281.

47. Babickova J, Klinkhammer BM, Buhl EM, et al. Regardless of etiology, progressive renal disease causes ultrastructural and functional alterations of peritubular capillaries. Kidney Int. 2017; 91: 70–85.

48. Desmoulière A, Darby IA, Gabbiani G. Normal and pathologic soft tissue remodeling: role of the myofibroblast, with special emphasis on liver and kidney fibrosis. Lab Invest. 2003; 83: 1689-1707.

49. Flanders KC. Smad3 as a mediator of the fibrotic response. Int J Exp. 2004; 85: 47-64.

50. Guarino M, Tosoni A, Nebuloni M. Direct contribution of epithelium to organ fibrosis: epithelial-mesenchymal transition. Human Path. 2009; 40: 1365–1376.

51. Zeisberg M, Maeshima Y, Mosterman B, et al. Renal fibrosis. Extracellular matrix microenvironment regulates migratory behavior of activated tubular epithelial cells. Am J Pathol. 2002; 160: 2001-2008.

52. Liu Y. New insights into epithelial-mesenchymal transition in kidney fibrosis. J Am Soc Nephrol. 2010; 21: 212-222.

53. Guo Y, Xiao L, Sun L, Liu F. Wnt/beta-catenin signaling: a promising new target for fibrosis diseases. Physiol Res. 2012; 61(4): 337-346.

54. Chung ACK, Lan HY. Molecular Mechanisms of TGF-b Signaling in Renal Fibrosis. Curr Pathobiol Rep. 2013; 1: 291-299.

55. Zheng H, Li W, Wang Y, et al. Glycogen synthase kinase-3 beta regulates Snail and β-catenin expression during Fas-induced epithelial-mesenchymal transition in gastrointestinal cancer. Eur J Cancer. 2013; 49(12): 2734-2746.

56. Patel S, Takagi K, Suzuki J, et al. RhoGTPase Activation Is a Key Step in Renal Epithelial Mesenchymal Transdifferentiation. J Am Soc Nephrol. 2005; 16(7): 1977-1984.

57. Zhang Y, Wang S, Liu S, et al. Role of Smad signaling in kidney disease. Int Urol Nephrol. 2015; 47: 1965–1975.

58. Verrecchia F, Mauviel A. Transforming Growth Factor-β Signaling Through the Smad Pathway: Role in Extracellular Matrix Gene Expression and Regulation. J Invest Dermatol. 2002; 118(2): 211-215.

59. Zhang J, Zhang X, Xie F, et al. The regulation of TGF-β/SMAD signaling by protein deubiquitination. Protein Cell. 2014; 5(7): 503–517.

60. Huang XR, Chung ACK,Wang XJ et al. Mice overexpressing latent TGF-b1 are protected against renal fibrosis in obstructive kidney disease. Am J Physiol Renal Physiol. 2008; 295: F118–F127.

61. Huang XR, Chung ACK, Zhou L et al. Latent TGF-b1 protects against crescentic glomerulonephritis. J Am Soc Nephrol. 2008; 19: 233–242.

62. Medina C, Santos-Martinez MJ, Santana A et al. Transforming growth factor-beta type 1 receptor (ALK5) and Smad proteins mediate TIMP-1 and collagen synthesis in experimental intestinal fibrosis. J Pathol. 2011; 224: 461–472.

63. Haupt A, Joberty G, Bantscheff M et al. Hsp90 inhibition differentially destabilises MAP kinase and TGF-beta signalling components in cancer cells revealed by kinase-targeted chemoproteomics. BMC Cancer. 2012; 12: 38.

64. Zhang K, Lu Y, Yang P et al. HILI inhibits TGF-beta signaling by interacting with Hsp90 and promoting TbetaR degradation. PLoS ONE. 2012; 7: e41973.

65. Wei MG, Sun W, He WM, et al. Ferulic Acid Attenuates TGF-β1-Induced Renal Cellular Fibrosis in NRK-52E Cells by Inhibiting Smad/ILK/Snail Pathway. Evidence-Based Complementary and Alternative Medicine. 2015; 2015: 619720.

66. Harney AS, Lee J, Manus LM, et al. Targeted inhibition of Snail family zinc finger transcription factors by oligonucleotide-Co(III) Schiff base conjugate. Proc Natl Acad Sci U S A. 2009; 106(33): 13667–13672.

67. Harney AS, Meade TJ, LaBonne C. Targeted inactivation of Snail family EMT regulatory factors by a Co(III)-Ebox conjugate. PLoS One. 2012; 7(2): e32318.

68. Secher T. Soluble NCAM. Adv Exp Med Biol. 2010; 663: 227-242.

69. Kiselyov VV. NCAM and the FGF-receptor. Adv Exp Med Biol. 2010; 663: 67-79.

70. Walmod PS, Kolkova K, Berezin V, Bock E. Zippers make signals: NCAM-mediated molecular interactions and signal transduction. Neurochem Res. 2004; 29: 2015–2035.

71. Mendiratta SS, Sekulic N, Hernandez-Guzman FG, et al. A novel alpha-helix in the first fibronectin type III repeat of the neural cell adhesion molecule is critical for N-glycan polysialylation. J Biol Chem. 2006; 281: 36052–36059.

72. Nelson RW, Bates PA, Rutishauser U. Protein determinants for specific polysialylation of the neural cell adhesion molecule. J Biol Chem. 1995; 270: 17171–17179.

73. Kiss JZ, Rougon G. Cell biology of polysialic acid. Curr Opin Neurobiol. 1997; 7: 640–646.

74. Brackenbury R, Sorkin BC, Cunningham BA. Molecular features of cell adhesion molecules involved in neural development. Res Publ Assoc Res Nerv Ment Dis. 1987; 65: 155-167.

75. Rao Y, Wu XF, Gariepy J, et al. Identification of a peptide sequence involved in homophilic binding in the neural cell adhesion molecule NCAM. J Cell Biol. 1992; 118: 937–949.

76. Rao Y, Wu XF, Yip P, et al. Structural characterization of a homophilic binding site in the neural cell adhesion molecule. J Biol Chem. 1993; 268: 20630–20638.

77. Soroka V, Kolkova K, Kastrup JS, et al. Structure and interactions of NCAM Ig1-2-3 suggest a novel zipper mechanism for homophilic adhesion. Structure. 2003; 11: 1291–1301.

78. Beggs H E, Baragona SC, Hemperly JJ, Maness PF. NCAM-140 interacts with the focal adhesion kinase p125 fak and the src-related tyrosine kinase p59fyn. J Biol Chem. 1997; 272: 8310–8319.

79. Schmid RS, Graff RD, Schaller MD, et al. NCAM stimulates the Ras-MAPK pathway and CREB phosphorylation in neuronal cells. J Neurobiol. 1999; 38: 542–558.

80. Povlsen GK, Ditlevsen DK, Berezin V, Bock E. Intracellular signaling by the neural cell adhesion molecule. Neurochem Res. 2003; 28(1): 127-141.

81. Berezin V, Bock E. NCAM mimetic peptides: Pharmacological and therapeutic potential. J Mol Neurosci. 2004; 22: 33–39.

82. Rutishauser U. Polysialic acid in the plasticity of the developing and adult vertebrate nervous system. Nat Rev Neurosci. 2008; 9: 26–35.

83. Tiong KH, Mah LY, Leong CO. Functional roles of fibroblast growth factor receptors (FGFRs) signaling in human cancers. Apoptosis. 2013; 18(12): 1447-1468.

84. Niethammer P, Delling M, Sytnyk V, et al. Cosignaling of NCAM via lipid rafts and the FGF receptor is required for neuritogenesis. J Cell Biol. 2002; 157: 521–532.

85. Marković-Lipkovski J, Müller CA, Klein G, et al. Neural cell adhesion molecule expression on renal interstitial cells. Nephrol Dial Transplant. 2007; 22: 1558–1566.

86. Klein G, Langegger M, Goridis C, et al. Neural cell adhesion molecules during embryonic induction and development of the kidney. Development. 1988; 102: 749–761.

87. KDOQI Clinical Practice Guidelines for Chronic Kidney Disease: Evaluation, Classification, and Stratification. National Kidney Foundation. 2002; p. 44.

88. Vansthertem D, Gossiaux A, Declèves AE, et al. Expression of nestin, vimentin, and NCAM by renal interstitial cells after ischemic tubular injury. J Biomed Biotechnol. 2010; 2010: 193259.

89. Gattenlöhner S, Waller C, Ertl G, et al. NCAM(CD56) and RUNX1(AML1) are up-regulated in human ischemic cardiomyopathy and a rat model of chronic cardiac ischemia. Am J Pathol. 2003; 163(3): 1081-1090.

90. Zhao X, Jankovic V, Gural A, et al. Methylation of RUNX1 by PRMT1 abrogates SIN3A binding and potentiates its transcriptional activity. Genes Dev. 2008; 22(5): 640-653.

91. Lam K, Zhang DE. RUNX1 and RUNX1-ETO: roles in hematopoiesis and leukemogenesis. Front Biosci (Landmark Ed). 2012; 17: 1120-1139.

92. Zeisberg M, Zeisberg EM. Precision renal medicine: a roadmap towards targeted kidney fibrosis therapies. Fibrogenesis Tissue Repair. 2015; 8: 16.

93. Yang L, Besschetnova TY, Brooks CR, et al. Epithelial cell cycle arrest in G2/M mediates kidney fibrosis after injury. Nat Med. 2010; 16(5): 535-543.

94. Lovisa S, LeBleu VS, Tampe B, et al. Epithelial-to mesenchymal transition induces cell cycle arrest and parenchymal damage in renalfibrosis. Nat Med. 2015; 21(9): 998-1009.

95. Tampe D, Zeisberg M. Potential approaches to reverse or repair renal fibrosis. Nat Rev Nephrol. 2014; 10(4): 226-237.

96. Meng XM, Zhang Y, Huang XR, et al. Treatment of renal fibrosis by rebalancing TGF-β/Smad signaling with the combination of asiatic acid and naringenin. Oncotarget. 2015; 6(35): 36984-36997.

97. Xu J, Lamouille S, Derynck R. TGF-β-induced epithelial to mesenchymal transition. Cell Res. 2009; 19(2): 156-172.

98. Meng XM, Huang XR, Xiao J, et al. Diverse roles of TGF-beta receptor II in renal fibrosis and inflammation in vivo and in vitro. The Journal of pathology. 2012; 2: 175-188.

99. Cavallaro U, Niedermeyer J, Fuxa M, Christofori G. N-CAM modulates tumour-cell adhesion to matrix by inducing FGF-receptor signalling. Nat Cell Biol. 2001; 3(7): 650-7.

100. Colombo N, Cavallaro U. The interplay between NCAM and FGFR signalling underlies ovarian cancer progression. Ecancermedicalscience. 2011; 5: 226.

101. Zecchini S, Bombardelli L, Decio A, et al. The adhesion molecule NCAM promotes ovarian cancer progression via FGFR signalling. EMBO Mol Med. 2011; 3(8): 480-494.

102. Tomlinson DC, Baxter EW, Loadman PM, et al. FGFR1-induced epithelial to mesenchymal transition through MAPK/PLCγ/COX-2-mediatedmechanisms. PLoS One. 2012; 7(6): e38972.

103. Miller MW, Luo J. Effects of ethanol and transforming growth factor beta (TGF beta) on neuronal proliferation and nCAM expression. Alcohol Clin Exp Res. 2002; 26(8): 1281-1285.

104. Roubin R, Deagostini-Bazin H, Hirsch MR, Goridis C. Modulation of NCAM expression by transforming growth factor-beta, serum, and autocrine factors. J Cell Biol. 1990; 111(2): 673-684.

105. Stewart HJ, Rougon G, Dong Z, et al. TGF-betas upregulate NCAM and L1 expression in cultured Schwann cells, suppress cyclic AMP-induced expression of O4 and galactocerebroside, and are widely expressed in cells of the Schwann cell lineage in vivo. Glia. 1995; 15(4): 419-436.

106. Thannickal VJ, Aldweib KD, Rajan T, Fanburg BL. Upregulated expression of fibroblast growth factor (FGF) receptors by transforming growth factor-beta1 (TGF-beta1) mediates enhanced mitogenic responses to FGFs in cultured human lung fibroblasts. Biochem Biophys Res Commun. 1998; 251(2): 437-441.

107. Kanda T, Funato N, Baba Y, Kuroda T. Evidence for fibroblast growth factor receptors in myofibroblasts during palatal mucoperiosteal repair. Arch Oral Biol. 2003; 48(3): 213-221.

108. Tur MK, Etschmann B, Benz A, et al. The 140-kD isoform of CD56 (NCAM1) directs the molecular pathogenesis of ischemic cardiomyopathy. Am J Pathol. 2013; 182(4): 1205-1218.

109. Metsuyanim S, Harari-Steinberg O, Buzhor E, et al. Expression of Stem Cell Markers in the Human Fetal Kidney. PLoS One. 2009; 4(8): e6709.

110. Kriz W, Kaissling B, Le Hir M. Epithelial-mesenchymal transition (EMT) in kidney fibrosis: fact or fantasy? J Clin Invest. 2011; 121(2): 468-474.

111. Loeffler I, Wolf G. Epithelial-to-Mesenchymal Transition in Diabetic Nephropathy: Fact or Fiction? Cells. 2015; 4(4): 631-652.

112. Diestel S, Hinkle CL, Schmitz B, et al. NCAM 140 stimulates integrin-dependent cell migration by ectodomain shedding. J Neurochem. 2005; 95: 1777–1784.

113. Schaffner F, Ray AM, Dontenwill M. Integrin α5β1, the Fibronectin Receptor, as a Pertinent Therapeutic Target in Solid Tumors. Cancers. 2013; 5: 27-47.

114. White LR, Blanchette JB, Ren L, et al. The characterization of alpha5-integrin expression on tubular epithelium during renal injury. Am J Physiol Renal Physiol. 2007; 292(2): F567-576.

115. Christensen C, Lauridsen JB, Berezin V, et al. The neural cell adhesion molecule binds to fibroblast growth factor receptor 2. FEBS Lett. 2006; 580(14): 3386-3390.

116. Shirakihara T, Horiguchi K, Miyazawa K, et al. TGF-β regulates isoform switching of FGF receptors and epithelial-mesenchymal transition. EMBO J. 2011; 30(4): 783-795.

117. Foster BA, Kaplan PJ, Greenberg NM. Characterization of the FGF axis and identification of a novel FGFR1IIIc isoform during prostate cancer progression in the TRAMP model. Prostate Cancer Prostatic Dis. 1999; 2: 76–82.

118. Xu-Dubois YC, Galichon P, Brocheriou I, et al. Expression of the transcriptional regulator snail1 in kidney transplants displaying epithelial-to-mesenchymal transition features. Nephrol Dial Transplant. 2014; 29(11): 2136-2144.

119. Strutz F, Zeisberg M, Ziyadeh FN, et al. Role of basic fibroblast growth factor-2 in epithelial-mesenchymal transformation. Kidney Int. 2002; 61(5): 1714-1728.

120. Matsui I, Ito T, Kurihara H, et al. Snail, a transcriptional regulator, represses nephrin expression in glomerular epithelial cells of nephrotic rats. Lab Invest. 2007; 87(3): 273-283.

121. Li C, Siragy HM. High glucose induces podocyte injury via enhanced (pro)renin receptor-Wnt-β-catenin-snail signaling pathway. PLoS One. 2014; 9(2): e89233.

122. Barrallo-Gimeno A, Nieto MA. The Snail genes as inducers of cell movement and survival: Implications in development and cancer. Development. 2005; 132: 3151-3161.

123. Boutet A, De Frutos CA, Maxwell PH, et al. Snail activationtion disrupts tissue homeostasis and induces fibrosis in the adult kidney. EMBO J. 2006; 25: 5603-5613.

124. Boutet A, Esteban MA, Maxwell PH, Nieto MA. Reactivation of Snail genes in renal fibrosis and carcinomas: a process of reversed embryogenesis? Cell Cycle. 2007; 6(6): 638-642.

125. Nam EH, Lee Y, Moon B, et al. Twist1 and AP-1 cooperatively upregulate integrin α5 expression to induce invasion and the epithelial-mesenchymal transition. Carcinogenesis. 2015; 36(3): 327-337.

126. Okada H, Danoff TM, Kalluri R, Neilson EG. Early role of Fsp1 in epithelial-mesenchymal transformation. Am J Physiol. 1997; 273(4 Pt 2): F563-574.

127. Zimmer DB, Cornwall EH, Landar A, et al. The S100 protein family: History, function, and expression. Brain Res Bull. 1995; 37: 417–429.

128. Nakatani K, Tanaka H, Ikeda K, et al. Expression of NCAM in activated portal fibroblasts during regeneration of the rat liver after partial hepatectomy. Arch Histol Cytol. 2006; 69(1): 61-72.

129. Marković-Lipkovski J, Životić M, Müller CA, et al. Variable Expression of Neural Cell Adhesion Molecule Isoforms in Renal Tissue: Possible Role in Incipient Renal Fibrosis. PLoS ONE. 2015; 10(9): e0137028.

130. Jiang J, Dean D, Burghardt RC, Parrish AR. Disruption of cadherin/catenin expression, localization, and interactions during HgCl2-induced nephrotoxicity. Toxicol Sci. 2004; 80: 170–182.

131. Prozialeck WC, Lamar PC, Appelt DM. Differential expression of E-cadherin, N-cadherin and beta-catenin in proximal and distal segments of the rat nephron. BMC Physiol. 2004; 4: 10.

132. Keller C, Kroening S, Zuehlke J, et al. Distinct mesenchymal alterations in N-cadherin and E-cadherin positive primary renal epithelial cells. PLoS One. 2012; 7(8): e43584.

133. Buchmaier BS, Bibi A, Müller GA, et al. Renal cells express different forms of vimentin:the independent expression alteration of these forms is important in cell resistance to osmotic stress and apoptosis. PLoS One. 2013; 8(7): e68301. .

134. Cho KH, Jeong KJ, Shin SC, et al. STAT3 mediates TGF-β1-induced TWIST1 expression and prostate cancer invasion. Cancer Lett. 2013; Vol. 336(1): 167-173.

135. Wang Y, Shi J, Chai K, et al. The Role of Snail in EMT and Tumorigenesis. Curr Cancer Drug Targets. 2013; 13(9): 963-972.

136. Tang H, Massi D, Hemmings BA, et al. AKT-ions with a TWIST between EMT and MET. Oncotarget. 2016; 7(38): 62767-62777.

137. Serrano I, McDonald PC, Lock FE, Dedhar S. Role of the integrin-linked kinase (ILK)/Rictor complex in TGFβ-1-induced epithelial-mesenchymal transition (EMT). Oncogene. 2013; 32(1): 50-60.

138. Gotzmann J, Mikula M, Eger A, et al. Molecular aspects of epithelial cell plasticity: implications for local tumor invasion and metastasis. Mutat Res. 2004; 566(1): 9–20.

139. Migdal M, Soker S, Yarden Y, Neufeld G. Activation of a transfected FGFR-1 receptor in Madin-Darby epithelial cells results in a reversible loss of epithelial properties. J Cell Physiol. 1995; 162(2): 266-276.

140. Rohani MG, Parks WC. Matrix remodeling by MMPs during wound repair. Matrix Biol. 2015; 44-46: 113-121.

141. Yang J, Hou Y, Zhou M, et al. Twist induces epithelial-mesenchymal transition and cell motility in breast cancer via ITGB1-FAK/ILK signaling axis and its associated downstream network. Int J Biochem Cell Biol. 2016; 71: 62-71.

142. Ye T, Wei X, Yin T, et al. Inhibition of FGFR signaling by PD173074 improves antitumor immunity and impairs breast cancer metastasis. Breast Cancer Res Treat. 2014; 143(3): 435-446.

143. Nguyen PT, Tsunematsu T, Yanagisawa S, et al. The FGFR1 inhibitor PD173074 induces mesenchymal-epithelial transition through the transcription factor AP-1. Br J Cancer. 2013; 109(8):2248-58.

144. Yanagita M. Inhibitors/antagonists of TGF-β system in kidney fibrosis. Nephrol Dial Transplant. 2012; 27: 3686-3691.

145. Di Marco GS, Reuter S, Kentrup D, et al. Treatment of established left ventricular hypertrophy with fibroblast growth factor receptor blockade in an animal model of CKD. Nephrol Dial Transplant. 2014; 29(11): 2028-2035.

146. Lei J, Li W, Yang Y, et al. TC-1 overexpression promotes cell proliferation in human non-small cell lung cancer that can be inhibited by PD173074. PLoS One. 2014; 9(6): e100075.

147. Lamont FR, Tomlinson DC, CooperPA, et al. Small molecule FGF receptor inhibitors block FGFR-dependent urothelial carcinoma growth in vitroand in vivo. Br J Cancer. 2011; 104(7): 75–82.

148. Regad T. Targeting RTK Signaling Pathways in Cancer. Cancers (Basel). 2015; 7(3): 1758-1784.

149. Liu F, Zhuang S. Role of Receptor Tyrosine Kinase Signaling in Renal Fibrosis. Int J Mol Sci. 2016; 17(5): E972.

150. Gudernova I, Vesela I, Balek L, et al. Multikinase activity of fibroblast growth factor receptor (FGFR) inhibitors SU5402, PD173074, AZD1480, AZD4547 and BGJ398 compromises the use of small chemicals targeting FGFR catalytic activity for therapy of short-stature syndromes. Hum Mol Genet. 2016; 25(1): 9-23.

151. Strutz F, Zeisberg M, Renziehausen A, et al. TGF-beta 1 induces proliferation in human renal fibroblasts via induction of basic fibroblast growth factor (FGF-2). Kidney Int. 2001; 59(2): 579-592.

Biography

Maja (Miroslav) Životić, was born on January 9th 1987 in Požarevac, Serbia. She attended Primary school in Veliko Gradište, and afterwards Gymnasium in Požarevac. In 2006 she started with study of medicine at University of Belgrade - Faculty of Medicine and graduated in 2012 with an average mark 9.85 (out of 10.00). She enrolled PhD studies on October 2012, course of Molecular Medicine at University of Belgrade - Faculty of Medicine. PhD thesis entitled "The role of interaction between fibroblast growth factor receptor and neural cell adhesion molecule in renal fibrosis" was approved by Scientific Council for medical sciences at University of Belgrade on March 29th 2016. Prof. dr Jasmina Marković-Lipkovski was appointed as scientific advisor for this thesis.

Since December 1st 2012 she has been empolyed as a scientific researcher of the project entitled *„Characterization of renal stem/progenitor cells in humans: identification of novel surface markers of multipotent renal cells with regenerative properties in kidney injuries"*, number OI 175047, Ministry of education, science and technological development of Republic of Serbia. During 2014/2015 she was a member of PPP-DAAD bilateral project between Serbia and Germany, entitled "*Characterization of Progenitor Cells for Kidney Regeneration ("ProKiReg"): Identity of NCAM positive Progenitors in fetal and adult Kidney"*. Since 2014 she has been employed as a teaching assistant at Institute of Pathology of the University of Belgrade - Faculty of Medicine, and became a resindent of pathology.

She is an active researcher of the bilateral project group (three years 2016-2018) founded by Alexandar von Humboldt Foundation. Project is entitled „*Induction of NCAM expression in adult human kidney: an adaptive cellular response to tissue hypoxia?"* (number 3.4-IP-DEU/1019337).

She was scientific advisor of students' scientific research papers with the international participations. She was awarded for her dedication to work with students by the Student Parliament of the University of Belgrade - Faculty of Medicine. Her scientific results were presented on the numerous national and international congresses, and she published 6 full text articles as author and co-author.

Biografija

Maja (Miroslav) Životić, rođena je 09.01.1987. u Požarevcu, Republika Srbija. Osnovnu školu završila je u Velikom Gradištu, a potom je srednjoškolsko obrazovanje nastavila u Požarevačkoj gimnaziji. Medicinski fakultet Univerziteta u Beogradu upisala je 2006. godine i diplomirala juna 2012. godine sa prosečnom ocenom na studijama 9,85. Doktorske akademske studije upisala je oktobra 2012. godine, smer Molekularna medicina, a izrada doktorske disertacije pod nazivom *„Uloga interakcije receptora za fibroblastni faktor rasta sa neuralnim ćelijskim adhezionim molekulom u fibrozi bubrega“* odobrena je na sednici Veća naučnih oblasti medicinskih nauka Univerziteta u Beogradu 29. marta 2016. godine. Za mentora doktorske disertacije imenovana je prof. dr Jasmina Marković-Lipkovski, redovan profesor Medicinskog fakulteta Univerziteta u Beogradu.

Od 01. decembra 2012. zaposlena je kao istraživač na projektu Ministrastva prosvete, nauke i tehnološkog razvoja Republike Srbije, pod nazivom *„Karakterizacija bubrežnih stem/progenitor ćelija kod čoveka: identifikacija novih površinskih markera multipotentnih bubrežnih ćelija koje mogu imati regenerativnu ulogu kod oštećenja bubrega“*, broj OI 175047. Bila je i član PPP-DAAD bilateralnog projekta između Ministarstva prosvete, nauke i tehnološkog razvoja Republike Srbije i DAAD fondacije SR Nemačke, pod nazivom *„Characterization of Progenitor Cells for Kidney Regeneration (“ProKiReg”): Identity of NCAM positive Progenitors in fetal and adult Kidney“* u toku 2014/2015 godine. Od 01. avgusta 2014. zaposlena je kao saradnik u nastavi na Katedri Patologije Medicinskog fakulteta Univerziteta u Beogradu, a potom od maja 2016. kao asistent na istoj Katedri. Specijalistički staž iz Patologije započela je 29. decembra 2014. Aktivan je član istraživačkog tima bilateralnog projekta (trogodišnjeg projekta 2016-2018.) Alexandar von Humboldt Fondacije „*Induction of NCAM expression in adult human kidney: an adaptive cellular response to tissue hypoxia?”* (broj 3.4-IP-DEU/1019337).

Bila je mentor studentskih radova prezentovanih na internacionalnim skupovima. Nagrađena je za posvećnost u radu sa studentima od strane Studentskog parlamenta Medicinskog fakulteta Univerziteta u Beogradu. Rezultate svojih istraživanja prikazivala je na brojnim naučnim skupovima u zemlji i inostranstvu, a publikovala je u celini 6 radova kao autor i koautor.

Prilog 1.

Izjava o autorstvu

Potpisani-a Maja Životić

broj upisa _____

Izjavljujem

da je doktorska disertacija pod naslovom

”The role of interaction between fibroblast growth factor receptor and neural cell adhesion molecule in renal fibrosis”

(„Uloga interakcije receptora za fibroblastni faktor rasta sa neuralnim ćelijskim adhezionim molekulom u fibrozi bubrega“)

- rezultat sopstvenog istraživačkog rada,
- da predložena disertacija u celini ni u delovima nije bila predložena za dobijanje bilo koje diplome prema studijskim programima drugih visokoškolskih ustanova,
- da su rezultati korektno navedeni i
- da nisam kršio/la autorska prava i koristio intelektualnu svojinu drugih lica.

Potpis doktoranda

U Beogradu, 16.03.2018.

Prilog 2.

Izjava o istovetnosti štampane i elektronske verzije doktorskog rada

Ime i prezime autora: Maja Životić

Broj upisa

Studijski program: Molekularna medicina

Naslov rada: „The role of interaction between fibroblast growth factor receptor and neural cell adhesion molecule in renal fibrosis" („Uloga interakcije receptora za fibroblastni faktor rasta sa neuralnim ćelijskim adhezionim molekulom u fibrozi bubrega")

Mentor: Prof. dr Jasmina Marković-Lipkovski

Potpisani 

izjavljujem da je štampana verzija mog doktorskog rada istovetna elektronskoj verziji koju sam predao/la za objavljivanje na portalu **Digitalnog repozitorijuma Univerziteta u Beogradu.**

Dozvoljavam da se objave moji lični podaci vezani za dobijanje akademskog zvanja doktora nauka, kao što su ime i prezime, godina i mesto rođenja i datum odbrane rada.

Ovi lični podaci mogu se objaviti na mrežnim stranicama digitalne biblioteke, u elektronskom katalogu i u publikacijama Univerziteta u Beogradu.

Potpis doktoranda

U Beogradu, 16.03.2018.

Prilog 3.

Izjava o korišćenju

Ovlašćujem Univerzitetsku biblioteku „Svetozar Marković“ da u Digitalni repozitorijum Univerziteta u Beogradu unese moju doktorsku disertaciju pod naslovom:

„The role of interaction between fibroblast growth factor receptor and neural cell adhesion molecule in renal fibrosis”

(„Uloga interakcije receptora za fibroblastni faktor rasta sa neuralnim ćelijskim adhezionim molekulom u fibrozi bubrega“)

---

koja je moje autorsko delo.

Disertaciju sa svim prilozima predao/la sam u elektronskom formatu pogodnom za trajno arhiviranje.

Moju doktorsku disertaciju pohranjenu u Digitalni repozitorijum Univerziteta u Beogradu mogu da koriste svi koji poštuju odredbe sadržane u odabranom tipu licence Kreativne zajednice (Creative Commons) za koju sam se odlučio/la.

1. Autorstvo
2. Autorstvo - nekomercijalno
3. Autorstvo – nekomercijalno – bez prerade
4. Autorstvo – nekomercijalno – deliti pod istim uslovima
5. Autorstvo – bez prerade
6. Autorstvo – deliti pod istim uslovima

(Molimo da zaokružite samo jednu od šest ponuđenih licenci, kratak opis licenci dat je na poleđini lista).

Potpis doktoranda

U Beogradu, 16.03.2018.

1. Autorstvo - Dozvoljavate umnožavanje, distribuciju i javno saopštavanje dela, i prerade, ako se navede ime autora na način određen od strane autora ili davaoca licence, čak i u komercijalne svrhe. Ovo je najslobodnija od svih licenci.

2. Autorstvo – nekomercijalno. Dozvoljavate umnožavanje, distribuciju i javno saopštavanje dela, i prerade, ako se navede ime autora na način određen od strane autora ili davaoca licence. Ova licenca ne dozvoljava komercijalnu upotrebu dela.

3. Autorstvo - nekomercijalno – bez prerade. Dozvoljavate umnožavanje, distribuciju i javno saopštavanje dela, bez promena, preoblikovanja ili upotrebe dela u svom delu, ako se navede ime autora na način određen od strane autora ili davaoca licence. Ova licenca ne dozvoljava komercijalnu upotrebu dela. U odnosu na sve ostale licence, ovom licencom se ograničava najveći obim prava korišćenja dela.

4. Autorstvo - nekomercijalno – deliti pod istim uslovima. Dozvoljavate umnožavanje, distribuciju i javno saopštavanje dela, i prerade, ako se navede ime autora na način određen od strane autora ili davaoca licence i ako se prerada distribuira pod istom ili sličnom licencom. Ova licenca ne dozvoljava komercijalnu upotrebu dela i prerada.

5. Autorstvo – bez prerade. Dozvoljavate umnožavanje, distribuciju i javno saopštavanje dela, bez promena, preoblikovanja ili upotrebe dela u svom delu, ako se navede ime autora na način određen od strane autora ili davaoca licence. Ova licenca dozvoljava komercijalnu upotrebu dela.

6. Autorstvo - deliti pod istim uslovima. Dozvoljavate umnožavanje, distribuciju i javno saopštavanje dela, i prerade, ako se navede ime autora na način određen od strane autora ili davaoca licence i ako se prerada distribuira pod istom ili sličnom licencom. Ova licenca dozvoljava komercijalnu upotrebu dela i prerada. Slična je softverskim licencama, odnosno licencama otvorenog koda.